SRI LANKAN GEOTECHNICAL SOCIETY

Geotechnical Engineering Project Day 2023

PROCEEDINGS

27th March 2024

PRESIDENT'S MESSAGE

Geotechnical Engineers help design structures that are either composed of soil or rock or are in contact with it. In essence, they engineer the interface between the natural and built environments. Research provides insight into the interaction and performance of structures with earth, such bearing failures, settlement damage, and failures due to emergent processes such as landslides and liquefaction.

As the President of the Sri Lankan Geotechnical Society, I am very pleased to send this message to the Proceedings of Project Day which will be held online on Thursday, 27th March 2024.

This annual event has been organized by SLGS since 2000 uninterruptedly with the objective of promoting research and enhancing the presentation skills of Civil Engineering students in Sri Lankan Universities.

The event features a competition among final year undergraduates who have conducted research projects in Geotechnical Engineering. The best projects will be selected by an independent committee of distinguished Geotechnical Professionals appointed by SLGS, based on the written paper and the presentation.

This year, we are proud to have 15 competitors from Sri Lankan Universities who have completed their undergraduate research projects on various Geotechnical Engineering aspects, including foundation design, deep excavation, ground settlement, slope stability, ground improvement, and rock mechanics.

This time we are continuing the same evaluation procedure which, we believe, will minimize any biasness in the competition. Competitors are expected to present their research objectives, procedure and findings in a four to six paged paper and to make a five minutes oral presentation. The best and the second-best paper / presentation will receive cash awards and certificates.

Many winners in the past year have proceeded to do higher studies and subsequently established good carriers in the field of Geotechnical Engineering as both academics and practicing engineers.

I would like to thank all the Students, Authors / Research Supervisors for their interest and commitment for submitting papers and making presentations in this Project Day. Without their participation, this event will not be a reality.

Also, I would like to thank panel of evaluators namely Dr. Samanthi Indiketiya, Dr. Manasi Wijerathna, Dr. Priyanath Ariyarathne, Dr. Chathuri Arachchige, Dr. Asitha Senanayake, Dr. Sahan Udakara and Dr. Waranga Dilanthi for their difficult task of evaluating all the papers and presentations within very short notice.

I am grateful to the members of the Organizing and the Executive Committees for being with me together offering their unstinting support to make this event successful.

A special thanks goes to Dr. Sampath Hewage for his untiring effort for organizing and coordinating the Project Day in this year.

I would like to thank Dr. Mark Ballouz, President International Society for Soil Mechanics and Geotechnical Engineering (ISSMGE) for his encouragement of conducting this event by SLGS. Also, I would like to thank key office bearers of South Asian Geotechnical Associations for their continuous support for SLGS activities.

I am certain that this Project Day will be another exciting and informative event by the Sri Lankan Geotechnical Society and I wish everyone a very effective and fruitful Seminar.

This year also the Society has / will organize/d Geo-forum, our monthly short presentation event followed by a Question and Answer session, Design Workshops and an Annual Seminar to enhance the knowledge of the engineers and other professionals engaged in Geotechnical and Foundation related works. Also, we are planning to have our International Conference in 2026 in Colombo. I cordially invite all of you to participate these events effectively to support the Sri Lankan Geotechnical Society for their continuous effort to enhance the knowledge in Geotechnical and Foundation Engineering of Engineers and other Professionals who are involved in the discipline.

Eng. K.L.S. Sahabandu
B.Sc.Eng.(Hons.), Pg. Dip.(Hyd.), M.Sc. (Struct.), C.Eng.,
M.I.C.E.(U.K.), M. Cons. E. (S.L.), F.I.E.(S.L.), Hon. F.S.S.E.(S.L.)
PRESIDENT
SRI LANKAN GEOTECHNICAL SOCIETY (SLGS)

SLGS EXECUTIVE COMMITTEE

Eng. K L S Sahabandu	President
Prof. H S Thilakasiri	Vice President
Prof. S A S Kulathilaka	Past President
Eng. K S Senanayake	Past President
Prof. U P Nawagamuwa	Hony. Secretary
Dr. K H S M Sampath	Assistant Secretary
Eng. R M Rathnasiri	Treasurer
Eng. M D J P Wickramasooriya	Assistant Treasure
Dr. N H Priyankara	Editor– Journal
Dr. S K Navaratnarajah	Editor– Newsletter
Dr. W A Karunawardena	Committee Member
Dr. J S M Fowze	Committee Member
Prof. L I N De Silva	Committee Member
Eng. R.M. Abeysinghe	Committee Member
Eng. Lasanda Padmasiri	Committee Member

Content

1	**Strength and Swell Characteristics of Expansive Road Subgrade Stabilized with Novel Rice Husk Ash Based One-Part Geopolymer.** *I. Krishnalojan, A. Sivasithamparam, M.C.M. Nasvi and L.C Kurukulasuriya* *Department of Civil Engineering, University of Peradeniya, Sri Lanka*	1
2	**Optimization of Deep Excavation Support Systems Using Finite Element Analysis: A Case Study.** V.S.S.D. Silva and L.I.N. De Silva *Department of Civil Engineering, University of Moratuwa, Sri Lanka*	7
3	**Influence of Gradation on Shear Behaviour of Railway Ballast Material.** M. Amalan, R. Tharmarajah and S. K. Navaratnarajah *Department of Civil Engineering, University of Peradeniya, Sri Lanka*	13
4	**Improvement of Gravel Roads Against Erosion Caused by Heavy Rain.** P.P.J. Kishok and N.H. Priyankara *Department of Civil and Environmental Engineering, University of Ruhuna, Sri Lanka*	17
5	**Shredded Rubber for Ballast Replacement in Rail Track Applications.** C. Thanusikan, E. Mathynushan and S.K. Navaratnarajah *Department of Civil Engineering, University of Peradeniya, Sri Lanka*	23
6	**Geotextile Encased Stone Columns (GESC) in Soft Soil.** W.D.I.C. Weerawardana and N.H. Priyankara *Department of Civil and Environmental Engineering, University of Ruhuna, Sri Lanka*	29
7	**Prediction of Geotechnical Properties of Expansive Soil Stabilized with Fly Ash using Artificial Neural Network.** K. Kirushanthan, T.Thigitharan and M.C.M. Nasvi *Department of Civil Engineering, University of Peradeniya, Sri Lanka*	34
8	**Seepage Control in Earthen Dams Using Soil-Cement-Bentonite Cutoff Wall.** M.S. Umar and N.H. Priyankara *Department of Civil and Environmental Engineering, University of Ruhuna, Sri Lanka*	40

9	**Strength Mobilization in Soft Clayey Soils Mixed with Quarry Dust and Cement in Early Curing.** R.D.M.P Rajapksha and W.M.N.R Weerakoon *Department of Civil Engineering, University of Sri Jayewardenepura, Sri Lanka*	46
10	**Stabilization of Subgrade Using Geosynthetics.** U.D.M. Kumara and N.H. Priyankara *Department of Civil and Environmental Engineering, University of Ruhuna, Sri Lanka*	51
11	**Partial Soil Replacement Strategies for Enhancing Soft Soil Conditions Beneath Shallow Foundations.** G.K.H. Wijesooriya and L.I.N. De Silva *Department of Civil Engineering, University of Moratuwa, Sri Lanka*	57
12	**Engineering Properties of Peat Soils - Mixed with Combination of Quarry Dust and Cement.** A.R.A. Mohammed and W.M.N.R. Weerakoon *Department of Civil Engineering, University of Sri Jayewardenepura, Sri Lanka*	64
13	**Novel Fly Ash based One-part Geopolymer for Stabilization of Expansive Road Subgrade.** K.R.H. Jayawardane, K.S.S. Rangana, M.C.M. Nasvi and L.C. Kurukulasuriya *Department of Civil Engineering, University of Peradeniya, Sri Lanka*	70
14	**Investigation of Consolidation Parameters of Sri Lankan Peat Soil.** C. H. Nerangama and W.M.N.R.Weerakoon *Department of Civil Engineering, University of Sri Jayewardenepura, Sri Lanka*	76
15	**Investigation of the Stability of Embankments on Soft Soil Deposits.** C.F. Robinson, T.M.D. Thilakarathne and H.S. Thilakasiri *Department of Civil Engineering, Sri Lanka Institute of Information Technology, Sri Lanka*	82

Strength and swell characteristics of expansive road subgrade stabilized with novel rice husk ash based one-part geopolymer

Krishnalojan I., Sivasithamparam A., Nasvi M.C.M., and Kurukulasuriya L.C.

Department of Civil Engineering, University of Peradeniya, Sri Lanka

ABSTRACT: Expansive soil presents challenges for road subgrade due to restricted bearing capacity and climate change fluctuations. Chemical stabilization, like ordinary Portland cement (OPC), is greenhouse gas-intensive. Geopolymer, has gained interest due to its low environmental impact. There are two types of geopolymers available: one-part and two-part. Two-part geopolymer (TP-GP) has drawbacks like mixing and handling complexity, making one-part geopolymer (OP-GP) recommended. Limited studies have focused on Rice husk ash (RHA)-based OP-GP. This study analyzes the strength and swell characteristics of RHA-based OP-GP with varying binder/dry soil and NaOH/RHA ratios to find the optimal OP-GP based on unconfined compression strength (UCS) and cost. The optimum OP-GP stabilized sample was OP-GP with B/S = 0.2 and NH/RHA = 0.15 based on both UCS and cost. Further, selected optimum OP-GP was compared with optimum TP-GP and 8% OPC stabilized samples using utility analysis based on UCS, CBR, swell pressure, cost, and carbon footprint.

KEY WORDS: Expansive soil, Soil stabilization, Geopolymer, Rice husk ash

1 INTRODUCTION

Expansive soils exhibit unique characteristics such as volume changing behavior and high moisture retaining ability. These traits are attributed to the presence of clay minerals like montmorillonite (Maheepala et al., 2022). Expansive soil damage, exacerbated by industrial waste amendments, incurs an annual global repair cost surpassing that of natural disasters, reaching $7 billion. In Sri Lanka, expansive soil occurs in arid, semi-arid and monsoonal areas due to the seasonal distribution of precipitation and evaporation/ transpiration cause wide fluctuation in the soil moisture, identified in Dambulla, Mahiyanganaya, Anuradhapura and Hambantota.

Soil stabilization is the process of altering the physical or chemical properties of soil to improve its strength, durability, and resistance to deformation. The most popular method is changing chemical properties, called as chemical stabilization as it's less expensive and lets us control the curing and setting times. OPC, is the most commonly used calcium-based binder for stabilizing soil. The International Energy Agency (IEA) reported that the global OPC production was responsible for around 2.2 billion tons of CO_2 emissions, or 8% of the total worldwide (Maheepala et al., 2022) and its lead to leaching and form carbonation shrinkage cracks (Khadka et al., 2018), despite the fact that OPC treated soil gains strength far more quickly within low cost.

Alkali-activated binders (AAB) are being diagnosed as a distinctly promising solution to tackle the issues related with stabilizers. Geopolymers are inorganic, amorphous, and three-dimensional polymeric chains formed between alumina-silicate materials. The adoption of AABs as a substitute of regular stabilizers can lead to a terrific discount of GHG emissions, ranging from 70 to 90% (Davidovits et al., 2015). Geopolymers can be classified into two distinct types based on the phase of alkali activator utilized: one-part and two-part. While OP-GP employs solid alkali activators, TP-G utilizes liquid alkali activators. Despite its associated challenges such as the complexity of mixing, handling, and sensitivity to environmental factors, OP-G is favored for soil stabilization purposes.

The total annual production of RHA would be approximately 0.1 million tons per year in Sri Lanka (Fernando et al., 2022). Currently, RHA has no commercial use in Sri Lanka, leading to its frequent disposal in landfills and causing wide-scale environmental pollution. Therefore, in our research, RHA is used as an aluminosilicate material, offering a sustainable alternative for cement soil stabilization. The aim of this research is to analyze the strength, swell characteristics and cost and carbon footprint of expansive road subgrade

stabilized with novel RHA-based OP-G, TP-G, and 8% OPC stabilization

Maheepala. et al., (2022) conducted a review on the expansive soil stabilization. It was found that incorporation of precursors in the range of 15– 20%, alkaline molarities between 5 and 10 M, along with strong alkalis (NaOH or KOH), Ca rich additives, and discrete fibers could enhance the stabilization performance with respect to unconfined compressive strength (UCS), swell, and durability. Tesanasin et al., (2022) conducted research on the properties of marginal lateritic soil (MLS) with one-part high calcium fly ash geopolymer. Beyond 20% NaOH, UCS and indirect tensile strength (ITS) reduced due to the heat generation of NaOH which led to expansion, microcracking, shortening of setting time, early precipitation of the geo polymer products and reduction of strength.

2 MATERIAL AND METHODOLOGY

2.1 *Materials*

The soil sample was collected from Wilgamuwa, Central Province, Sri Lanka. (7°32'34.9"N 80°54'52.1"E). The RHA sample used in this study was collected from Divulapitiya rice mill, Negombo, Sri Lanka. and chemical components such as NaOH and Na_2SiO_3 were brought from local market in Colombo, Sri Lanka. The classification of an expansive soil sample was determined by performing laboratory tests such as such as sieve and hydrometer analysis (BS 1377: Part 2: 1990), Atterberg limit tests (BS 1377: Part 2: 1990), standard proctor compaction test (BS 1377: Part 2: 1990), specific gravity test (BS 1377: Part 4: 1990), swell pressure test (BS 1377: Part 5: 1990) and unconfined compressive strength (UCS) test (BS 1377: Part 7: 1990).

Table 1. Results of characterization testing of expansive soil

Properties	Values
Specific gravity	2.67
Liquid limit (%)	55
Plastic limit (%)	29
Plasticity index (%)	26
Soil Classification (USCS)	CH
Maximum swell pressure (kPa)	210
Maximum Swell percentage (%)	4.7
UCS(MPa)	0.32
MDD (kN/m^3) (Standard Compaction)	14.91
OMC (%)	23.8
MDD (kN/m^3) (Modified Compaction)	17.7
OMC (%)	14
CBR	2.5

The results of the raw soil characterization are given in Table 1. Based on the characterization results, this soil is classified as clay of high plasticity (CH) according to USCS.

2.2 *Methodology*

2.2.1 *Mix composition for OP-G*

The mix composition parameters shown in Table 2 were selected based on the literature. A series of 16 UCS specimens were casted with different binder (RHA + NaOH)/ dry soil (B/S) ratios and solid NaOH/ RHA (NH/RHA) ratios to determine the optimal mix for OP-G stabilization in terms of 7 Days UCS strength and cost.

2.2.2 *Sample preparation*

The method used to prepare the OP-GP stabilized expansive soil sample is described in Fig. 1. Soil mix was prepared by mixing raw soil with prescribed amount of water by following the method adopted by Wu et al., (2021). Thereafter, geopolymer mix was prepared by mixing RHA, NaOH with prescribed amount of water. Immediately both mixes were mixed to prepare the geopolymer stabilized soil mix.

Table 2. Mix Optimization for OP-GP

Mix Parameter (weight ratio)	Values	Reference
B/S	0.1,0.15,0.2,0.25,0.3	Wu et al 2021
NH/RHA	0.1,0.15,0.2,0.25	Wu et al 2021, Zheng et al. 2021

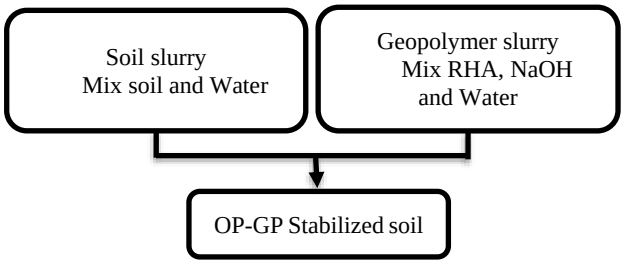

Fig. 1 Sample preparation method

The required quantity of water was added, taking into account both the soil and geopolymer binder. The soil, RHA and solid NH mixture underwent a thorough mixing with the water to achieve a homogenous consistency. Three different mixing water contents (Cases 1 to 3) were trialed to obtain the optimum water content for high UCSs.

✓ Case 1: Total weight of water = Total weight of solids x OMC
✓ Case 2: Total weight of water = Total weight of solids x 1.2 OMC
✓ Case 3: Total weight of water = Total weight of solids x 1.4OMC

Based on the UCS results and the appearance of cracks in cases 1 and 2, Case 3 was selected to prepare all the samples. Stabilized samples were fully wrapped using cling wrap and cured under room temperature for 7 days.

2.2.3 *UCS Test for OP-GP samples*

In compliance with BS 1377-Part 7:1990 standards, a motorized machine was utilized to measure the UCS of OP-GP stabilized samples. The platen displacement rate was kept constant at 1 mm/min. Three test specimens were excluded from the mold to determine UCS values, which guaranteed a standard deviation of less than 10% of the average strength after seven days.

2.2.4 *Selecting Optimum OP-G*

The optimal OP-GP stabilized soil sample was chosen by evaluating UCS test results and the cost per unit volume of stabilized soil. A thorough cost analysis, specially concentrating on manufacturing and transportation expenses, was carried out for all samples. The overall utility of each sample was calculated, taking into account UCS and cost/UCS, with weights of 0.3 and 0.7 assigned to both responses, respectively.

2.2.5 *Comparing the Optimum OP-G, TP-G and 8 % OPC based Utility function*

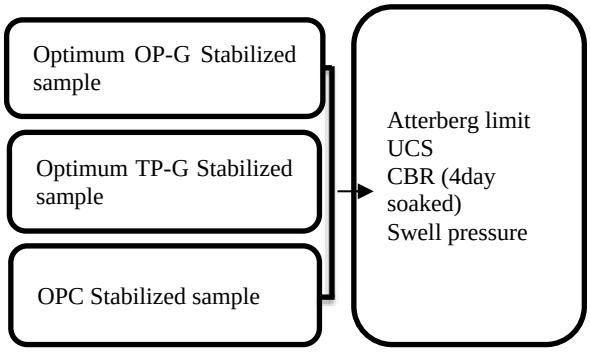

Fig. 2 Testing carried out for different stabilized sample

This research compared the previously found optimum OP-GP stabilized soil with an optimum TP-GP stabilized soil sample, as well as an 8% OPC stabilized soil sample. The TP-GP stabilized soil was made using a liquid alkaline activator with a NH concentration of 5 M and a 70:30 ratio of Na_2SiO_3 (NS) to NH. The same optimal ratios determined for OP-GP were applied to the TP-GP formulation. The 8% OPC-stabilized soil was created by adding 8% OPC and OMC. Following a curing period of 28 days, the stabilized soil samples underwent various tests, detailed in Fig. 2.

An in-depth analysis was carried out for all three soil samples, focusing on both the expenses incurred and the environmental impact, specifically during the production of raw materials. The study involved calculating the mass of different materials per unit volume for each soil sample to assess costs, and local market prices were applied to determine the unit cost of each material. To determine emissions associated with each sample, the functional equations and inventory data from Fernando et al. (2021) were utilized.

This study used a simplified version of Multi-Attribute Utility Theory (MAUT) to rank stabilizers. Criteria such as swell pressure, UCS, CBR, cost per UCS, and emission were identified and assigned weights to reflect their importance. Utility functions were developed for each criterion, with different functions used based on whether higher or lower values were preferred. Overall utility scores were computed for each stabilizer percentage, and the most suitable percentage was determined based on the highest score. The methodology followed was outlined by Taufik et al. (2021).

3 RESULTS AND DISCUSSION

3.1 *Strength characteristics of OP-GP stabilized samples and optimum OP-GP based on utility analysis*

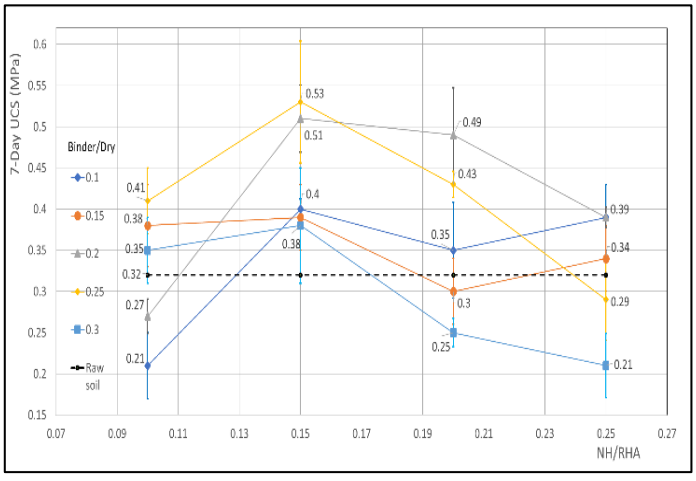

Fig. 3 The variation of UCS with NH/RHA ratios for OP-GP

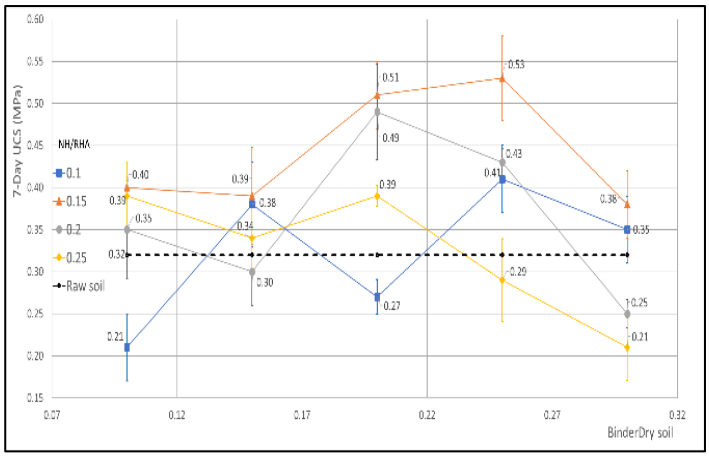

Fig. 4 The variation of UCS with B/S ratios for OP-G

Fig. 3 and 4 show the variation of UCS of OP-GP stabilized soil with NH/RHA and B/S respectively. According to Fig. 3 and 4, the optimum B/S ratio and NH/RHA ratio for higher UCS were found to be 0.25 and 0.15.

A contour plot was developed to show the variation of UCS with B/S and NH/RHA. As depicted in Fig. 5, three zones were identified as follows: zone 1: High amount of water content zone, zone 2: Optimum UCS zone, zone 3: High amount of geopolymer binder zone. Fig. 5 shows the variation of UCS with NH/RHA for constant B/S and Figure 6 shows the variation of UCS with B/S for constant NH/RHA.

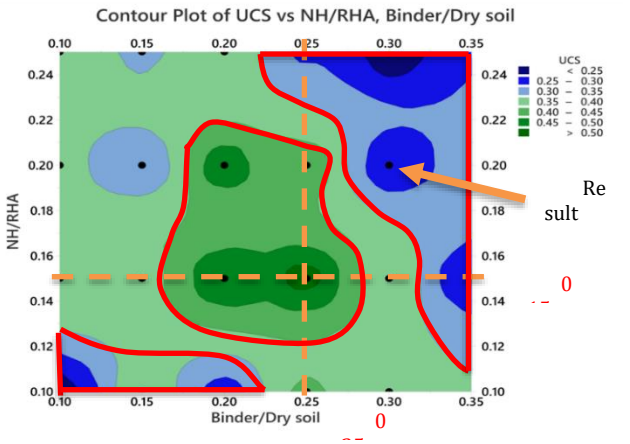

Fig. 5 Contour plot for 7-D UCS with B/S and NH/RHA

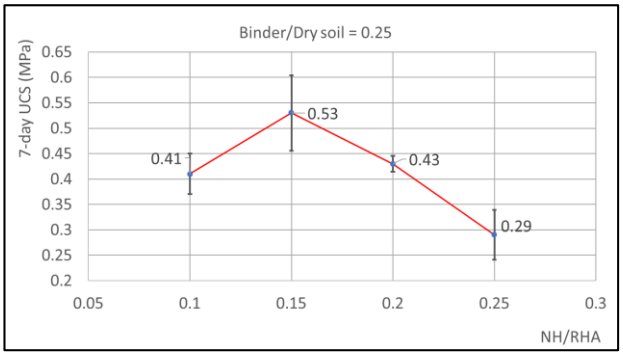

Fig. 6 The variation of UCS with NH/RHA

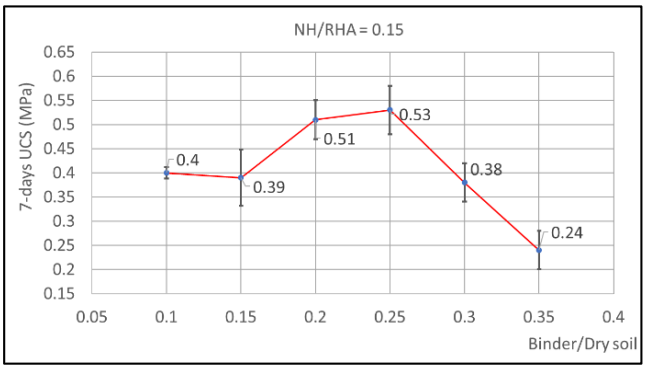

Fig. 7 The variation of UCS with B/S

The mixture reached a UCS value of 0.53 MPa after 7 days of curing. It can be seen from Fig. 6 that as the NH/RHA ratio increases, the UCS value of stabilized soil increases to the optimal value and then decreases again. The increase in UCS is due to the polymerization reaction to form C-A-S-H gel. The decrease in UCS of NH/RHA above 0.15 is due to expansion because of the heat generation of NaOH, and therefore microcracking. It can be seen from Fig. 7 that as the B/S ratio increases, the UCS value of stabilized soil increases to the optimal value and then decreases again. The initial increment might be due to quantity of RHA could induce pozzolanic reaction and form cementitious compounds that have strength increase, while the additional amount of RHA could act as unbounded particles, forming weak bonds between the soil and the cementitious compounds formed (Pushpakumara et al., 2022).

Table 3. Utility results of top 5 samples of OP-GP

Binder/Dry soil	NH/RHA	Cost/ UCS	UCS	U (Cost/UCS)	U (UCS)	Overall Utility Response	Rank
0.20	0.15	52.25	0.51	4.92	9.95	6.43	1
0.25	0.15	59.91	0.53	4.50	10.36	6.26	2
0.10	0.15	36.93	0.40	5.97	7.37	6.39	3
0.20	0.20	69.41	0.49	4.06	9.52	5.70	4
0.15	0.10	38.58	0.38	5.84	6.82	6.13	5

All mixtures were ranked based on the overall utility response calculated for each sample, taking into account UCS and cost/UCS. The utility results of the top five samples (out of 16 samples) are shown in Table 3. Based on Table 3, the mix having B/S = 0.2, and NH/RHA = 0.15 was found to be the best stabilized mix in terms of cost/UCS.

3.2 *Strength and swell characteristics of OP-GP, TP-GP and OPC stabilized samples*

Table 4. Variation of the Atterberg limits

Atterberg limit	Raw Soil	OP-GP	TP-GP	OPC
LL (%)	55	38	39	54
PL (%)	29	36	34	37
PI (%)	26	2	5	17

As shown in Table 4, LL values of the OP-GP, TP-GP, and OPC stabilized samples were 38, 39 and 54%. Therefore, only OP-GP and TP-GP samples met the ICTAD guidelines (see Table 5) with values lower than 40%. Specifically, the PI values for soil stabilized with OP-GP, TP-GP, and OPC decreased by 92%, 80%, and 34%, respectively. But PI value of OPC did not meet the ICTAD guidelines given in Table 5. The results of the study indicated that the utilization of OP-GP and TP-GP binders leads to a reduction in the plasticity of the soil, as evidenced by the significant decrease in PI values compared to untreated soil. This decrease in PI is attributed to the reduction in water affinity resulting from the soil being coated with a geometric gel, particularly in the geopolymer-stabilized samples compared to those stabilized with OPC.

Table 5. ICTAD specifications for subgrade

Engineering properties	Subgrade specifications by Road Development Authority of Sri Lanka
LL	<40%
PI	<15%
4-days soaked CBR at 95% MDD (Modified)	>15%

Table 6. Strength and swell results of stabilized samples

Sample	Raw Soil	OP-GP	TP-GP	OPC
Swell pressure (kPa)	163.66	95.3	115	108.03
UCS (MPa)	0.32	0.69	0.65	2.77
CBR (%)	12	20	18	81

Table 6 presents the strength and swell results of OP-GP, TP-GP, and OPC stabilized samples. The UCS values for OP-GP, TP-GP, and OPC stabilized samples were 0.69, 0.65 and 2.77 MPa respectively (see Table 6). Furthermore, the UCS values of the stabilized soil samples significantly increased compared to untreated soil, with percentage increases of 115%, 103% and 765% for OP-GP, TP-GP, and OPC stabilized samples respectively. This highlights the positive impact of cement in strengthening these mixtures due to the introduction of cementitious bonding, which enhances cohesion within the soil structure, and the formation of hydration products like calcium silicate hydrates.

Specifically, the CBR values for OP-GP, TP-GP, and OPC stabilized soil samples were determined to be 20%, 18%, and 81%, respectively as shown in Table 6. The 4 days soaked CBR values for the stabilized soil samples also met the standards set by ICTAD (refer Table 5), with values higher than 15% indicating the suitability of these stabilized samples for subgrade applications.

Moreover, the swell pressure values of the soil samples stabilized with OP-GP, TP-GP, and OPC were lower than those of the natural soil sample, with observed percentage reductions ranging as 42%, 30% and 34% respectively.

3.3 *Cost and Carbon footprint*

Table 7. Cost and emission factors of raw materials

Materials	Cost (USD/kg)	Emission factors (kg CO_2-eq/ kg)
RHA	-	0.0027
OPC	0.15	0.94
NH	0.96	1.425
NS	0.8	0.78

Table 7 indicates emission factors of materials obtained from Fernando et al. (2021) and cost factors obtained from local markets. According to Table 8, the cost per m^3 of stabilized soil to gain 1 MPa of UCS was estimated as 41.19 USD for OP-GP. It can be seen that the cost of the geopolymer based stabilizers is significantly high compared to OPC due to high cost of NH. And also, cost/UCS of OPC stabilized sample showed lower value not only the lower cost but also the high UCS of OPC sample. But total emission from 1 m^3 of OPC stabilized soil is adversely large compared to OP-GP and TP-GP indicating its environmental damage.

3.4 *Utility analysis based on Multi-Attribute Utility Theory*

If the weights assigned for swell pressure, UCS, CBR, Cost/ UCS and emission were 0.2, 0.15, 0.15, 0.3, 0.2 respectively, OP-GP, TP-GP and OPC can be ranked as shown in Table 9 computing overall utility for each stabilizer. The greatest emphasis was placed on cost-effectiveness by assigning the highest weight to cost/UCS, influencing the optimal selection. While OPC stabilizer demonstrated superior performance across various indicators such as UCS, CBR and cost/UCS, OP-GP emerged as a

Table 8. Cost and emission values for OP-GP, TP-GP and OPC stabilized samples

Item	Cost (USD/m^3)					Emission (kg CO_2-eq/ m^3)					28-day UCS (MPa)	Cost/UCS (USD/m^3/ MPa)
	RHA	OPC	NH	NS	Total	RHA	OPC	NH	NS	Total		
OP-GP	-	-	28.42	-	28.42	0.53	-	42.19	-	42.72	0.69	41.19
TP-GP	-	-	4.59	23.59	28.18	0.62	-	6.81	23	30.43	0.65	43.35
OPC	-	18.24	-	-	18.24	-	114.61	-	-	114.61	2.77	6.58

viable alternative with reasonable UCS, lower emission and super performance in reducing swell, ranking as the second optimal choice in terms of overall utility. As an alternative for OPC, OP-GP can be utilized in stabilizing road subgrade as it has become the second optimal choice based on overall utility.

Table 9. Results of utility analysis

Sample	OP-GP	TP-GP	OPC
U(Swell pressure)	1	0	0.35
U(UCS)	0.02	0	1
U(CBR)	0.03	0	1
U(Cost/UCS)	0.06	0	1
U(Emission)	0.85	1	0
Overall Utility	0.4	0.2	0.67
Rank	2	3	1

4 CONCLUSION

Following conclusions were drawn based on the findings. (B/S=binder/dry soil, NH=NaOH)

- The samples with 1.4 OMC exhibited the highest UCS and were found to be free of surface cracks.
- Highest UCS were found at OP-GP with B/S = 0.25 and NH/RHA = 0.15
- Lowest cost/UCS were found at OP-GP with B/S = 0.2 and NH/RHA = 0.15 which is having the lowest total cost and second highest UCS out of all samples. That was the optimum OP-GP stabilized sample based on both UCS and cost.
- The utilization of OP-GP and TP-GP binders led to a notable decrease in soil plasticity, as demonstrated by the significant reduction in PI values compared to untreated soil in contrast to those stabilized with OPC.
- OP-GP and TP-GP binders effectively reduced PI values by 92% and 80%, respectively, meeting ICTAD guidelines. OPC failed to meet LL and PI specifications, highlighting the superiority of geopolymer stabilizers in reducing soil plasticity.
- OP-GP and TP-GP stabilized samples demonstrated UCS increases of up to 115% and 103%, respectively, compared to untreated soil. OPC showed the highest UCS value with a percentage increment of 765%.
- CBR values for OP-GP, TP-GP, and OPC stabilized samples met ICTAD standards while OPC stabilization exhibited incredible increment of CBR compared to OP-GP and TP-GP.
- OP-GP stabilized soil sample exhibited lowest swell pressure value compared to TP-GP, and OPC treated soil, with a percentage reduction of 42%.
- OP-GP demonstrated higher costs due to NH expenses but had lower emissions per unit strength achieved. OPC had a lower cost/UCS but higher emissions, highlighting environmental concerns. Therefore, OP-GP emerged as a more environmentally sustainable alternative.
- While OPC ranked highest in overall utility due to superior performance in UCS, CBR, and cost/UCS, OP-GP emerged as a viable alternative, ranking second in utility with reasonable UCS, lower emissions, and superior performance in reducing swell pressure.
- Therefore, OP-GP can be recommended as a sustainable alternative to OPC for road subgrade stabilization.

REFERENCES

Davidovits, J., 2015. False Values on CO_2 Emission for Geopolymer Cement/concrete Published in Scientific Papers, pp. 1–9. Technical paper, 24

Fernando, S., Gunasekara, C., Law, D.W., Nasvi, M.C.M., Setunge, S. and Dissanayake, R., 2021. Life cycle assessment and cost analysis of fly ash–rice husk ash blended alkali-activated concrete. Journal of Environmental Management, 295, p.113140

Maheepala, M., Nasvi, M., Robert, D., Gunasekara, C., & Kurukulasuriya, L.. 2022 A comprehensive review on geotechnical properties of alkali activated binder treated expansive soil. Journal of Cleaner Production, 363, 132488.

Taufik, I., Alam, C.N., Mustofa, Z., Rusdiana, A. and Uriawan, W., 2021, March. Implementation of Multi-Attribute Utility Theory (MAUT) method for selecting diplomats. In IOP Conference Series: Materials Science and Engineering (Vol. 1098, No. 3, p. 032055). IOP Publishing

Tesanasin, T. Suksiripattanapong C., Duc B., Tabyang W. 2022 Engineering properties of marginal lateritic soil stabilized with one-part high calcium fly ash geopolymer as Pavement Materials.

Wu, J., Min Y., Li B., Zheng X. 2021 Stiffness and strength development of the soft clay stabilized by the one-part geopolymer under one-dimensional compressive loading, *Soils and Foundations*, 61(4), pp. 974–988

Optimization of Deep Excavation Support Systems Using Finite Element Analysis: A Case Study

V.S.S.D. Silva, L.I.N. De Silva
Department of Civil Engineering, University of Moratuwa, Sri Lanka

ABSTRACT: This study proposes a method to optimize the design of retaining walls during deep excavations using measured field monitoring data and a two-dimensional finite element (FE) analysis. Some studies indicate that the elastic modulus (E_{50}) of soil can be increased by several times to obtain the unloading-reloading modulus (E_{ur}) of the soil. The back analysis technique was used to calibrate the elastic modulus of the soil by comparing the lateral wall deformation profile obtained from the FE analysis with the inclinometer data acquired from the site. The prop forces obtained from the numerical analysis were compared with those obtained from different empirical methods used to evaluate prop forces on multi-propped retaining structures. It was found that E_{50} can be increased between 2 and 4 times to obtain the E_{ur} of soil. The reduction in maximum bending of the wall was analyzed by assigning different stiffness values for soil in the numerical model. The study highlights that the maximum bending moment that acts on the retaining wall can be reduced between 20% and 40% through the optimization of the retaining wall design.

KEY WORDS: Deep excavation, Finite element analysis, Elastic modulus, Back analysis

1 INTRODUCTION

Construction projects that involve deep excavation work have become a common feature due to the scarcity of land. The retaining structures are constructed before conducting deep excavation work to avoid excessive horizontal and vertical ground movement, which can cause severe damage to the surrounding structures. The wall displacement caused by deep excavation depends on many factors, such as soil condition, ground condition, surcharge load, construction method, groundwater level, strut spacing and stiffness, and retaining wall stiffness (Hsiung et al, 2016). Accurate estimation of wall deformation during the design stage is difficult due to the lack of detail in the soil strata below ground level. To reduce risk, designers have used conservative design approaches.

Coulomb (1776) first introduced the limit equilibrium method to calculate the lateral forces acting on retaining walls due to the presence of soil. Rankine theory was introduced as a result by extending the theory to an infinite body (Rankine, 1857). Various methods are currently being used to evaluate the earth pressure distribution of the retaining wall and the prop forces of the support system used in deep excavations. The Apparent Earth Pressure Diagram (APD) and Distributed Prop Load (DPL) methods introduced by Terzaghi and Peck (1967) and Twine and Roscoe (1999), respectively, stand as the most widely utilized empirical methods for calculating earth pressure distributions and prop forces acting on multi-propped retaining walls. Fig. 1 and Table 1 present the charts of APD and DPL methods, respectively. Here, H refers to the depth of excavation and γ refer to the unit weight of the soil.

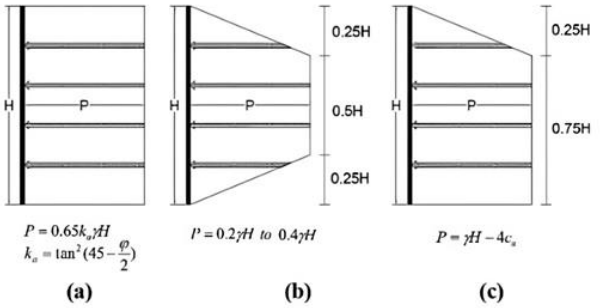

Fig. 1 Apparent earth pressure diagrams introduced by (Terzaghi & Peck, 1967). (a) Sands, (b) Stiff-hard clays, and (c) Soft to medium clay

Table 1. Magnitude of the distributed prop load for different soil types (ArcelorMittal Commercial RPS, 2016)

Class	Soil	Over retained height	DPL
AS	Same as AF for medium strength clay		
AF	Medium strength clay	Top 20%	0.2 γH
		Bottom 80%	0.3 γH
	Low strength clay with stable base	Top 20%	0.5 γH
		Bottom 80%	0.65 γH
	Low strength clay with enhanced base stability	Top 20%	0.65 γH
		Bottom 80%	1.15 γH
BS	High to very high strength clay	All	0.5 γH
BF	High to very high strength clay	All	0.3 γH
C	Granular soil, dry	All	0.2 (γ-γ_w)H
	Granular soil, submerged	Above water	0.2 γH
		Below water	0.2 (γ-γ_w)H + γ_w(z-d_w)

Empirical methods cannot estimate the wall displacement. Advances in technology have led to the design of computer software to investigate and analyze the behavior of retaining structures with greater accuracy. Currently, many studies are performed using finite element models for deep excavations. Soil stiffness was found to be the parameter that has the dominant control over excavation-induced ground movement (Hou et al, 2009; Hsiung, 2009; Ramadan and Meguid, 2020). There are different types of soil stiffness parameters. Some of them are the elastic modulus (E_{50}), the unloading-reloading modulus (E_{ur}), and the initial tangent modulus (E_0), which are presented in Fig. 2.

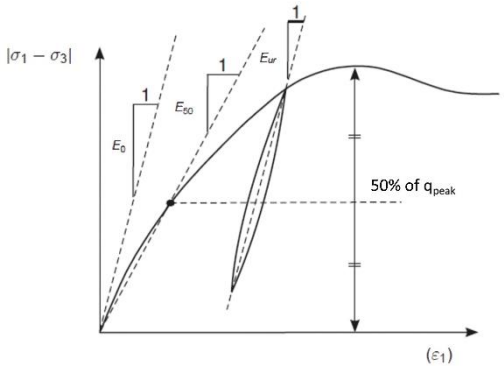

Fig. 2 Definition of E_{50} and E_{ur} in drained triaxial test

The back analysis technique is commonly used in studies to calibrate the critical parameters to minimize the deviation between numerically computed results and field observation results (Calvello & Finno, 2004). The Hardening Soil (HS) and Mohr-Coulomb (MC) models are widely used constitutive models.

Bentley Systems (2020) recommends using E_{ur} instead of E_{50} as the soil stiffness parameter for the construction work of tunnels and basements where deep excavations are involved. Given that the surrounding soil experiences changes in stress conditions due to the unloading of soil during excavation, E_{ur} is the governing parameter of soil stiffness. Previous studies have found that E_{50} can be increased by several integer multiples to obtain the E_{ur} of soil (Duc et al., 2020; Nguyen & Luu, 2013). Increasing soil stiffness helps improve soil stability, directly reducing forces and moments that act on the retaining structure. It reduces the reinforcement requirement needed to withstand the moments generated on the structure. Optimizing the design approach can significantly reduce the construction cost of retaining structures.

This study proposes a method using two-dimensional analysis to select appropriate parameters and modeling procedures in the numerical modeling of retaining structures using field test data. To achieve this, the investigation includes analyzing the effect of the elastic modulus of soil on the lateral wall deformation, evaluating prop forces and earth pressure distributions using numerical and empirical methods, and evaluating the bending moment envelopes through numerical and empirical methods.

2 SITE DESCRIPTION

An excavation carried out to construct a hospital complex in Colombo was selected for this study. It is in a heavily congested area with several multi-story buildings near the site boundary. The hospital building consists of 15 floors, including two basements. The excavation area has a maximum length and width of 47 and 33 meters, respectively. The typical plan view of the excavation area is presented in Fig. 3. There are two levels of excavation at the site. The general excavation of 8.6 m and 10.3 m for areas that locate the lift and services. The excavation area was retained by a 0.88 m thick secant pile wall having a socketed depth of 0.5 m into the bedrock. For the excavation reaching a depth of 8.6 m, two levels of lateral support were used, while three levels of lateral bracing supported a depth of 10.3 m. The shoring system used props with an effective length and spacing of 4 m. The excavated area primarily consisted of residual soil, and the ground conditions were assessed using information from four boreholes.

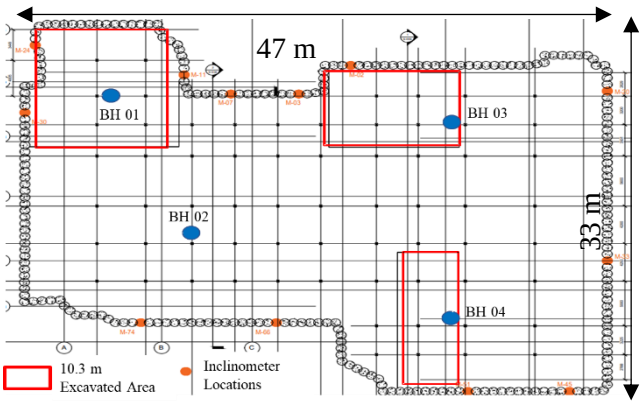

Fig. 3 Excavation area with borehole and inclinometer locations

3 METHODOLOGY

3.1 *Instrumentation*

Ground instruments were placed at appropriate locations to monitor the ground movement. The monitoring plan included twelve inclinometers (Fig. 3). The lateral movements of the walls were monitored using a 500 mm long inclinometer torpedo. The readings were taken in the excavation direction at intervals of 0.5 m. Measurements were taken once every two weeks according to the monitoring plan

to ensure that ground movements were within the acceptable range. The data obtained from the measurements were used to validate the numerical models used in this study. The elastic modulus of the soil was calculated using the SPT N values obtained from the field test data. Eq. (1), introduced by Yoshida and Yoshinaka (1972), was used to calculate the elastic modulus using the SPT N data. E_b is the modulus of deformation and N is the standard penetration resistance. The values obtained from the equation were multiplied by two before being used for modeling work.

$$E_b = 6.78\,N^{0.998} = 7N \quad (1)$$

The friction angle (Ø) was calculated using Eq. (2) extracted from Japanese Railway Standards, which uses the standard penetration resistance for a drill with a standard energy ratio of 70% (N_{70}).

$$Ø = 0.45\,N_{70} + 20^0 \quad (2)$$

3.2 *Numerical Modeling*

PLAXIS 2D finite element software was used in this study. Two-dimensional plane strain triangular mesh elements consisting of fifteen displacement nodes were used to analyze the structure. The boundaries were established twice the maximum excavation depth away from the secant pile wall, and a 25 m thick soil body mesh was used to represent the total thickness of the soil layers. Movements in all directions were restricted at the bottom boundary, and vertical movements were enabled at both vertical boundaries of the model. Soil properties were assigned for soil layers according to the borehole data. The excavation area mainly consists of sandy soil. Therefore, an effective stress drained analysis was performed. The idealized soil properties based on field test data for borehole one is presented in Fig. 4.

Soil		1 Clayey sand (SPT N = 6)	2 Clayey Sand (SPT N = 26)	3 Silty clayey sand (SPT N = 34)	4 Clayey sand (SPT N = 50)	5 Fine sand (SPT N = 15)	6 HWR (SPT N = 8)
Depth (m)		0.0 to -2.5	-2.5 to −3.5	-3.5 to -7.5	-7.5 to -10.0	-10.0 to -13.2	-13.2 to -15.5
Material Model		Mohr-Coulomb	Mohr-Coulomb	Mohr-Coulomb	Mohr-Coulomb	Mohr-Coulomb	Mohr-Coulomb
γ_{unsat}	[kN/m³]	16.00	20.00	20.00	21.00	17.00	16.00
γ_{sat}	[kN/m³]	17.00	21.00	21.00	22.00	18.00	17.00
k_x	[m/s]	10^{-6}	10^{-6}	10^{-6}	10^{-6}	10^{-4}	10^{-6}
k_y	[m/s]	10^{-6}	10^{-6}	10^{-6}	10^{-6}	10^{-4}	10^{-6}
E_{ref}	[kN/m²]	12000	40000	50000	70000	22000	14000
ν	[-]	0.350	0.300	0.300	0.250	0.300	0.350
c_{ref}	[kN/m²]	3.00	8.00	8.00	10.00	0.00	3.00
φ	[°]	24.00	30.00	32.00	38.00	28.00	25.00
ψ	[°]	0.00	0.00	2.00	8.00	0.00	0.00
$R_{inter.}$	-	0.67	0.67	0.67	0.67	0.67	0.67

Fig. 4 Soil properties of Borehole 1

One-dimensional fixed-end anchor elements were used as struts in the support system. Plate elements with a uniform thickness were used to model the secant pile wall. Young's modulus and Poisson's ratio of the wall were set as 31 GPa and 0.2, respectively. Different surcharge values were used depending on the buildings available on the surrounding ground surface. The medium mesh distribution was selected for the analysis as recommended by Likitlersuang et al. (2013). The mesh was refined near the retaining wall to increase the accuracy of the results.

4 RESULTS AND DISCUSSION

4.1 *Effect of the elastic modulus of soil on the lateral deformation of the wall*

One of the main objectives of this study is to perform a parametric study to increase the elastic modulus of soil used in deep excavation work. The back analysis technique was used to calibrate the elastic modulus of the soil. The M-74, M-66, M-33, and M-51 inclinometer measurements were considered to minimize the corner effect and maintain the plane strain behavior for greater accuracy. Figs. 5 and 6 present the lateral wall deformation profile obtained from the M-66 inclinometer readings compared with the wall deformation profiles obtained from the numerical analysis for different integer multipliers of the elastic modulus of the soil.

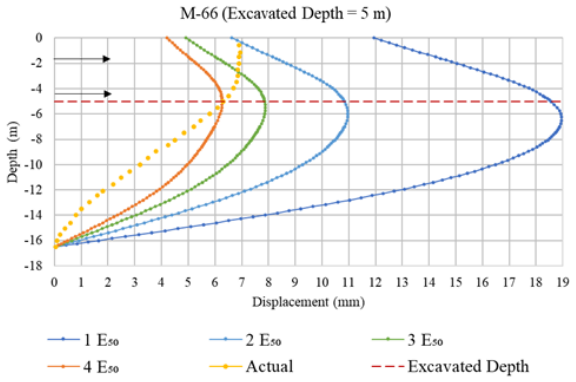

Fig. 5 Comparison of lateral wall deformation at 5 m excavation depth

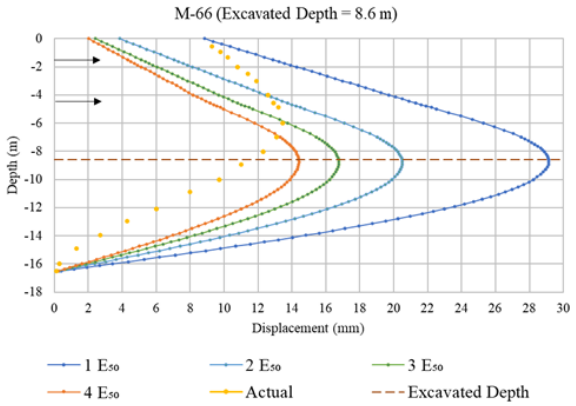

Fig. 6 Comparison of lateral wall deformation at 8.6 m excavation depth

The results indicate that the maximum wall deformation obtained from the inclinometer readings was between the deformation profiles obtained for 2 and 4 times the elastic modulus of the soil at a 5 m excavation depth (Fig. 5). It has been increased to a higher multiple of the elastic modulus of soil with the increase in excavation depth up to 8.6 m (Fig. 6). A similar behavior was also observed for the readings of the M-74 inclinometer. In both cases, it can be observed that the maximum deflection point has been fitted between higher integer multipliers with the increase in the depth of excavation. According to the literature, the plane strain behavior reduces with increasing excavation depth, where the three-dimensional corner effect reduces the wall deformation from the plane strain behavior. Although the selected inclinometers are located a certain distance from the corner, the lateral deformation of the actual wall underestimates the results obtained from the numerical analysis with increasing excavation depth.

Furthermore, model validation was performed using field monitoring data. After calibrating the model using the back analysis technique, the maximum deflection point of the actual behavior was found between the deformation profiles of 2 to 4 times the elastic modulus of the soil at a depth of excavation of 5 m. The maximum deformation of the actual wall is about 40% of the maximum deformation of the profile obtained from the numerical analysis using the elastic modulus as soil stiffness. This reduction narrows to 35% when 2 E_{50} is used as soil stiffness.

4.2 *Evaluation of prop forces using numerical and empirical methods*

Prop forces were evaluated using numerical analysis for different excavation depths to compare with different empirical methods for validation. Table 2 presents the prop forces obtained from the numerical analysis compared to the Terzaghi & Peck and DPL methods, considering soil as sand and clay separately. Strut levels 1, 2, and 3 are located at elevations of -1.5 m, -4.575 m, and -7.9 m, respectively, from the ground level.

Table 2. Comparison of Prop Forces

Stage	Strut Level	Finite Element Analysis	Peck Method (Sand)	Peck Method (Clay)	DPL Method (Sand)	DPL Method (Clay)
		(kN/m)	(kN)	(kN)	(kN)	(kN)
Stage 5	1	101.77	118.15	119.73	88.16	220.4
Stage 6	1	58.05	148.75	150.8	132.15	330.32
	2	325.79	215.54	318.07	233.96	396.61
Stage 8	1	33.74	164.01	162.04	156.77	391.95
	2	360.89	205.55	330.38	241.63	412.58
	3	308.84	268.73	430.22	260.96	384.21

The prop forces obtained from both methods for sandy soil had higher values for the uppermost strut level and lower prop forces for the second and third strut levels at all stages of excavation. A similar behavior was observed by Chee (2014). One of the critical observations in that study was that the lateral earth pressure of the sand exceeds the pressure obtained from the empirical calculations at higher depths. When the earth pressure of the soil obtained from the numerical analysis exceeds the values obtained from the empirical calculations, the prop forces increase in the numerical analysis, since they directly influence the forces acting on the support system. The results obtained for clay soil from both Peck and DPL methods provide results closer to the FE analysis than those obtained for sandy soil for lower strut levels. The DPL method for clay soil provides the highest prop forces out of all.

4.3 *Evaluation of lateral earth pressure distribution using numerical and empirical methods*

In addition to calculating the prop forces, the lateral earth pressure distribution was observed along the wall to verify the values obtained in Section 4.2. Fig. 7 compares the earth pressure distributions obtained from the numerical analysis with the empirical equations used to calculate the strut forces in Section 4.2.

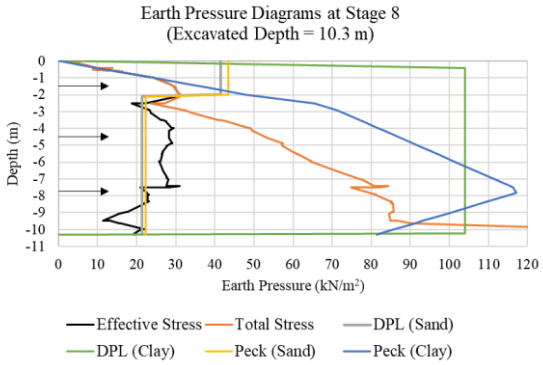

Fig. 7 Comparison of lateral earth pressure distributions

The DPL method considering clay soil provides the highest soil earth pressure, creating the most conservative earth pressure diagram, resulting in the highest prop forces in Section 4.2. In both Peck and DPL methods, assuming sandy soil led to a reduced earth pressure distribution below the groundwater level due to the replacement of submerged unit weight with unsaturated unit weight. The effective earth pressure diagram obtained from the FE analysis did not show any significant reduction below groundwater level. FE analysis presents a higher effective earth pressure distribution below the groundwater table than the values obtained from the Peck and DPL methods considering sandy soil. As

a result, lower prop force values were obtained for the second and third prop levels from Peck and DPL methods considering sandy soil compared to the FE analysis.

4.4 *Effect of soil stiffness on the bending moment envelope*

One of the key objectives of this study is to carry out a parametric investigation to evaluate the reduction in bending moments that act on the retaining structure due to the enhancement of soil stiffness used in deep excavation analysis. The E_{50} of the soil was observed to increase by 2 – 4 times to obtain the E_{ur} of the soil to have an accurate wall behavior with respect to the actual conditions. With increasing stiffness, the retaining structure experiences reduced bending moments. Using numerical modeling, the percentage of reduction in the bending moment with the increase in soil stiffness was evaluated at different excavation depths. They were compared with the bending moment envelopes obtained from different empirical methods used earlier (Figures 8,9 and 10). The arrows signify the respective props levels.

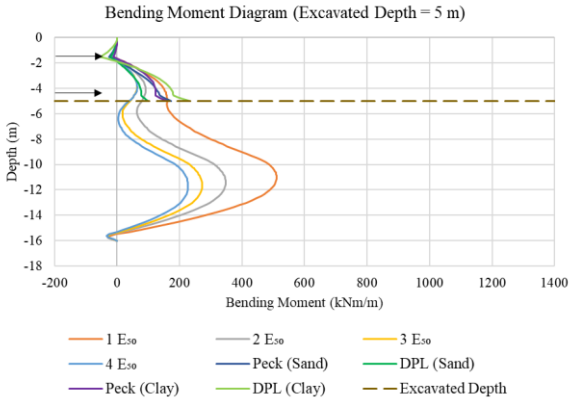

Fig. 8 Comparison of bending moment envelopes at 5 m excavation depth

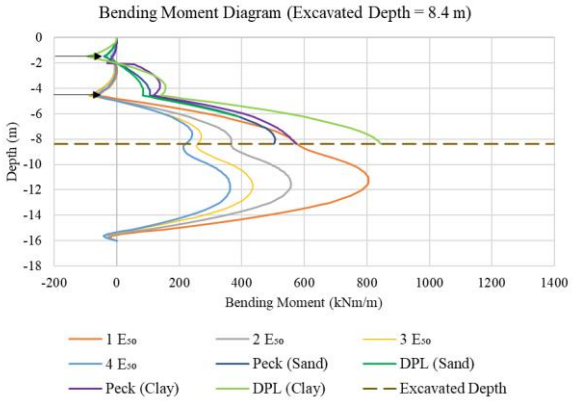

Fig. 9 Comparison of bending moment envelopes at 5 m excavation depth

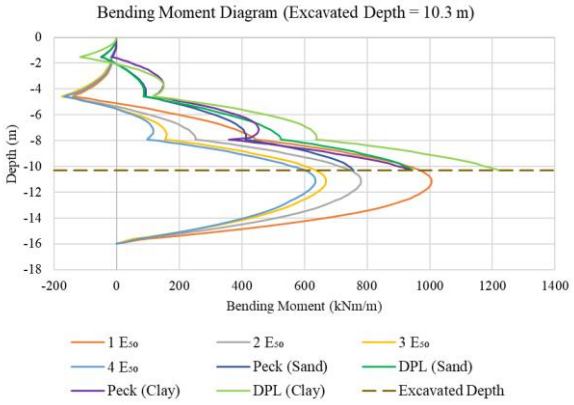

Fig. 10 Comparison of bending moment envelopes at 5 m excavation depth

The bending envelopes obtained using various empirical methods for all three excavation depths follow the same pattern obtained using numerical analysis. The deviation between the bending moment envelopes increases with increasing excavation depth. The bending moment envelope obtained from the DPL method considering clay soil has the highest bending moment values, providing the most conservative design with the highest reinforcement requirement. The highest lateral earth pressure distribution obtained during the earth pressure comparison led to the highest bending moments at all three stages.

A significant deviation was observed between the profiles at all three stages when comparing the bending moment envelopes obtained for different soil stiffness values. The largest deviation was observed between the E_{50} and $2E_{50}$ bending envelopes. The deviation of bending moment envelopes between two adjacent multipliers of the elastic modulus decreases as the value of the elastic modulus increases. The percentage reduction in bending between the $4E_{50}$ and E_{50} envelopes decreases with increasing excavation depth. A conservative approach was taken using the 10.3 m excavation graph for the analysis. Compared to the maximum bending moment obtained for E_{50}, there is a reduction of 40% in the maximum bending moment for the $4E_{50}$ envelope at the excavation depth of 10.3 m. When comparing the maximum bending moment obtained for E_{50}, there is a reduction of 20% in the maximum bending moment for $2E_{50}$ at the same depth.

5 CONCLUSION

The elastic modulus (E_{50}) values derived from the SPT N data can be multiplied by 2 to 4 times to obtain the unloading-reloading modulus (E_{ur}) value that would reasonably predict the wall movement in the FE analysis. As the depth of excavation increases, the lateral deformation

was underestimated mainly due to the impact of the corner effects. Considering sandy soil, both Peck and DPL methods produced higher prop force values for the first prop level, while the second and third prop levels had lower values than the numerical analysis results. The lower earth pressure distribution obtained from the DPL and Peck methods compared to the earth pressure distribution of the FE analysis caused this result.

A significant deviation was observed between the bending moment profiles at all three stages when the elastic modulus of the soil increased with different integer multiples. The deviation between the two adjacent multipliers of the elastic modulus decreases as the value of the elastic modulus increases. The DPL method for clay soil provides the highest bending moment envelope at all excavation stages compared to other methods. All other methods yield bending moment envelopes closer to the envelope obtained by assigning the E_{50} value in the numerical analysis. The maximum bending moment can be reduced from 20% to 40% by increasing soil stiffness between $2E_{50}$ and $4E_{50}$. This study suggests that the reinforcement requirement for flexure can be reduced in proportion to the reduction in the maximum bending moment.

ACKNOWLEDGMENTS

Special thanks to the Department of Civil Engineering at the University of Moratuwa and to the International Construction Consortium (Pvt) Ltd project team that worked on the Los Angeles Medical Center Hospital project for the continuous support of the research.

REFERENCES

ArcelorMittal Commercial RPS. (2016). *Piling Handbook* (9th ed.). Imprimerie Centrale.

Bentley Systems. (2020). *PLAXIS 2D - Material Models Manual*.

Calvello, M., & Finno, R. J. (2004). Selecting parameters to optimize in model calibration by inverse analysis. *Computers and Geotechnics*, *31*(5), 410–424. https://doi.org/10.1016/j.compgeo.2004.03.004

Chee, B. J. S. (2014). *Analysis of strut forces for braced excavations in sand* (Issue May 2023). http://hdl.handle.net/10356/60052

Coulomb, C. A. (1776). Essai Sur Une Application Des Maximis et Minimis a Queques problems Des Statique Relatifsa1‟ Architecture. *Nem. Div. Sav. Acad, Sci*, *7*.

Duc, T. N., Vo, P., & Thi, T. T. (2020). Determination of unloading—reloading modulus and exponent parameters (m) for hardening soil model of soft soil in ho chi minh city. *Proceedings of the International Conference on Sustainable Civil Engineering and Architecture 2019*, *80*(January), 677–689. https://doi.org/10.1007/978-981-15-5144-4_65

Hou, Y. M., Wang, J. H., & Zhang, L. L. (2009). Finite-element modeling of a complex deep excavation in Shanghai. *Acta Geotechnica*, *4*(1), 7–16. https://doi.org/10.1007/s11440-008-0062-3

Hsiung, B.-C. B. (2009). A case study on the behaviour of a deep excavation in sand. *Computers and Geotechnics*, *36*(4), 665–675. https://doi.org/10.1016/j.compgeo.2008.10.003

Hsiung, B.-C., Yang, K.-H., Aila, W., & Hung, C. (2016). Three-dimensional effects of a deep excavation on wall deflections in loose to medium dense sands. *Computers and Geotechnics*, *80*, 138–151. https://doi.org/10.1016/j.compgeo.2016.07.001

Likitlersuang, S., Surarak, C., Wanatowski, D., Oh, E., & Balasubramaniam, A. (2013). Finite element analysis of a deep excavation: A case study from the Bangkok MRT. *Soils and Foundations*, *53*(5), 756–773. https://doi.org/10.1016/j.sandf.2013.08.013

Nguyen, V., & Luu, C. (2013). Influence of unloading soil modulus on horizontal deformation of diaphragm wall. *Proceeding of International Symposium on New Technologies for Urban Safety of Mega Cities in Asia*, *October*, 1247–1255.

Ramadan, M. I., & Meguid, M. (2020). Behavior of cantilever secant pile wall supporting excavation in sandy soil considering pile-pile interaction. *Arabian Journal of Geosciences*, *13*(12). https://doi.org/10.1007/s12517-020-05483-8

Rankine, W. J. M. (1857). II. On the stability of loose earth. *Philosophical Transactions of the Royal Society of London*, *147*, 9–27.

Terzaghi, K., & Peck, R. B. (1967). Soil mechanics in engineering practice (2nd edition). In *John Wiley & Sons, Inc* (Second Edi). John Wiley & Sons. https://books.google.lk/books?id=AnbHzgEACAAJ

Twine, D., & Roscoe, H. (1999). *Temporary propping of deep excavations-guidance on design, C517*. Construction Industry Research and Information Association. https://doi.org/https://doi.org/10.1680/geot.10.P.072

Yoshida, I., & Yoshinaka, R. (1972). A Method to Estimate Modulus of Horizontal Subgrade Reaction For a Pile. *Soils and Foundations*, *12*(3), 1–17. https://doi.org/https://doi.org/10.3208/sandf1972.12.3_1

Influence of Gradation on Shear Behavior of Railway Ballast Material

M. Amalan, R. Tharmarajah and S. K. Navaratnarajah
Department of Civil Engineering, University of Peradeniya, Sri Lanka

ABSTRACT: The ballast layer in railway track infrastructure undergoes deformation and degradation from moving train loads and environmental changes. To enhance track performance and cut maintenance costs, it is imperative to study ballast shear behavior and degradation under diverse loading conditions. This study investigates the influence of gradation on the shear behavior of railway ballast materials. The research methodology involves laboratory testing of ballast samples with different gradations. Shear strength parameters are determined using Large-scale direct shear tests. The study uses three gradations of particle size distributions commonly found around and within the Indian upper and lower limit gradation standard. Furthermore, a numerical model was developed to study the influence of ballast gradation and investigate the influence of vertical stress by carrying out a parametric study with different normal stresses.

KEY WORDS: Ballast, Gradation, Shear strength, Breakage, DEM

1 INTRODUCTION

The ballast layer, the largest component in the track system, transfers loads from sleepers to the underlying layers and provides rapid drainage. Over time, ballast materials break and become fouled, affecting track performance and longevity. The shear strength of the ballast provides lateral confinement and resistance to maintain the geometry of the track structure. The shear behavior of ballast varies with different factors. Ballast gradation is one such factor that affects shear strength. The particle size distribution of ballast is not the same for all countries. It varies considering the subgrade properties, load application, climate, the strength of the parent rock, etc. Gradations are selected mainly by considering the strength and drainage properties of the ballast layer. Researchers studied the shear behavior of the ballast by conducting large-scale direct shear tests and triaxial tests. In Sri Lanka, ballast particle sizes ranging from 19 to 63 mm are used in rail tracks. There is no unique gradation used in Sri Lankan tracks rather Indian ballast gradation is used. Therefore, this study mainly focuses on understanding the effect of different gradations on the shear behavior of the ballast used in the rail tracks in Sri Lanka.

2 LITERATURE REVIEW

The shear behavior of railway track ballast plays a critical role in ensuring the stability and performance of tracks, impacting safety and operational efficiency (Indraratna, 2016). Key factors affecting shear behavior include particle size distribution, angularity, compaction, moisture content, and confining pressure (Danesh et al., 2018). The particle size distribution (PSD), void ratio, and degree of saturation are intricately tied to ballast behavior (Indraratna et al., 2005). The ideal gradation should balance drainage benefits with higher strength and reduced settlement, as suggested by Guo et al. (2022). The uniformity coefficient (Cu) is crucial, with larger values associated with higher shear strength. Global ballast specifications vary with different countries adopting various crushed rock particles based on quality and availability (Anbazhagan et al., 2012). Degradation can lead to the accumulation of fines, reducing drainage, causing water retention and track settlement (Danesh et al., 2018). In terms of shear resistance breakage indices, such as the ballast breakage index (BBI), indicate increased breakage under higher stress (Venuja et al., 2023).

While many studies stress the importance of factors like ballast gradation, shear behavior, and degradation in railway tracks, Sri Lanka lacks specific standards for ballast gradation, and there haven't been many studies on how different gradations affect shear behavior. Our research aims to explore the impact of different ballast gradations on the shear behavior of ballast used in Sri Lanka. This study specifically focuses on conducting large-scale direct tests with three different ballast gradations to suit the unique conditions of the Sri Lankan railway system.

3 METHODOLOGY

3.1 *Laboratory test using large-scale direct shear tests*

In this study, ballast material was collected from Ambepussa quarry. Property tests were conducted according to the accepted standards. Then the ballast was washed, dried, and sieved using 19, 25, 37.5, 50, and 63 mm sieves to separate particles into required size ranges for the direct shear test. The main aim of this study is to analyze the effect of gradation on the shear behavior of railway ballast. For that, three gradations were chosen considering Indian gradation limits as shown in Fig. 1. Indian gradation limits are considered in this study as it is adopted in Sri Lankan rail tracks. Here PSD A1 is in between the upper and lower limits of Indian standards which is normally adopted in Sri Lankan rail tracks. PSD A2 is obtained by increasing the percentage of particles between 19 - 37.5 mm size ranges, beyond the upper limit. On the other hand, PSD A3 is obtained by increasing the percentage of particles between 37.5 - 63 mm size ranges.

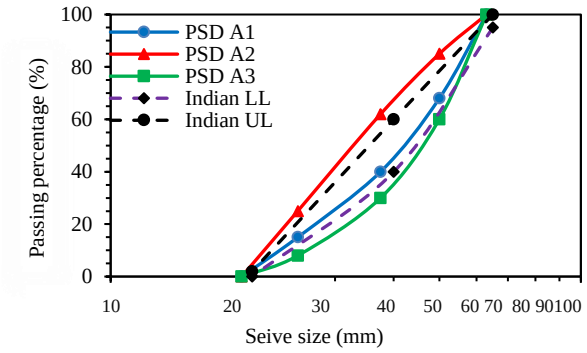

Fig. 1 Different Particle Size Distribution

Test specimen was prepared based on the gradation, which was selected for the test. According to the required density of 1550 kg/m³ and the volume of the apparatus, required mass of ballast was calculated. Then according to the selected gradation, inclusion of particle size range was considered. Particles were filled into the apparatus in three layers. Before filling, particles were colored (different colors for three layers as shown in Fig. 2) and numbered (different numbers for different size ranges) to identify the breakage easily. With different colors, it could be easy to identify at which layer maximum breakage occurs, and with the numbers, it can be identified which size range particles are broken.

Fig. 2 Colored particles for three layers

Particles were filled into the large-scale direct shear test apparatus in three layers. Each layer was compacted manually using a rubber-padded vibratory hammer to obtain field density. Fig. 3 shows the large-scale direct shear test apparatus used for the experiment. Three different normal stresses were selected as 30 kPa, 60 kPa and 90 kPa. Constant horizontal shear was applied manually using hydraulic jack as 4 mm/min in the bottom cylinder.

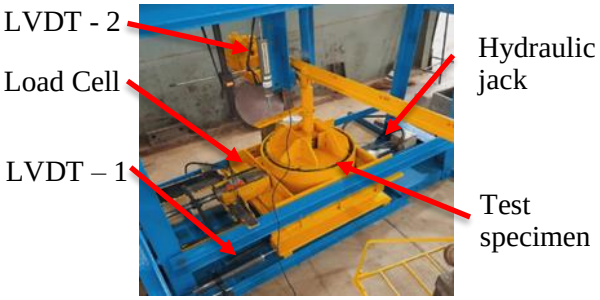

Fig. 3 Large-scale direct shear test apparatus

Firstly, three different gradations were tested for one common normal stress, 60 kPa. Then PSD 1 and PSD 3 gradations were tested for 90 kPa normal stress. All tests were done until 15% shear strain ballast reach.

3.2 *Numerical model using DEM*

Discrete Element Method (DEM) is one of the leading approaches in numerical analysis. Since ballast particles are discrete granular angular particles, DEM was chosen for this study. Particle shape is one of the key factors, which decides the mechanical behavior of ballast particles, real ballast particles were scanned in 3D using a scanning device and imported as multi-sphere clump particles to the DEM software (EDEM). Then the particles were generated according to the selected gradation. The following Fig. 4 illustrates the modelled experimental setup with generated particles.

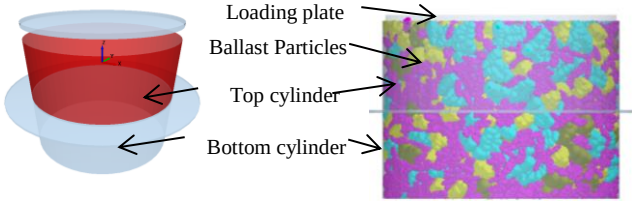

Fig. 4 DEM model of shear test

4 RESULTS AND DISCUSSIONS

4.1 *Experimental results*

Shear stress and strain were calculated using the shear load and horizontal displacement data obtained from the data logger. Fig. 5 shows the shear stress and vertical strain variation for different PSDs for 60 kPa normal stress. As expected, inclusion of larger size particles shows some significant effect in shear behavior. Shear increased with inclusion of larger-sized particles. In contrast, dilation decreased due to void increasing with inclusion of large-size particles.

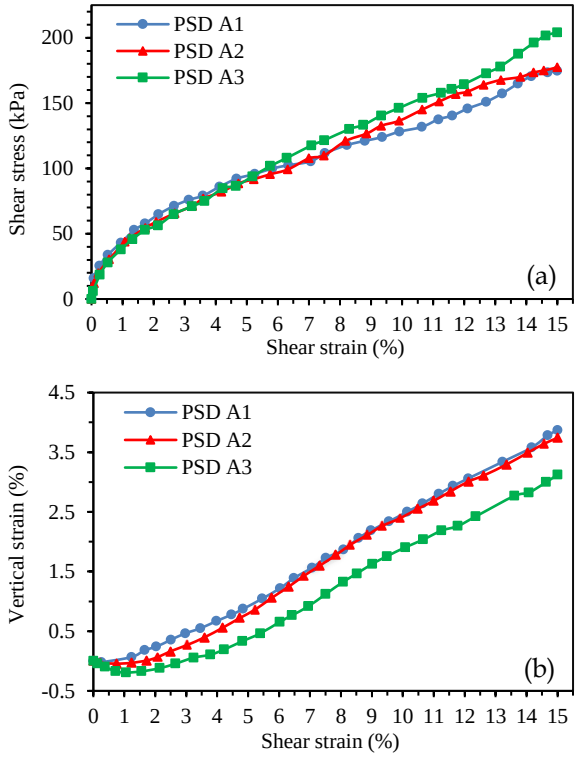

Fig. 5 (a) Shear stress and (b) vertical strain variation with shear strain for 60 kPa normal stress

Then the normal stress was increased to 90 kPa and test was done for PSD A1. As expected, shear stress was increased with normal stress as shown in the Fig. 6.

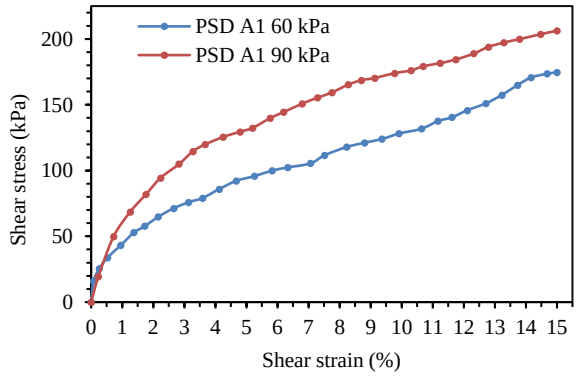

Fig. 6 Shear stress variation with shear strain

Results obtained for the Ambepussa (A) material were compared with the results obtained for the ballast collected from Gampola (G) (Venuja et al., 2022). The Ambepussa ballast showed higher shear resistance than the Gampola ballast particles. Fig. 7 shows the comparison of the results.

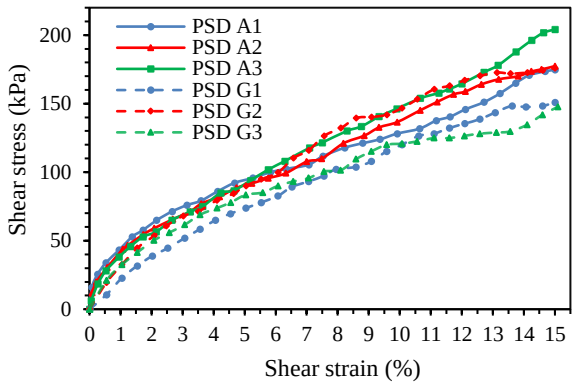

Fig. 7 Shear stress vs shear strain for different gradations under 60 kPa normal stress

Breakage was analyzed using BBI method (Indraratna et al., 2005). Comparatively higher breakage occurred in middle layer, because of shear was applied in the middle layer. Considerable breakage was observed in the top layer, because normal stress was applied in top layer zone. As expected, inclusion of larger particles decreased the breakage. Fig. 8 shows the breakage results for different gradations.

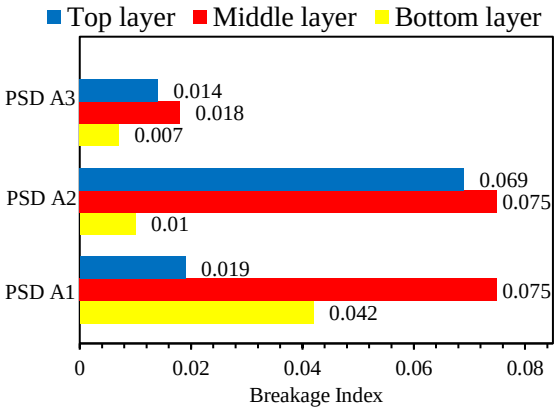

Fig. 8 Breakage results under 60 kPa normal stress

4.2 *Numerical analysis results*

PSD A1 with 60kPa normal shear stress results was used to calibrate the numerical model. Using these calibrated coefficients, the same model was run for the other two gradations. Numerical results were obtained and compared with experimental results as shown in Fig.9. An acceptable agreement was observed in this comparison. Then the normal stress

had been changed to 30 kPa and 90 kPa and simulation was done for PSD A1. Fig.10 shows the obtained results.

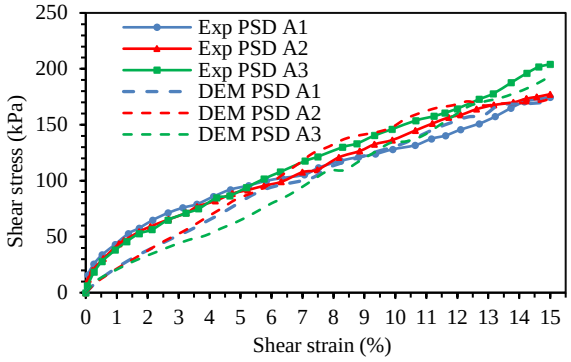

Fig. 9 Comparison of shear stress vs shear strain results of both experiment and numerical analysis under 60 kPa normal stress

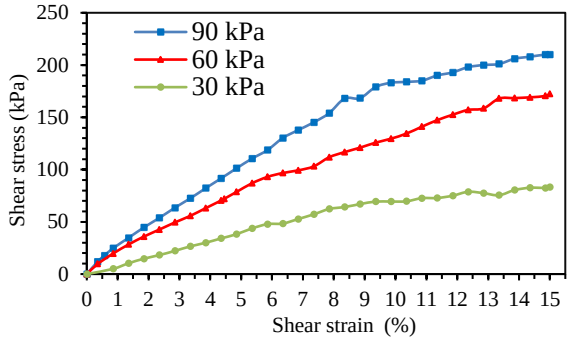

Fig. 10 Comparison of shear stress vs shear strain for PSD A1

5 CONCLUSION

This research elaborates on the effect of particle size distribution on the shear behavior of ballast. For that, three different gradations were chosen, and large-scale direct shear tests were conducted. In addition to this, numerical simulation using DEM was carried out. Shear stress increased with increasing normal stress. In contrast, dilation is reduced due to the high compaction of materials. The presence of a higher number of larger particles resulted in higher shear strength. The shear behavior of the ballast changes with gradation. High shear strength was obtained for the gradation with a higher number of larger-size particles. Numerical results showed acceptable agreement with the experimental results. So, the validated model can be used to conduct parametric studies under higher normal stresses. In terms of gradation, the selected new gradation PSD A3 shows better in resisting shear and reducing ballast breakage. So, further extending the same study for the permeability behavior will guide to find a better gradation limit to use for rail track foundation.

ACKNOWLEDGMENTS

We extend our sincere gratitude to the Civil Engineering Department at the Faculty of Engineering, University of Peradeniya, for providing us with the opportunity to undertake this research project. Additionally, we are deeply thankful to the lab staff of the Geotechnical Laboratory for their invaluable support and assistance throughout this endeavor. Their guidance, expertise, and willingness to assist with experimental procedures have been instrumental in the successful completion of this project. We are truly appreciative of the resources, facilities, and encouragement extended to us, which have significantly contributed to the realization of this research.

REFERENCES

Anbazhagan, P., Bharatha, T. P., & Amarajeevi, G. (2012). Study of Ballast Fouling in Railway Track Formations. In dian Geotechnical Journal, 42(2), 87–99. Doi: 10.1007/s40098-012-0006-6

Danesh, A., Palassi, M., & Mirghasemi, A. A. (2018). Effect of sand and clay fouling on the shear strength of railway ballast for different ballast gradations. Granular Matter, 20(3). doi:10.1007/s10035-018-0824-z

Guo, Y., Marikine, V., & Jing, G. (2022). Railway ballast. In Elsevier eBooks (pp. 295–317).

Indraratna, B., Sun, Y., & Nimbalkar, S. (2016). Laboratory As sessment of the Role of Particle Size Distribution on the De formation and Degradation of Ballast under Cyclic Loading. Journal of Geotechnical and Geoenvironmental Engineer ing, 142(7), 04016016. doi: 10.1061/(asce)gt.1943-5606.0001463

Indraratna B, Lackenby J, Christie D (2005) Effect of confining pressure on the degradation of ballast under cyclic loading. Geotechnique 55(4):325–328

Venuja, S., Navaratnarajah, S.K., Bandara, C.S., Jayasinghe, J.A.S.C. (2023). Experimental and Numerical Study on the Shear-Strain Behavior of Ballast with Different Gradations. In: Dissanayake, R., et al. ICSBE 2022. ICSBE 2022. Lec ture Notes in Civil Engineering, vol 362. Springer, Singa pore. https://doi.org/10.1007/978-981-99-3471-3_18

Improvement of Gravel roads against Erosion caused by heavy rain

Kishok P.P. J and N.H. Priyankara

Department of Civil and Environmental Engineering, University of Ruhuna, Galle, Sri Lanka

ABSTRACT: In Sri Lanka, where more than 50% of the roads are unpaved, this research focuses on the critical issue of erosion and the poor condition of unpaved gravel roads, which provide problems with transportation during rainy seasons and environmental hazards during dry periods. The primary goal is to use waste products from the sugar industry to minimize erosion and improve gravel road engineering. This study has the potential to lower accident rates, minimize the impact on the environment, and support rural development. Especially in low-traffic areas, gravel roads are a more affordable option than expensive asphalt roads. The byproducts of sugar cane, especially 5% spent wash and 2% bagasse ash, show potential as additions that improve the characteristics of roads. Field investigations show that erosion primarily affects the sides of the road while the middle of the road is stable and maintains road usage.

KEY WORDS: Unpaved roads, Erosion, Bagasse ash, Spent-wash, Engineering properties

1 INTRODUCTION

1.1 *Background*

With more than 50% of its roads still being unpaved, unpaved gravel roads are a common but challenging aspect of Sri Lanka's transportation system. In addition to creating substantial mobility concerns, these roads also contribute to environmental problems including dust pollution and erosion (*National Highways*, 2020).

Due to poor maintenance, gravel roads are very difficult to use, especially when it rains and they become muddy, slippery, and rough. Excessive dust on gravel roads during the dry season affects travel and may be harmful to the health of local residents as well as drivers and other road users. This makes it very evident that ongoing maintenance is necessary to keep the road in good condition. Due to financial limitations, the majority of Sri Lanka's gravel roads are not well maintained, and as a result, after the rainy season, they are not in a usable condition.

1.2 *Aim*

the Aim of this research is to control the erosion of the gravel roads using byproducts of sugar industries to increase road accessibility, lower maintenance costs, and support rural development.

1.3 *The Objectives*

The Objectives of the research study are to estimate the deformation characteristics of gravel roads under climatic variation and to improve the Engineering characteristics of the base material of gravel roads using sugar cane byproducts.

1.4 *Measuring erosion*

Measuring erosion is a crucial aspect of understanding and addressing these challenges. A study by the University of Koblenz-Landau employed a rain simulator to measure erosion on unpaved roads, shedding light on erosion processes (Zemke, 2016). Additionally, research conducted at Ben Gurion University in Israel utilized a clay-based geopolymer to strengthen soil and mitigate soil erosion, offering valuable insights into erosion control techniques (Hanegbi & Katra, 2020). Furthermore, A study at the University of Technology Sydney in Ultimo, NSW, Australia, conducted field monitoring of unpaved road erosion, providing essential data for understanding the real-world behavior of such roads (Pardeshi et al., 2020).

A comprehensive approach was used in the research methodology to solve the problem of erosion on gravel roads. Three main works were involved in this study; Field monitoring the Deformation of the Gravel road, Laboratory Tests for Improve the Base Material of the Gravel Road and Erosion Test using a Rainfall Simulator

2.1. Field monitoring

The work begins with field monitoring. The objective of this approach was to understand how erosion affects gravel roads throughout time. It required precise measurements of the actual changes to the geometry of the road. the Buruduwalaga road in the Monaragala district was selected for this monitoring process because it was relatively new

and had less erosion. Leveling was done three times over the span of a three-month period from march 2023 to June 2023 to make a reliable monitoring process.

With the PRDA's help, field monitoring began underway in the Monaragala District on March 22, 2023. Nails and bottle lids were used to mark points throughout the road's cross section at 20-meter intervals. Initial heights were measured using a leveling machine, and a nearby bridge served as the benchmark. There were more monitoring sessions on May 7 and June 13. Point identification, level measurement, and data recording were all consistent operations. These measures offer essential information on the characteristics and deformation of the gravel road under various climatic situations, enabling erosion assessment by comparing reduced levels over time.

1.5 *Laboratory Testing*

Laboratory tests on the gravel road's base material were done after field monitoring. These tests provided an essential source of fundamental data by determining the material's Engineering properties. The Table 1 shows the laboratory tests that were conducted under this methodology and the Physical and Engineering Parameters obtained.

Table 1 Conducted laboratory tests and the parameters

Laboratory Tests	**Physical and Engineering Parameters**
Sieve analysis	Particle Size Distribution
Atterberg limit tests	Liquid limit (LL) Plastic limit (PL) Plasticity Index (PI)
Standard Proctor Compaction test	Optimum moisture content (OMC) Maximum dry density
Pycnometer test	The specific gravity
The California Bearing Ratio (CBR) test – 4 days soaked	CBR Value
Moisture content test	Natural moisture content Saturated moisture content
Direct shear test	Shear strength parameters

From the different sub base samples, the sample from the Waththegama (G3) was selected to do further the mixing process with Bagasse ash. That G3 sample was selected due to high availability of the sample compare to the other samples. Then Bagasse ash, a byproduct of the sugar industry, was added to the samples in order to improve the engineering properties of the basic material. The base material was combined with several weight proportions of Bagasse ash, and laboratory tests were repeated to determine which mix produced the best results.

The research added Spent wash to the previously determined best mixture, building on improvements made with Bagasse ash. Another set of laboratory study were done to determine the optimum proportion of Bagasse ash and Spent wash to effectively resist erosion. Different weight percentages of spent wash were applied.

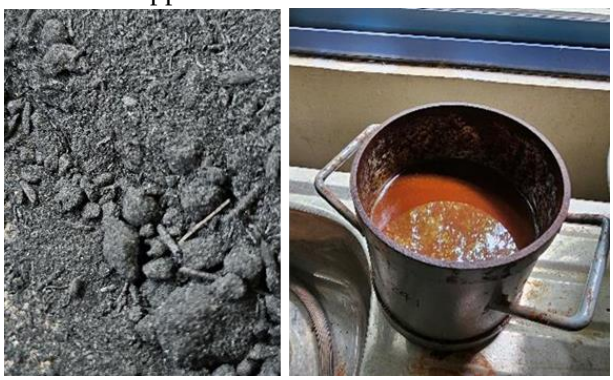

Fig. 1 Bagasse ash and Spent wash

1.6 *Erosion Test*

For the erosion test, two samples were created: the first used simply Waththegama soil under the optimal conditions, while the second used the selected mix of 2% Bagasse ash and 5% Spent wash. Both samples were put into a mold with dimensions 500 x 500 x 150 mm in size, with three layers of compaction. Factors such as slope, compaction, and the intensity of rainfall can significantly impact the rate of erosion (Odi Enyegue et al., 2021), (Cao et al., 2015). Therefore, these factors were kept constant for both samples. After a 24-hour period of air drying, an erosion test was performed with runoff water and eroded material collected in a bucket. The erosion test was conducted under a 180 mm/hr rainfall intensity. After an hour-long test, eroding particles were sorted using wet sieving, allowed to oven dry for 24 hours, and then weighed to determine their effectiveness.

Fig. 2 Sample Preparation and the Erosion test

2 RESULTS AND DISCUSSION

2.1 *Field Monitoring results*

Field Monitoring results shows significant reductions and increments have occurred in the levels of each selected road lines. There was nearly 200mm of erosion that occurred in one side of some road line, with a nearly equal elevation increase observed in the other side of the same lines during the time period between the first two measurements. This suggests that eroded particles appear to be sliding along the slope during erosion events and the eroded particles have accumulated at the lowest elevation point. Furthermore, the data indicates that the elevation of the center point remains relatively stable throughout the monitoring period. Significant reductions and increments have occurred in the levels of each selected road lines.

The following graph analyze some heavily affected road line to understand this road's erosion.

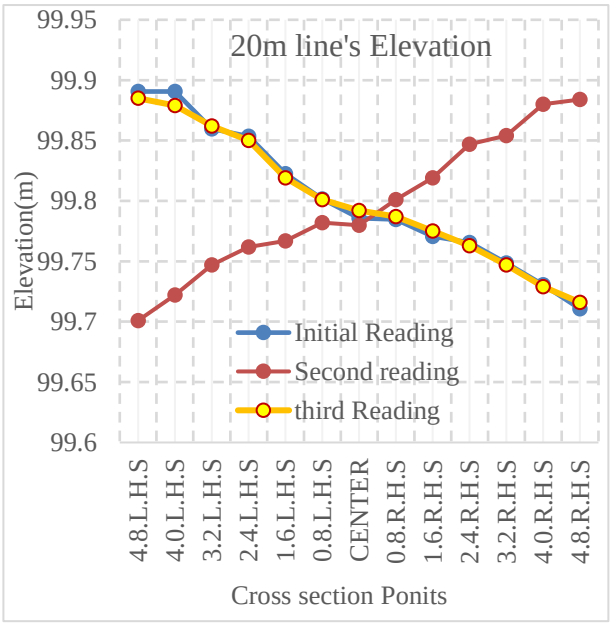

Fig. 3 Reduced levels of the of the 20m Road line throughout the monitoring period

2.2 *Basic Engineering Properties of the materials*

The basic properties of the subbase (Waththegama) and Subgrade materials are shown below.

Table 2 Summary of the basic properties of samples

Test	**Parameters**	**Subbase Materiel**	**Sub-grade Materiel**
Atterberg	Liquid Limit (%)	35	-
	Plastic Limit (%)	14	-
	Plasticity index (%)	21	-
Standard Proctor Compaction	Maximum dry unit weight (kN/m3)	18.5	18.5
	Optimum moisture content (%)	9.7	9.8
Particle Size Distribution	Cu	6.25	20.83
	Cc	1.12	1.20
	Gravel %	18.00	11.50
	Sand %	80.45	64.71
	fine %	1.55	23.79
	Classification	SW	SM
Specific Gravity test	Specific Gravity G. S	2.65	2.64
California Bearing Ratio	CBR (%)	12.65	17.5
Shear strength Parameters	Cohesion (kPa)	20.14	0
	Friction Angle	39.4	41.89

2.3 *Mixing Progress results*

Table 3 Summary of the Bagasse ash Mix Results

Parameters	**W % of Bagasse ash**				
	0%	**2%**	**5%**	**10%**	**15%**
Liquid Limit (%)	34	35	40	51	52
Plastic Limit (%)	27	26	31	39	41
Plasticity index (%)	7	9	10	12	11
Maximum dry unit weight (kN/m3)	18.5	18.13	17.4	17.16	16.88
Optimum moisture content (%)	9.7	10.1	12.4	15.3	15.7
Cohesion (kPa)	20.1	13.16	15.73	11.29	10.34
Friction Angle	39.4	39.5	37.5	39.93	34.83
CBR Value	12.7	12.9	4.86	6.05	14.14

When comparing the plastic limit and cohesion, it appears that the 5% bagasse ash mix is slightly better than the 2% mix. However, the 5% mix exhibits a very low CBR value. Conversely, although the 15% mix has a better CBR, it shows low maximum dry unit weight and cohesion values. Therefore, it seems that the sample containing 2% bagasse

ash demonstrates a slightly better improvement compared to other percentages.

Table 4 Summary of the Spent wash Mix Results

Parameters	**W % of Spent wash**				
	0%	**2%**	**5%**	**10%**	**15%**
Liquid Limit (%)	34.6	35	29.5	34.5	35.6
Plastic Limit (%)	25.6	31	25.6	32.2	34.9
Plasticity index (%)	9.0	4.0	3.9	2.3	0.7
Maximum dry unit weight (kN/m3)	18.13	18.2	18.12	18.16	18.1
Optimum moisture content (%)	10.1	10.8	11.2	11.4	15
Cohesion (kPa)	13.16	16.47	17.96	14.72	12.96
Friction Angle	39.5	35.68	39.0	40.81	47.49
CBR Value	12.9	12.4	14.19	10.32	

When analyzing the results, it appears that as the weight percentage of spent wash increases, the Plasticity Limit decreases, while Cohesion and CBR values increase up to 5% and then decrease. Friction angle and Maximum dry unit weight show little to no significant change. Comparing these values, it's shows that the 5% spent wash content having significant improvements in properties, particularly in CBR Value and Cohesion, which are crucial properties for the gravel road's resistance against erosion. `

2.4 *Erosion Testing*

Table 5 Erosion Test Results

Sample No.	1	2
Ingredients	Soil only	Soil with 2% Bagasse ash and 5% spent wash
Rain intensity (mm/Hr)	178	186
Eroded Mass (g)	123.2	60.2
Amount of Erosion (kg/m^2)	**0.49**	**0.24**

The mixed sample exhibits a higher resistance to erosion when compared to the soil without any mixture. Surface erosion appears similar for both samples after the erosion test. However, a greater amount of erosion occurred in the 1st sample due to the collapse of the corner of the soil sample, while the 2nd sample's corner remained stable throughout the test.

3 CONCLUSIONS AND FUTURE DIRECTIONS

3.1 *Field monitoring*

In conclusion, the Buruduwalaga gravel road field monitoring and analysis in the Monaragala district have clarified the erosion patterns and their effects on road deformation. It was clear during the three-month observation period that erosion mostly affected the corners of the road, causing significant decreases and increases in elevation levels along specific road lines. Notably, the center of the road maintained a fair amount of stability, which is good for passengers because it made for easier traveling. The eroded particles were not washed away, even with erosion depths of up to 200 mm, which was greater than the thickness of the base material of the road. Instead, they built up on the opposite side, reversing the slope's direction in the road's cross-sectional profile.

Additionally, according to the study's findings, there were no major problems like potholes or significant travel difficulties brought on by erosion during the monitoring period. Even though erosion did happen, the road's overall usability was not changed much, mostly because of the stability of the road's middle section. Overall, this research offers direction on how to deal with erosion-related issues and preserve the longevity and safety of gravel roads in the area, contributing crucial information for road maintenance and engineering activities in the Monaragala district.

3.2 *Laboratory Testing*

In conclusion, this study used sugar cane by-products, namely bagasse ash and Spent wash, to improve the engineering Properties of gravel road base materials against erosion. Following the testing of three different base material samples, Sample G3 (Waththegama) was chosen due to its greater availability and comparable qualities to the other two. In the study, the effects of bagasse ash and spent wash on a range of soil properties, such as Atterberg limits, Standard Proctor Compaction, direct shear, and California Bearing Ratio (CBR) values, were thoroughly examined. The results showed several key findings:

3.2.1 Effect of the Bagasse Ash

Different impacts were observed on soil parameters when bagasse ash was added to the gravel

sample. Liquid Limit and Plasticity Index increased together with the percentage of bagasse ash. As the ash content increased, the maximum dry unit weight decreased and the maximum moisture content increased. The greatest CBR value was observed at 15% ash concentration, but the cohesion value is low compare to 2% mix. The 5% mix have a high amount of cohesion, but really low CBR value. So, when analyzing the samples mixed with different percentages of bagasse ash based on their obtained basic properties, it appears that the sample containing 2% bagasse ash shows a slightly better improvement compared to other percentages.

3.2.2 Effect of the Spent Wash

The addition of Spent wash produced significant impacts on soil characteristics, much like bagasse ash. The Liquid Limit and Plastic Limit climbed while the Plasticity Index decreased as the percentage of spent wash increased. The Optimum moisture content increased slightly while the Maximum dry unit weight remained mostly unchanged. Cohesion initially increased up to 5% spent wash content in the Direct Shear test but afterward decreased. Up to 10% mix, the friction angle was largely constant but after 15% spent wash was added, it significantly increased. Unfortunately, the excessive moisture content prevented CBR testing for the 15% spent wash content. Comparing these values, it's shows that the 5% spent wash content having some improvements in properties.

3.2.3 Optimal Mix Proportions

The study reveals that a 5% spent wash content combined with 2% bagasse ash may provide an optimal mix for stabilizing the gravel road base material against erosion. This is because of the overall improvement in characteristics, particularly CBR values and cohesiveness as shown in the figures below.

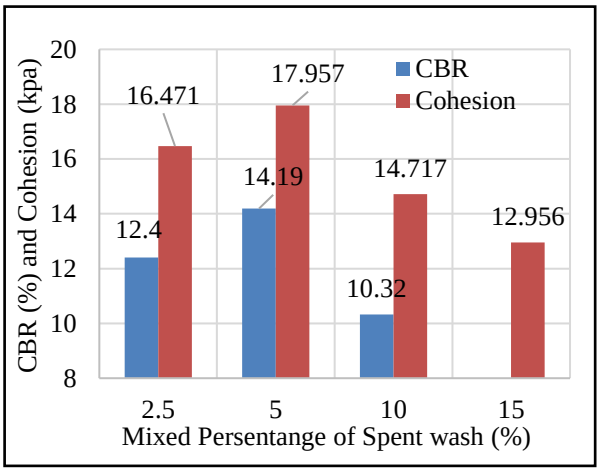

Fig. 5 CBR and Cohesion values vs weight percentage of Spent wash

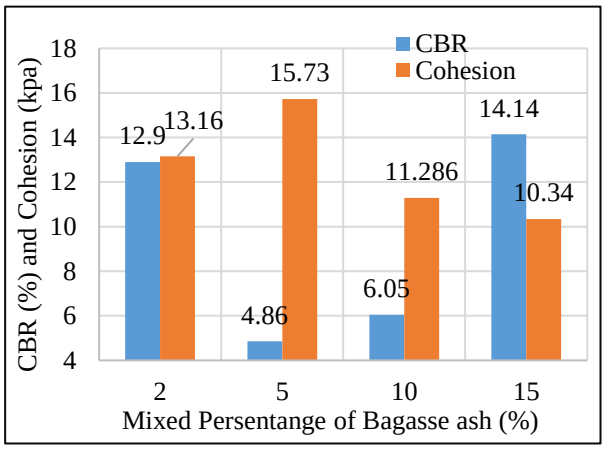

Fig. 4 CBR and Cohesion values vs weight percentage of Bagasse Ash

3.3 *Erosion Test*

Two samples were made, one using only The G03 soil (Waththegama) and the other using a mixture of 2% bagasse ash and 5% spent wash. Both samples were compacted under the optimum Conditions. These samples went through an hour of artificial rainfall at an intensity of 180 mm/hr for the erosion test. The findings of the erosion test clearly show that the soil mix has a positive impact on erosion resistance. When compared with the sample made up only of soil, the mixed sample showed a much stronger resistance to erosion. While the amount of surface erosion for the two samples seemed to be similar, the first sample had more erosion, primarily because its corner collapsed during the test.

These results show the way selected mix proportions bind soil particles, increase cohesion, and eventually strengthen the gravel road edges. This is significant in regions with a lot of rain because it indicates that this mixture might make gravel road surfaces stronger by withstanding strong rainfall even at 180 mm/hr.

3.4 *Future directions*

The report's future directions highlight the necessity of a comprehensive and continuing strategy to solve erosion-related problems with gravel road development and maintenance. The report recommends the use of waste resources like bagasse ash and spent wash in the construction of roads and makes suggestions for long-term field monitoring programs to monitor erosion patterns and deformation as well as mix proportions to increase erosion resistance. Future road engineering efforts must also include innovative erosion testing methods, involvement of stakeholders, and environmental effect studies. Programs for public involvement and awareness are

also suggested in order to ensure community support for the construction of sustainable road infrastructure.

4 ACKNOWLEDGMENTS

I would like to extend my heartfelt thanks to the Department of Civil and Environmental Engineering, Faculty of Engineering, University of Ruhuna, And Dr. J.M.R.S. Appuhamy, head, Department of Civil and Environmental Engineering for providing me with the resources and facilities to conduct my research. I would also like to extend my gratitude to the PRDA of Monaragala District for their invaluable assistance with providing the samples and assisting with the leveling work for this research.

5 REFERENCES

Cao, L., Zhang, K., Dai, H., & Liang, Y. (2015). Modeling Interrill Erosion on Unpaved Roads in the Loess Plateau of China. *Land Degradation and Development*, *26*(8), 825–832. https://doi.org/10.1002/ldr.2253

Hanegbi, N., & Katra, I. (2020). A clay-based geopolymer in loess soil stabilization. *Applied Sciences (Switzerland)*, *10*(7). https://doi.org/10.3390/app10072608

National Highways. (2020, July). http://www.rda.gov.lk/source/rda_roads.htm

Odi Enyegue, T. T., Mbiakouo-Djomo, E. F., Tsanga, H., Kenmogne, F., Bayiha, B. N., Tchemou, G., Njeugna, E., & Fokwa, D. (2021). Effects of Soil Compaction in the Fight against Unpaved Roads Degradation Due to Erosion Caused by Heavy Rain: Proposition of a Specific CBR Evaluation Model. *Engineering*, *13*(03), 95–104. https://doi.org/10.4236/eng.2021.133008

Pardeshi, V., Nimbalkar, S., & Khabbaz, H. (2020). Field Assessment of Gravel Loss on Unsealed Roads in Australia. *Frontiers in Built Environment*, *6*. https://doi.org/10.3389/fbuil.2020.00003

Zemke, J. J. (2016). Runoff and soil erosion assessment on forest roads using a small-scale rainfall simulator. *Hydrology*, *3*(3). https://doi.org/10.3390/hydrology3030025

Shredded Rubber for Ballast Replacement in Rail Track Applications

C. Thanusikan, E. Mathynushan and S.K. Navaratnarajah
Department of Civil Engineering, University of Peradeniya, Sri Lanka

ABSTRACT: Railway transportation, a widely adopted mode globally, relies heavily on ballast materials to support tracks and ensure structural stability. Traditional choices like crushed stone, gravel, and slag dominate due to their cost-effectiveness and technical merits. However, prolonged exposure to cyclic loading and environmental factors alters their properties. This study explores the potential of shredded rubber as a sustainable alternative to traditional ballast. Shredded rubber presents advantages such as durability, shock absorption, noise reduction, and sustainability. The research focuses on determining the optimal shredded rubber percentage as a weight-based replacement for ballast. Large-scale direct shear experiments, conducted under varied normal stress conditions (30, 60, and 90 kPa), provide essential parameters. Discrete element method simulations further predict these parameters. The study recommends incorporating 10-15% shredded rubber by weight to mitigate peak shear stress and dilation effects, resulting in a notable 52–57% reduction in ballast breakage and enhanced durability for rail track applications.

KEY WORDS: Ballasted track, Shredded rubber, Crumb rubber, Numerical simulation

1 INTRODUCTION

The railway transportation system is increasingly demanding, with ballasted tracks being a traditional mode of transportation. Ballast performance depends on the mechanical behavior of the ballast material, which can deteriorate due to repetitive loading and environmental conditions. Shredded rubber is derived from recycling automotive and truck scrap tires. This study aims to combine shredded rubber with ballast particles to reduce ballast degradation and noise, making it a cost-effective and environmentally friendly solution in the railway transportation system. Experimental analysis was done with direct shear tests (DSTs), and numerical analysis was also done with software. In numerical analysis, the discrete element method (DEM) is used in rail track applications to simulate particle behavior in ballast materials. DEM allows for the analysis of particle interactions, settlement, deformation, and track degradation under different loading conditions. This helps engineers to optimize ballast design, assess track performance, and evaluate maintenance strategies, contributing to the development of efficient and sustainable rail track systems. In this study, numerical models were developed to simulate the DSTs of rubber intermixed with ballast using DEM by scanning and importing the actual shapes of rubber and ballast particles.

The main functions of railway ballast is to facilitate the drainage of water from the superstructure and mitigate the stresses resulting from train loads on the underlying layers. Ballast movement during long-term train loadings can cause settlement and stiffness changes, reducing strength. Techniques such as elastic inclusions like rubber mats, tire derived aggregates, and polyurethane-based inclusions improve railway ballast serviceability (Esmaeili et al., 2016). Guo et al. (2022) proposed a cost-effective and environmental friendly solution of mixing crumb rubber with ballast particles derived from shredded waste tire, which has been proven to effectively reduce ballast degradation and noise. Gong et al. (2019) conducted large-scale direct shear tests on specimens of 500–350 mm in size and found that boundary effects can be ignored if the chamber dimension to particle size ratio is greater than 7- 8%. The tests were conducted at three normal loads and stress levels. Ballast and TDA were mixed, and a sinusoidal load was applied for a compacted state. The study suggests 10% rubber content provides the optimum solution.

Numerical models aid in studying complex systems, allowing researchers to analyze variables, conduct simulations, and explore potential outcomes through DEM. Guo et al. (2019) performed DSTs on the rubber-protected ballast (RPB) and built a DST model and a three-sleeper track model with the DEM. ‘PFC2D’ is utilized in this study. The 2 primary components used to simulate ballast particles are discs, which are often insufficiently accurate to accurately represent the natural characteristics of railway ballast (Indraratna et al., 2014). The bonded particle model (BPM) is a method used to model irregular particle shapes, focusing on clumps or clusters. Clumps are rigid particles that remain

unbreakable despite large forces applied. Clusters, on the other hand, are rigid less particles that can break if the force is greater than the defined value. Both models have been widely used in studies.

In this investigation, ballast and rubber particles were gathered and blended according to weight percentages. Subsequently, laboratory DSTs were carried out with varied sample mixtures, and a numerical model was developed for comparing outcomes with experimental results.

2 EXPERIMENTAL ANALYSIS METHOD

2.1 *Material Preparation*

For this study, the fresh ballast material typically used in ballasted rail tracks in Sri Lanka was collected from Gampola Railway Unit. Sieve analysis was carried out to separate ballast aggregates into 4 different size groups: 19–25, 25–37.5, 37.5–50, and 50–63 mm. The test samples were prepared by mixing each sieved size of ballast aggregates according to the defined particle size distribution (PSD), as depicted in Fig. 1, which lies between the upper and lower limits of Indian standard gradation of ballast, widely adopted by the Department of Railways, Sri Lanka. Fig. 2 shows the ballast particle size ranges.

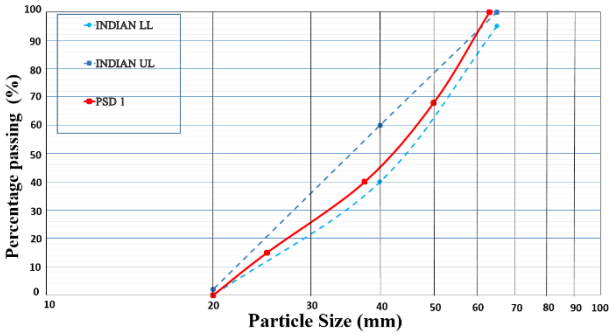

Fig. 1 Upper limit and lower limit of the Indian gradation and particle size curve used in current study.

Fig. 2 Ballast Particles size ranges

Subsequently, the samples underwent washing and drying to eliminate impurities. After obtaining the necessary samples from the previously separated four different-sized ballast samples, they were color-coded with three different colors to distinguish the three layers within the samples for testing. This coloring process was essential due to the presence of three distinct layers in the DST apparatus. Following the painting, the particles were systematically numbered as 1, 2, 3, and 4, facilitating the differentiation of the four size ranges of particles. This procedural step played a crucial role in conducting breakage analysis.

For the preparation of rubber samples required amount of rubber particles was collected from Jaffna from waste tyre materials. The collected rubber particles were cut according to the particle size distribution, and they were separated as shown in Fig. 3. Then considering proposed percentages by weight rubber particles were mixed with ballast as shown in Fig. 4.

Fig. 3 Rubber Particles size ranges

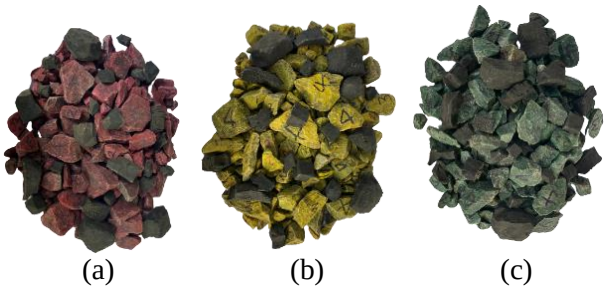

Fig. 4 Prepared mixture of samples (a) bottom layer, (b) middle layer, (c) top layer.

2.2 *Large Scale Direct Shear Test*

For the Experimental analysis large scale direct shear test apparatus was used. The apparatus has a circular shear plane and can accommodate a 400 mm diameter and 300 mm height test specimen. The shear plane was maintained at 150 mm height, allowing the sample to separate into two equal portions using top and bottom cylinders with 150 mm depth. The top cylinder movement was restricted, while the bottom cylinder was displaced laterally at a constant rate of 4 mm/min using a hydraulic jack. A lever-arm system was used to apply normal stress through the top loading plate, which rested on the test sample and moved vertically throughout the test. The reaction force on the top cylinder during shearing was measured by the load cell, while the lateral displacement of the bottom cylinder was measured by Linear Variable Differential Transducers (LVDT). Data from the load cell and two LVDTs were recorded from the data logger. Fig. 5 shows the large-scale direct shear test apparatus setup with connected load cell and LVDTs. After the Material preparation the mixture of Ballast intermixed with Rubber was filled to the apparatus. Fig. 6 shows the Sectional view of cylinder and loading setup

Fig. 5 Large scale direct shear test apparatus

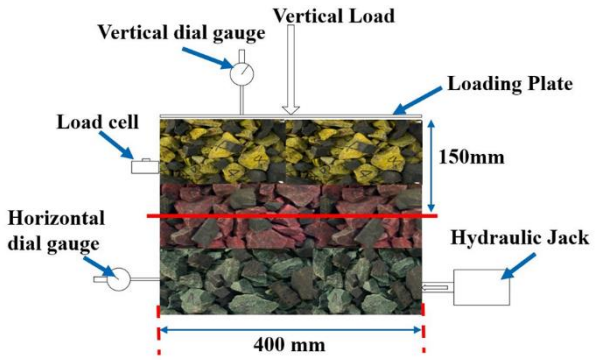

Fig. 6 Sectional view of cylinder and loading setup

2.3 *Breakage Analysis*

In this study, the investigation of ballast breakage in different tested samples were calculated using the Ballast Breakage Index (BBI), a key parameter influencing the overall performance and settlement of the ballast layer. According to Indraratna et al. (2005) the calculation of the BBI involved conducting sieve analysis at the end of each test to obtain particle size distributions of ballast samples after shearing and comparing that of with before the testing. The results from these BBI analyses provided insights into the optimum percentage of rubber mixed with ballast. Fig. 7 illustrates the Ballast Breakage Analysis being performed in the laboratory.

Fig. 7 Ballast Breakage Analysis

3 NUMERICAL ANALYSIS METHOD

3.1 *Model development*

Laboratory tests take more time, consume a lot of materials and increases the possibility of errors in the results. In order to address that, a virtual model will be helpful in quickly obtaining shear strength parameters without requiring a lot of laboratory work. The Discrete Element Method (DEM) was used to create the virtual model for the direct shear test.

3.2 *Particle generation*

The shape of the aggregate is crucial in numerical modelling to simulate the behavior of angular ballast aggregates and rubber particles. A library of CAD templates for variously shaped ballast and rubber particles was produced using 3D scanning, representing each size range of ballast and rubber in accordance with the particle size distribution. The novel method is constructing the nearly realistic shape of ballast and rubber particles in DEM utilizing CAD templates of the original ballast and rubber particles. CAD templates were imported to the DEM software to represent the four various size ranges of ballast and rubber, in this study four chosen ballast and rubber particles were created. The irregular particle shapes were generated as clumps (unbreakable). Clumps are rigid particles that does not break no matter how large the force is applied. The number of spheres for each particles were optimized considering the time efficiency of simulation. Fig. 8 and 9 show the generated ballast and rubber particles using overlapping method.

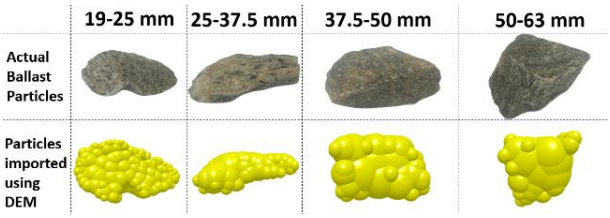

Fig. 8 Unbreakable particle shapes of Ballast

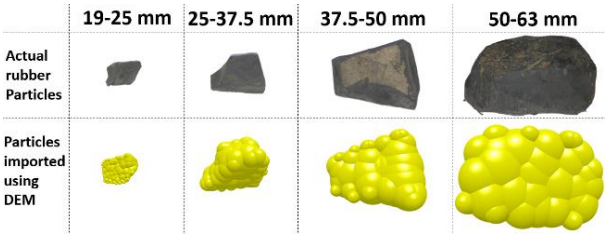

Fig. 9 Unbreakable particle shapes of Rubber

3.3 *Large scale direct shear test model*

The test apparatus was modelled according to the actual dimensions using steel material as shown in

Fig. 10. The top cylinder is stationary, and the bottom cylinder is movable in the shearing direction with a constant velocity of 4 mm/min. Vertical force is applied to the top surface of the top cylinder, while shear displacement is applied to the bottom cylinder in shearing direction.

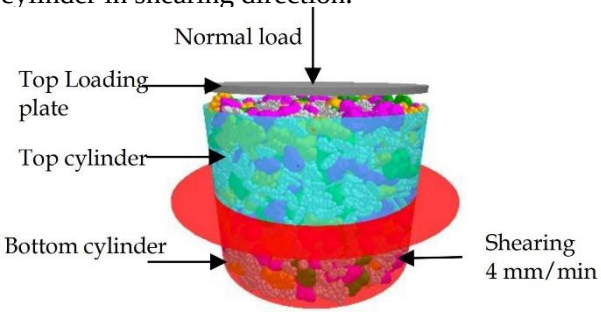

Fig. 10 DEM of Large-scale direct shear test

3.4 *Simulation and validation*

The particles were injected into the cylinder according to the selected particle size distribution. The loading was applied after particle filled. Since the Numerical software cannot provide direct test results, the total force acting on the bottom box over time was analyzed in order to calculate the shear stress. The model was calibrated by comparing the outcomes of the numerical model with the experimental results. To characterize the interaction behavior between two materials, there are three different kinds of parameters (Coefficient of restitution, Coefficient of static friction and Coefficient of rolling friction). The parameters for five different types of interactions (ballast-ballast, ballast-rubber, ballast-steel, rubber-steel, and rubber-rubber) were adjusted in order to calibrate the model. The model was initially calibrated for ballast interactions, then adjusted for rubber interactions and checked with variety of mixes. The procedure was finished to guarantee the consistency and accuracy of the model.

4 RESULTS AND DISCUSSION

4.1 *Experimental Results*

4.1.1 Shear Behavior

The reaction force on the top cylinder obtained from the load cell was used to calculate the shear stress against the shear strain. Since the shear area (A) was changing with the shear displacement as shown in Fig. 11, it was calculated using Equation (1), reported by Olson and Lai (1989), where D and x denote the diameter of the test specimen and the shear displacement respectively,

$$A = \frac{D^2}{2}\{cos^{-1}\left(\frac{x}{D}\right) - \left(\frac{x}{D}\right)\sqrt{1-\left(\frac{x}{D}\right)^2}\} \quad (1)$$

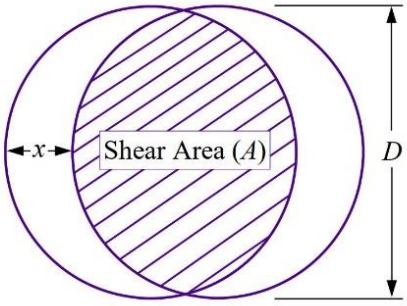

Fig. 11 Shear area for calculating shear stress

Fig. 12 shows the comparison of shear stress varies with shear strain for the normal stress of 60 kPa. As expected, the peak shear stress value is reduced with the increasing rubber percentages because rubber is typically less rigid and has lower shear strength compared to traditional ballast materials. As the rubber content increases, it can act as a softer material between the ballast particles, leading to decreased inter particle friction and, consequently, reduced shear strength.

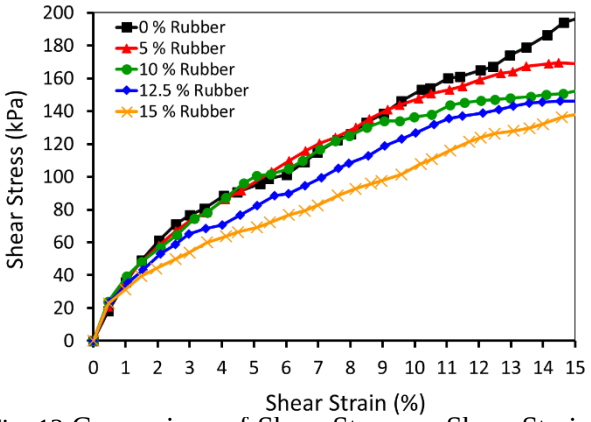

Fig. 12 Comparison of Shear Stress vs Shear Strain for 60 kPa Normal Stress

4.1.2 Compression/Dilation Behaviour

In the large-scale direct shear test with ballast particles and rubber, the addition of rubber influenced both dilation and compression behaviors during shear stress. Dilation behavior was evident in the tendency of materials to separate or increase in volume, indicating expansion and increased void spaces due to added rubber. This observation provided valuable insights into shear strength and potential particle rearrangement within the ballast layer. Conversely, rubber incorporation likely altered compression behavior, resulting in volume reduction or material compaction under shear stress.

This modification could have significant implications for the compaction characteristics of ballast particles, potentially reducing void spaces and impacting overall density and stability in the ballast layer. Understanding these behaviors was crucial for evaluating deformation characteristics and assessing the influence of rubber content on the mechanical response of the ballast layer in railway track applications.

Fig. 13 illustrated the vertical strain variation with shear strain under a normal stress of 60 kPa. Positive vertical strain indicated upward movement, representing particle dilation, while negative vertical strain indicated particle compression during shear. Tests with 0% rubber exhibited prominent dilation due to the angularity and hardness of the ballast particles, facilitating particle rolling. However, as rubber content increased, overall sample compressibility rose, reducing the dilation effect, and compression intensified. This comprehensive understanding is essential for optimizing railway track design and ensuring the stability and performance of the ballast layer under varying conditions.

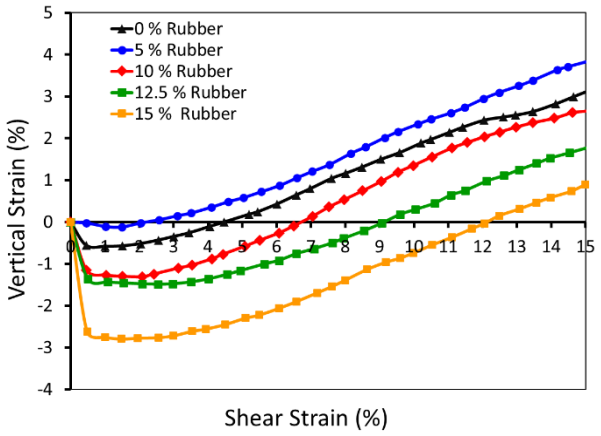

Fig. 13 Comparison of Vertical Strain vs Shear Strain for 60 kPa normal stress

4.1.3 Ballast Breakage

Fig. 14 shows how the ballast breakage index (BBI) and peak shear stress vary with different rubber percentages. Breakage occurred, especially at high normal stress during direct shear tests (DSTs), significantly influencing the mechanical behavior and durability of the track. Increasing rubber content decreased BBI as rubber particles are more deformable and less brittle than traditional ballast materials. This reduction in brittleness, accompanying higher rubber percentages, leads to less ballast particle breakage during loading and deformation, consequently lowering peak shear stress values.

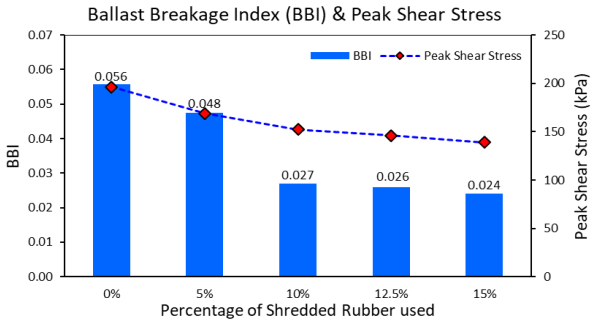

Fig. 14 Comparison of BBI and Peak Shear Stress with percentage of Rubber

4.2 *Numerical Results*

4.2.1 Calibration and Validation

The calibration process began with the application of a 60 kPa load to the 0% rubber sample. Then, until numerical results showed a satisfactory agreement with experimental findings, iterative calibration was performed. After calibrating coefficients for ballast-ballast and ballast-steel interactions, the introduction of rubber to the sample initiated a specific calibration process for interaction coefficients related to rubber. To calibrate the coefficients for each interaction, this was continued to do. Fig. 15 shows the validation of numerical results with 0% rubber (ballast only) and 10% rubber for the normal stress of 60kPa.

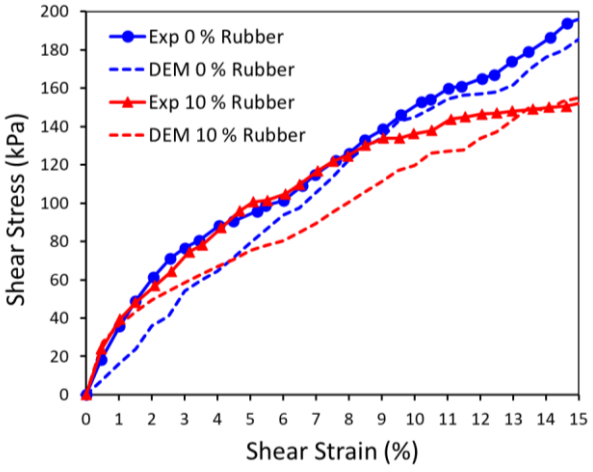

Fig. 15 Validation of shear stress vs shear strain results of both experiment and numerical (DEM) analysis under 60 kPa normal stress

4.2.2 Shear Behavior

Following the validation, the calibrated interaction coefficients were employed to conduct the simulations, exploring diverse rubber percentages and var-

ious normal stress values. The peak shear stress obtained from the numerical and experimental models was nearly identical. Fig. 16 shows the comparison of experimental and numerical analysis results for the applied normal stress of 60 kPa.

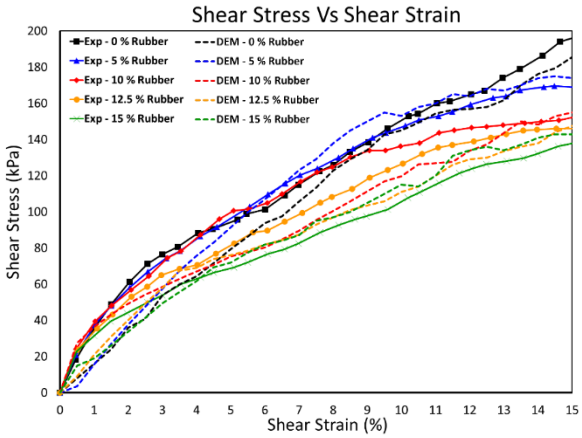

Fig. 16 Comparison of shear stress vs shear strain results of both experiment and numerical (DEM) analysis under 60 kPa normal stress

CONCLUSIONS

The study on the impact of rubber content on ballast mixtures found a strong correlation between increased rubber content and reduced peak shear stress. The study found that adding 10-15% shredded rubber to the mix significantly reduced ballast breakage by 52–57%. At the same time, the peak shear stress reduction (152-140 kPa) is marginal. Based on the laboratory test results and numerical simulation, the optimal rubber content range of 10–15% was identified, balancing shear stress reduction and improving durability in ballast mixtures. This research provides practical insights for optimizing ballast with rubber compositions in engineering applications, promoting structural integrity and performance longevity.

ACKNOWLEDGMENTS

Our sincere thanks to the Head of the Department of Civil Engineering Faculty of Engineering University of Peradeniya, who has given immense support to conduct the study.

REFERENCES

Esmaeili, M., Zakeri, J. A., Ebrahimi, H., & Khadem Sameni, M. (2016). Experimental Study on Dynamic Properties of Railway Ballast Mixed with Tire Derived Aggregate by Modal Shaker Test. Advances in Mechanical Engineering, 8(5), 168781401664024.

Gong, H., Song, W., Huang, B., Shu, X., Han, B., Wu, H., & Zou, J. (2019). Direct Shear Properties of Railway Ballast Mixed with Tire Derived Aggregates: Experimental and Nu merical Investigations. Construction And Building Materi als, 200, 465–473

Guo, Y., Shi, C., Zhao, C., Markine, V., & Jing, G. (2022a). Numerical Analysis of Train-Track-Subgrade Dynamic Per formance with Crumb Rubber in Ballast Layer. Construction And Building Materials, 336, 127559

Guo, Y., Zhao, C., Markine, V., Jing, G., & Zhai, W. (2020). Calibration For Discrete Element Modelling of Railway Bal last: A Review.Transportation Geotechnics, 23, 100341.

Indraratna, B., Lackenby, J., & Christie, D. (2005). Effect Of Confining Pressure on The Degradation of Ballast Under Cyclic Loading. Géotechnique, 55(4), 325–328.

Indraratna, B., Ngo, N. T., Rujikiatkamjorn, C., & Vinod, J. S. (2014). Behavior Of Fresh and Fouled Railway Ballast Sub jected to Direct Shear Testing: Discrete Element Simulation. International Journal of Geomechanics, 14(1), 34–44.

Olson, R.E., Lai, J. Direct Shear Testing; Chaoyang University of Technology: Taichung, Taiwan, 1989; pp. 1–14.

Geotextile Encased Stone Columns (GESC) in Soft Soil

W.D.I.C. Weerawardana and N.H. Priyankara
Department of Civil and Environmental Engineering, University of Ruhuna, Sri Lanka

ABSTRACT: In response to land scarcity, marshy lands with challenging soft soil are being utilized for infrastructure. Soft soil, characterized by high moisture, compressibility, and low shear strength, is often improved using stone columns. But to address the drainage issues in Stone Columns (GCP) caused by soft clay intrusion, and enhance performance in extremely soft soil, the need has arisen to use Geotextile Encased Stone Columns (GESC). As such in this research, the effect of stiffness of geotextile and the cell pressure on sand column was evaluated experimentally. A parametric study was conducted through PLAXIS using these observation data to investigate the influence factors that may have a direct impact on the factor of safety, including the stiffness of geotextile. The results of this analysis highlight the importance of geotextile in the global stability of geotextile-encased stone columns (GESC) installed in very soft soil.

KEY WORDS: Gravel Compaction Piles, Geotextiles, Numerical modeling, Parametric study

1 INTRODUCTION

Every section in the world develops with time including the construction field as well. Before starting any construction, it's crucial to check the ground conditions. Buildings stand on the ground, therefore it's important to know if the soil can support them. Some types of soil can support the loads, while others can't. This depends on the characteristics of the soil layers. The reason behind that inability may be the characteristics of a particular soil layer.
They are low strength, high compressibility, large creep deformation, and high moisture content. Hence, as a solution to overcome the above problem, unsuitable places can be abandoned for infrastructure development. But due to the rapid increase of population and developments, places with ground subsoil conditions have become limited. As a result, roadway embankments, are being constructed in marshy lands and low areas with weak subsoil strata. As such many challenging problems have to be overcome during the construction stage on soft soil deposits including low bearing capacity, excessive settlement and slope instability.
When considering the construction in low land areas and in marshy lands, there are two options can be adopted. Namely,

I. Transfer the structural load to underlain hard stratum through piles.
II. Improve the engineering characteristics of soft soil.

However, when considering the structures like roads occupying a large plan area and moderately loaded buildings, the use of the pile foundation is not an economical solution. Therefore, ground improvement techniques are more appropriate in such situations. The ground improvement is principally based on two concepts namely densification and solidification. In densification, soil particles are paced together reducing the voids while in solidification, soil particles are bound together with an external binder. Out of these two methods. The densification technique is the most popular method due to its low cost. Even though, reloading is the most common densification technique it consumes more time. In addition, due to low shear strength gain, there is uncertainty in the stability of the 2 embankments during construction. As such, Geotechnical Engineers prefer to use Gravel Compaction Piles (GCP) to improve soft soil especially when the soft soil thickness is more.
Stone columns or granular pile technique is mostly used to improve the soft soil because it has higher stiffness and drainage capability than surrounding weak soil. Hence, the settlement of the GCP improved composite ground is less than that of the

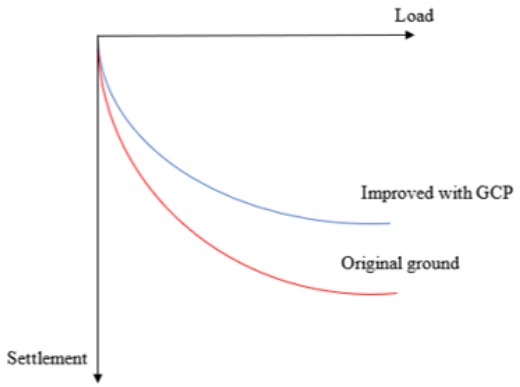

Fig. 1 Concept of GCP improvement

original ground as shown in **Error! Reference source not found.**.

According to (J. M. Mckenna, 1975) stone columns are not restrained by the surrounding soft clay, which leads to excessive bulging and soft clay squeezing into the voids of the stone aggregates, reducing the bearing capacity of the stone column as well as its drainage capacity. However, when the stone columns are installed in very soft soils, surrounding soft soil may not provide significant confining pressure from the surrounding. Therefore, (Han, 2015) geosynthetic encased stone columns as a convenient technique to improve soft soils which are having undrained shear strengths lower than 15 kPa.

In Sri Lanka, GCPs have been successfully used as a ground improvement technique in many projects, namely Outer Circular Highway Northern Section-1 (OCH-NS1), the Colombo-Katunayaka expressway project, etc. In these projects, GCPs have been used to improve soft soil in places where high embankments were constructed on peat deposits with high layer thickness. However, in the Southern Expressway Extension Project from Matara-Beliatta, though GCP technique has been used. It failed. After certain investigations to find the reason for this failure, a lack of knowledge of some basic conditions was found. The effect of drainage conditions of GCPs, and very low confining pressure around the GCP may be some of the reasons for the cause of failure. Hence, in this research study, the performance of the Geosynthetics Encased Gravel Compaction Piles on soft soil improvement will be studied using a series of Laboratory Triaxial tests. The effect of Geosynthetics on the drainage behavior as well as the deformation behavior of GCP will be studied. Only very limited research studies have been done in the world related to the performance of encased GCP. No research has been done in Sri Lanka to study the drainage performance of Geosynthetics Encased GCP. As such, findings of this research study will be helpful to overcome the uncertainties in the design of the GCP

2 METHADOLOGY

In order to find the behavior of GESC improved composite ground, following procedure was carried out. The overall research methodology is included a literature review, laboratory testing, and numerical analysis and which is illustrated using the flow chart as shown in Fig. 2.

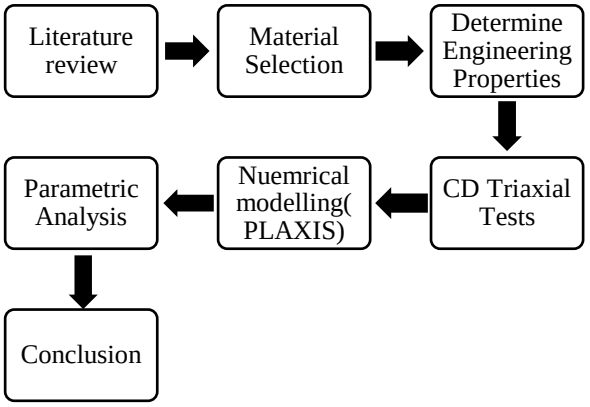

Fig. 2 Methodology adopted

2.1 *Material Selection*

Generally, Aggregate base course (ABC) material is used in GCP. But basically, this study concentrates on the effect of the geotextile, so then river sand is used as the infill material of GESC. Aggregate base coarse cannot be used as an infill material when conducting triaxial testing due to the particle size.

2.2 *Laboratory Experiments*

In this research project, a series of Consolidated Drained (CD) triaxial tests were conducted on woven geotextile sleeves to achieve two main objectives. First, to investigate the impact of geotextile on Gravel Compaction Piles (GCP), focusing on shear strength parameters such as effective cohesion (c') and effective frictional angle (Φ'), a series of triaxial series on both ordinary (without geotextile encasement) and encased sand columns under varying confining pressures (50 kPa, 100 kPa, and 150 kPa) was conducted. Second, the research studies the effect of confining pressure, representing the stress applied by the surrounding soft soil in GCP-improved ground. This was involved triaxial consolidated drained tests on a 100/50 fabricated geotextile sleeve for encased sand columns, conducted at different confining pressures (25 kPa, 50 kPa, 75 kPa, 100 kPa, 150 kPa, and 200 kPa).

2.3 *Numerical Modelling*

Numerical modeling using PLAXIS software will be conducted to evaluate the stability of the geosynthetic encased stone column-supported embankments. Further parametric analysis will be performed to understand the effect of geotextile encased sand columns on different strengths.
The material sets used in (Alkhorshid, 2018) are directly used for the model. Those values are mentioned in Table 1. For the soft soil layer, hardening soil model has used. Hardening soil model is a hyperbolic model of the elastoplastic kind and was developed within the context of friction hardening

plasticity. Therefore, that the effect of confining pressure can be easily find. Parameters in the hardening model can be shown below. Failure parameters as in Mohr-Coulomb model (Brinkgreve, 2002).

Table 1.Material sets used for the unit cell (Alkhorshid, 2018)

Material properties	Soft clay	Stone column	Embankment	Locally weak zone
Material model	HS	M-C	M-C	SSM
γ_{sat} (kN/m^3)	16	19	22	18
E' (kPa)	-	45000	42000	-
φ' (°)	23	39	35	5
ψ (°)	0	5	0	0
c' (kPa)	7	0	6	5
ν'	0.2	0.3	0.33	-
E_{50}^{ref} (kPa)	2313	-	-	-
E_{oed}^{ref} (kPa)	1850	-	-	-
E_{ur}^{ref} (kPa)	6938	-	-	-
c_c	-	-	-	6
c_s	-	-	-	0.6
e	-	-	-	3
P^{ref} (kPa)	100	-	-	-
OCR	1	-	-	-
K_0	0.6	0.37	0.43	0.91
m (power)	1	-	-	-

Validation was conducted by comparing settlement results at the top of the column and embankment heights with various methods. The methods included in this comparison are the analytical techniques of (Raithel, 2000), (Pulko & Majes, 2011), and (Zhang, 2014), alongside the numerical method developed by (N.R. Alkhorshid, G.L.S. Araújo, E.M. Palmeira, 2018) using PLAXIS. The graph available in same literature review was employed for this validation.The geometry of the unit cell (Alkhorshid, 2018) is shown in Fig. 3.

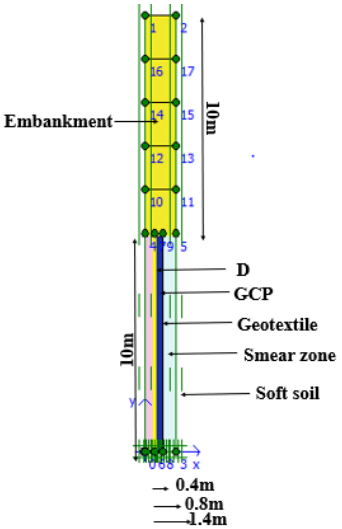

Fig. 3 Geometry of the unit cell

3 RESULTS AND DISCUSSION

3.1 *The effect of the strength of geosynthetics on granular columns*

Table 2 presents comprehensive findings from the triaxial test conducted on the ordinary sand column and the geosynthetic-encased sand columns (GESC) with varying geotextile strength. The results reveal a substantial increase in cohesion and a minor improvement in the friction angle. Consequently, increasing the stiffness of geotextile leads to higher values of cohesion and friction angle in comparison to the ordinary sand column.

An increase in stiffness leads to greater lateral confinement of the geotextile infill material against the geotextile encasement. This enhanced lateral confinement, in turn, increases the shear stress within the column. Table 3 shows the summary of stiffness of sand column obtained from experimental data.

Table 2.Shear strength parameters

		Cohesion	Friction Fangle
Ordinary sand column		18	32.21
GESC	100/50	25	32.42
	200/50	33	35.07
	600/50	40	36.87

Table 3.Summary of stiffness of sand column

		Stiffness (kPa)		
Cell pressure(kPa)		50	100	150
Ordinary sand column		6923.08	14646.24	20942.41
GESC	100/50	7000.00	20000.00	33846.15
	200/50	7309.94	20725.39	26500.00
	600/50	7894.74	20400.00	25102.88

3.2 *The effect of the strength of geosynthetics on granular columns*

As depicted in Table 4 when subjected to a cell pressure of 100kPa, the geosynthetic-encased sand columns (GESC) displayed lower axial strain compared to the ordinary sand column (OSC) for axial strains below 2.2%. Conversely, for axial strains exceeding 2.2%, the OSC exhibited lower deviator

stress. And also, this observation is particularly evident at a cell pressure of 150kPa.

The increasing the cell pressure leads to higher deviator stress values, and this relationship is inversely correlated with axial strain.

Table 4.Comparison about deviator stress and axial strain between OSC and 100/50 GESC

Cell Pressure (kPa)	Deviator stress(kPa)		Axial strain (%)	
	OSC	100/50 GESC	OSC	100/50 GESC
50	180	210	2.6	3
100	325	360	2.2	1.4
150	400	440	1.9	1.3

3.3 *The global stability of geosynthetic encased granular column improved ground*

To find the effect of geotextile around the pile, first a stiffness value has selected. Eoed – 2000 kN/m has selected for the analysis. Subsequently, the stiffness values of the geotextile were adjusted. The analysis focused on the variation of the stiffness of the infill material of the Geotextile-Encased Sand Column (GESC) in relation to the stiffness values of the geotextile, with all other parameters held constant. Table 5 presents the values of the geotextile and the stiffness of the infill material of the GESC, corresponding to the cell pressures employed in the triaxial tests.

a) Lateral deformation for a particular point with different stiffness values.

It is evident that as the stiffness of the surrounding soil increases at particular point (point D in Fig. 3;located 1m below from the ground level), lateral deformation decreases, resulting in improved stability. Thus, it can be observed that the lateral displacement behavior remains consistent across all three different cell pressure conditions. The geotextile serves as a confinement for the Geotextile-Encased Sand Column (GESC). When soil attempts to displace laterally, the geotextile exerts its stiffness to resist this movement. Higher stiffness in the geotextile corresponds to increased resistance, thus enhancing the overall stability of the system.

Table 5.Lateral displacement at point D

Stiffness of the geotextile (kN/m)	Lateral displacement (m)		
	50kPa	100kPa	150kPa
1000	0.017	0.009	0.00658
2000	0.016	0.008	0.00647
6000	0.007	0.007	0.00622

b) Lateral deformation for a particular geotextile stiffness value over the depth after 150 days.

Variation of lateral displacement for different geotextile stiffnesses with respect to the depth can be observed in **Error! Reference source not found.**. For lower stiffness values, graph shows a bulging shape. With the increment of the stiffness, it had changed the direction towards the pile. That movement of the geotextile should be the reason for the direction of lateral displacement.

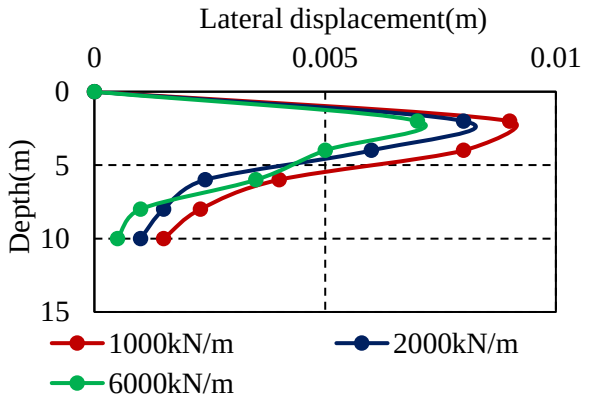

Fig. 4 Lateral displacement Vs Time curves for different gaeotextile stiffnesses

4 CONCLUSION

The following conclusions can be drawn based on the results of this study.

1. Geotextile encased sand columns continued to yield higher shear strengths as the axial strains increased, unlike the ordinary sand columns which approached steady state at relatively low axial strains.
2. The encasing of geotextile encasement not only increase the cohesion to the shear strength parameters, but it also increased the friction angle of the column to a value greater than the friction angle of an ordinary sand column.
3. The geotextile encasement elevates the stiffness of the infill material in the Geotextile-Encased Sand Column (GESC) to a level exceeding that of an ordinary sand column.
4. Increasing the stiffness of the geotextile in GESC results in higher shear strength parameters.

Specifically, cohesion exhibits a significant increase, while the friction angle experiences a slight improvement.
5. Increasing the stiffness of the geotextile in the Geotextile-Encased Sand Column (GESC) leads to a corresponding increase in the stiffness of the infill material relative to the geotextile stiffness.
6. Another factor influencing GESC behavior is the surrounding confining pressure. As the cell pressure increases, the stiffness of the Geotextile-Encased Sand Column (GESC) also increases, resulting in a corresponding reduction in axial strain.
7. Furthermore, an increase in cell pressure also results in an increase in the shear strength parameters.
8. In the unit cell model, it is well-described that the reduction of lateral displacement decreases with an increase in the stiffness of the geotextile. Thus, with improved single GESC stability, it can be concluded that overall stability increases.
9. The stiffness of geotextile materials significantly influences lateral displacement behavior. As geotextile stiffness increases, there is a noticeable shift in displacement direction toward the pile, which can be attributed to the material's elastic properties.

REFERENCES

Alkhorshid, N. A. (2018). Numerical Analysis of Soft Clay Reinforced with Stone Columns . *Numerical and Analytical EvaluationsSoils and Rocks, 41(3)*, pp.333-343.

Brinkgreve, R. B. (2002). Plaxis version 8 Material Models Manual. Netherlands.

Han, J. (2015). *Principles and Practice of Ground Improvement.* Georgia: John Wiley & Sons.

J. M. Mckenna, W. A. (1975, march 1). geotechnical. *No AccessPerformance of an embankment supported by stone columns in soft ground, 25*(1), 214-215.

N.R. Alkhorshid, G.L.S. Araújo, E.M. Palmeira. (2018). Behavior of Geosynthetic-Encased Stone Columns in Soft Clay: Numerical and Analytical Evaluations. *Soils and Rocks*, 333-343.

Pulko, B., & Majes, B. &. (2011). Geosynthetic encased stone columns: Analytical calculation model. . *Geotextiles and geomembranes*, 29-39.

Raithel, M. &. (2000). Calculation models for dam foundations with geotextile coated sand col umns. e. *Proc. International Conference on Geotechnical and Geological Engineering, Melbourn*.

Zhang, L. &. (2014). Deformation analysis of geotextile-encased stone columns. *Int. J. Geomech*, 1-10.

Prediction of Geotechnical Properties of Expansive Soil Stabilized with Fly Ash using Artificial Neural Network

K.Kirushanthan, T.Thigitharan and M. C. M. Nasvi

Department of Civil Engineering, University of Peradeniya, Sri Lanka

ABSTRACT: Expansive soils are considered as problematic soils since they exhibit high swelling and shrinkage when exposed to changes in moisture content. Chemical stabilization is a popular method employed to enhance geotechnical properties and reduce volume change characteristics in expansive soils. Geotechnical engineering properties of the stabilized soils are required in the analysis and design of structures constructed on these soils. However, conducting traditional laboratory experiments to determine the geotechnical properties are time-consuming, costly, and energy intensive. Recently soft computational approaches, such as Artificial Neural Network (ANN), have been used to predict the geotechnical properties. Since there are very limited studies to predict the geotechnical properties of expansive soil stabilized with fly ash (FA) by using ANN, this study aimed to develop predictive models to determine the geotechnical properties (optimum moisture content (OMC), maximum dry density (MDD), and 28-day unconfined compressive strength (UCS)) of expansive soil stabilized with FA using ANN in PYTHON language. For this purpose, a large number of data were collected from relevant literature to develop these models. All the proposed models were successfully trained and validated (R^2 Value for training and validation were $R^2 = 0.951$ and $R^2 = 0.911$ for OMC model, $R^2 = 0.989$ and $R^2 = 0.901$ for MDD model and $R^2 = 0.993$ and $R^2 = 0.915$ for UCS_28d (UCS) model respectively. Sensitivity analysis showed that OMC (53%) and MDD (46%) of the natural soil are the most influential parameter for the OMC model and MDD model respectively, whereas fly ash/soil ratio (41%) is the most influential parameter for UCS model.

KEY WORDS: Expansive soil, Soil stabilization, Fly ash, Artificial Neural Network (ANN), Sensitivity analysis

1 INTRODUCTION

Expansive soil is a type of soil that expands when it absorbs water and shrinks when it dries. This expansion and contraction can cause damage to structures built on expansive soils. Expansive soil at shallow depths and other poor ground conditions are common problems faced in geotechnical engineering, and these problematic soils pose enormous challenges to the proposed infrastructural development (Das et al., 2010). Most often, the option of soil replacement is not economical, and there is a need to perform some form of ground improvement or stabilization prior to construction. Soil stabilization may be done chemically or mechanically, depending on the peculiarity of the problem at hand. However, the treatment of most expansive soils will involve the use of chemical stabilization which involves adding chemical agents to the soil to modify its properties. Irrespective of the method used, it becomes imperative to investigate the performance of such stabilized soils using key parameters of the soil such as unconfined compressive strength (UCS), maximum dry density (MDD), optimum moisture content (OMC), California bearing ratio (CBR), plasticity index (IP), liquid limit (LL), plastic limit (PL), etc. (Chew, et al., 2004; Eyo, et al., 2020). Such geotechnical engineering properties of the stabilized soils are required in the analysis and design of infrastructure built on these soils. However, conducting a large number of laboratory experiments to find the geotechnical properties is time consuming, incur high cost and energy intensive. Analytical tools can be used to develop models to predict different physical and mechanical properties of soils and consequently the reduction of both the time consumption and cost. In addition, the analytical models have been applied as an effective approach with high performance compared with the statistical models.

Analytical tools such as artificial neural networks (ANNs) (Leong et al., 2018) multivariable regression (MVR) (Adhikari et al., 2019), genetic programming (Leong et al., 2018), etc. have been widely used to predict the geotechnical properties of stabilized soils. Among these techniques, ANN reflects the behavior of the human brain, it allows computer programs to recognize patterns and solve common problems in the fields of machine learning and deep learning.

To date, there are only a limited number of studies available to predict the geotechnical properties of expansive soil stabilized with FA using ANN. Hence, this research aims to predict the geotechnical engineering properties of expansive soil stabilized with FA using ANN.

2 LITERATURE REVIEW

Smith et al., (2018) has conducted a comprehensive study on the use of FA as a soil stabilizer. The research highlighted a significant improvement in soil strength and a reduction in expansive characteristics of soil treated with FA. This finding underscores the potential of FA as a promising agent for stabilizing expansive soils. The authors concluded that the introduction of FA in soil stabilization experiments resulted in a notable enhancement of soil strength and a reduction in expansive soil behavior.

Jones and Brown (2016) explored the application of ANNs in geotechnical engineering, specifically in modelling soil behavior. The study demonstrated the efficacy of ANNs in capturing intricate relationships within expansive soils. This insight supports the utilization of ANNs as a valuable tool for predicting geotechnical properties in soil stabilization projects. The authors concluded that machine learning techniques, particularly ANN, can be useful in estimating the strength properties of stabilized expansive soils.

Brown and Taylor (2019) investigated the use of ANN in predicting the compressive strength of expansive soils treated with different stabilizers, including FA. The study showcased the effectiveness of ANN in modelling the complex relationships involved in soil stabilization, contributing to the advancement of predictive modelling in geotechnical engineering. The authors concluded that the use of ANN can be a better solution to predict compressive strength in expansive soils treated with different stabilizers.

Wang and Zhang (2018) investigated the use of Artificial Neural Networks (ANNs) to predict the shear strength of expansive soils treated with various stabilizers including FA, lime, and cement. Their study aimed to develop a model that could accurately estimate shear strength based on soil and stabilizer properties. The ANN model achieved R^2 value of 0.91, indicating a strong correlation between predicted and observed shear strength values. Sensitivity analysis revealed that the ANN model gave considerable importance to parameters such as stabilizer type, curing time, and soil density. Specifically, the model identified FA content, curing time, and initial moisture content as the most influential factors affecting shear strength. Wang and Zhang concluded that ANNs are effective tools for predicting the shear strength of stabilized expansive soils, with the developed model showing a high R^2 value of 0.91. The sensitivity analysis highlighted key parameters that should be considered in soil stabilization projects, providing valuable guidance for engineering applications with various stabilizers.

Li and Wu (2019) investigated the use of Artificial Neural Networks (ANNs) to predict the swelling potential of expansive soils stabilized with different additives, including lime, gypsum, and FA. Their study aimed to develop a model to accurately estimate swelling potential based on soil and additive properties. The ANN model achieved R^2 value of 0.88, indicating a strong correlation between predicted and observed swelling potential values. Sensitivity analysis revealed that the ANN model emphasized parameters such as additive type, cur-ing time, and initial soil moisture content. Notably, FA content, curing time, and initial moisture con-tent were identified as the most influential factors affecting swelling potential. Li and Wu concluded that ANNs are effective in predicting the swelling potential of stabilized expansive soils, with the developed model demonstrating a high R^2 value of 0.88. The sensitivity analysis provided insights into crucial parameters for soil stabilization projects, offering valuable guidance for engineering applications using various additives.

3 METHODOLOGY

3.1 *Data collection and treatment*

An extensive compilation of databases containing results from numerous experimental studies were undertaken. The required data for the development of the three ANN models are OMC, MDD, and 28-day Unconfined Compressive Strength (UCS). The amount of data needed depends on several factors, such as the complexity of the problem, the size of the input space and the number of parameters in the model. As a rule of thumb, it is often recommended to have a sufficiently large dataset that provides a representative sample of the underlying population or distribution (Touzet et at., 1995). Hence, it was decided to collect significant number of data points not less than 50 data for each set.

It is important to remove outliers from the collected data and Cook's Distance method was used for this purpose. Cook's distance D_i of observation k is given by following Equation 1 (Jeremiah, et al., 2021).

$$D_i = \frac{\sum_{i=1}^{n}(\hat{y}_i - \hat{y}_{i(k)})^2}{pMSE} \quad (1)$$

where $\hat{y}_i$ is the i^{th} fitted response value; $\hat{y}_i(k)$ is the i^{th} fitted response value when the fit excludes observation k; MSE is the mean squared error; and p is the number of coefficients in the regression model.

3.2 *ANN model development*

ANN models for OMC, MDD and UCS were developed by using PYTHON language. The input and output parameters of the developed ANN models for OMC, MDD and 28day UCS are shown in Fig. 1.

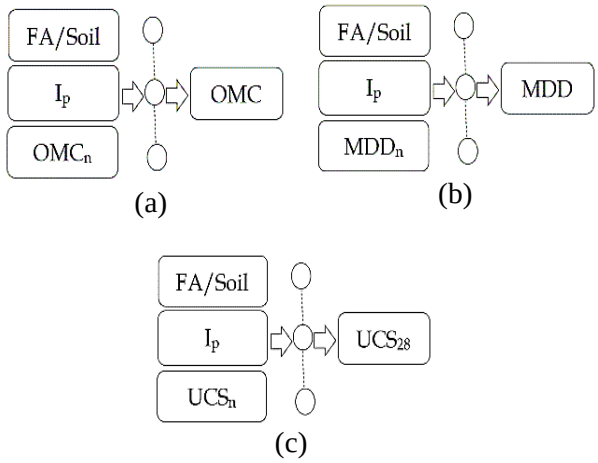

Fig. 1: Input parameters used for ANN models: (a) OMC Model, (b) MDD Model and (C) UCS Model.

To obtain a statistically consistent training and testing data, 70% of the experimental data were used for training the model and the remaining 30% of the data was used for testing and validating the ANN model (Gunasekara et al., 2020). As part of the pre-processing, the input and output variables were normalized to fall in the range [-1, 1] to make the learning rate high and to have a consistency while training the ANN model. Relu activation function was used as the activation function in the development phase of ANN models.

Number of neurons in the hidden layer was varied to find the optimum architecture. The performance of ANN model was reported in terms of two statistical parameters namely, coefficient of determination (R^2) and root mean square error (RMSE). The optimum architecture of ANN models were characterized by high R^2 value and low RMSE value.

4 RESULTS AND DISCUSSION

The typical ANN architecture of the developed ANN models is shown in Fig. 2. The model architecture for all the three models (OMC, MDD and UCS) consist of three hidden layer and the number of neurons in the 1st, 2nd and 3rd hidden layers were 256, 128 and 32 respectively. The final model architecture is in the form 3-256-128-32-1. The number of epochs used for MDD, OMC and UCS models were 150, 200 and 200 respectively as these numbers provided a better performance on predicting the output parameters of the respective models.

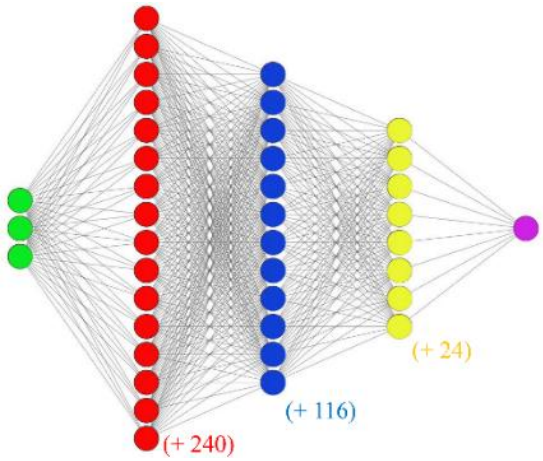

Fig. 2: Architecture of developed ANN models (OMC, MDD and UCS).

4.1 *MDD model*

Model training and validation plots for MDD model are shown in Fig. 3. According to Fig. 3, the training data set has high performance compared to the validation and target data sets. The R^2 value for training and validation data set are 0.989 and 0.901 respectively. The root mean squared error (RMSE) for training and validation data set are 0.030 and 0.162 respectively.

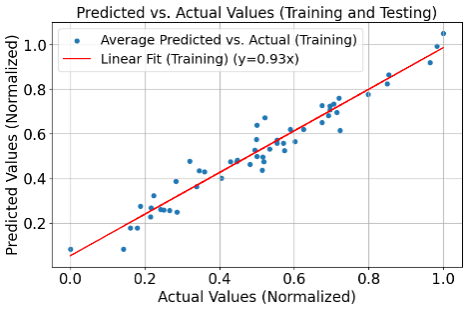

(a)

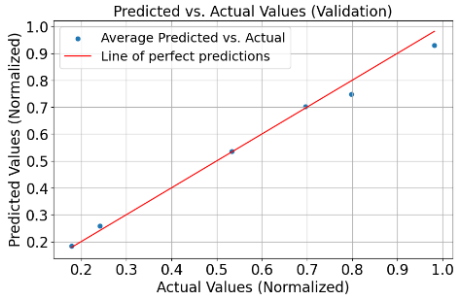

(b)

Fig. 3: Coefficient of determination (R^2) values of MDD – ANN model (a)Training and (b) Validation

4.2 *OMC model*

Model training and validation plots for OMC model are shown in Fig. 4. According to Fig. 4, the training data set has high performance compared to the validation and target data sets. The R^2 value for training and validation data set are 0.951 and 0.911 respectively. The root mean squared error (RMSE) for training and validation data set are 0.037 and 0.196 respectively.

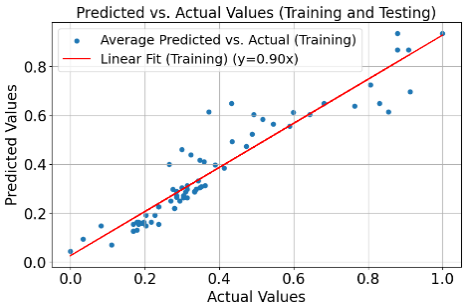

(a)

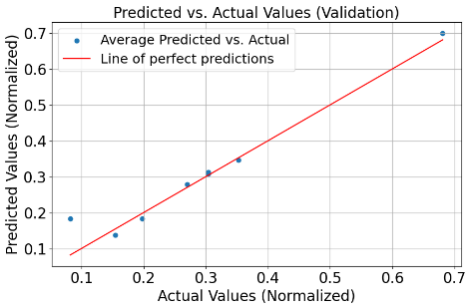

(b)

Fig. 4: Coefficient of determination (R^2) of OMC – ANN model (a)Training and (b) Validation

4.3 *UCS model*

Fig. 5 shows the model training and validation plots for the UCS model. According to Fig. 5, the training data set has high performance compared to the validation and target data sets. The R^2 value for training and validation data set are 0.993 and 0.915 respectively. The root mean squared error (RMSE) for training and validation data set are 0.017 and 0.271 respectively.

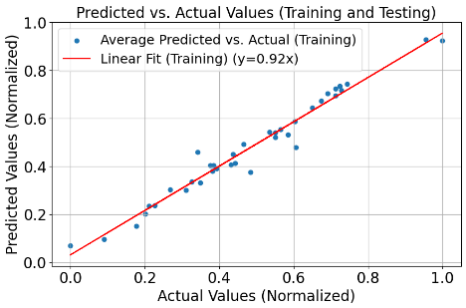

(a)

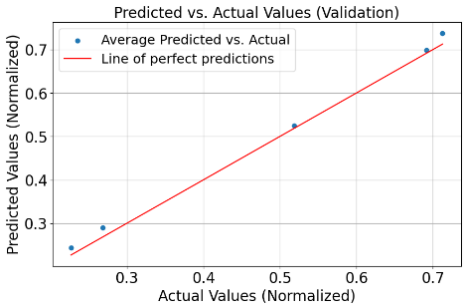

(b)

Fig. 5: Coefficient of determination (R^2) values of UCS – ANN model (a)Training and (b) Validation.

4.4 *Sensitivity analysis*

The correlation matrix method (Leong et al., 2018) was used to find the input variable contribution to the model and the obtained sensitivity plots for the three developed ANN models are shown in Fig. 6. According to Fig. 6, the sensitivity ranks OMC of the natural soil as the most influential parameter (53%) followed by FA/Soil ratio (34%) and I_P (13%) is the less influential parameter for OMC model. In the MDD model, MDD of the natural soil is the most influential parameter (46%) followed by FA/Soil ratio (32%) and I_P (22%). In the UCS model, FA/Soil ratio is the most influential parameter (41%) followed by UCS of natural soil (38%) and I_P (23%) .

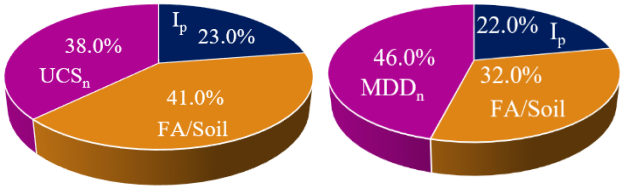

UCS

(a)

MDD

(b)

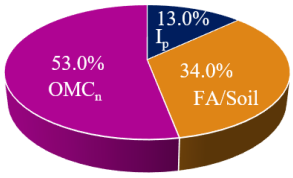

OMC

(c)

Fig. 6: Sensitivity analysis plots of developed (a) UCS, (b) OMC and (c) MDD models.

5 CONCLUSIONS

Artificial Neural Network (ANN) can be used to predict the unconfined compressive strength (UCS), maximum dry density (MDD) and optimum moisture content (OMC) of the expansive stabilized with fly ash (FA). The models for OMC, MDD and UCS share a consistent optimum architecture of 3-256-128-32-1. However, optimum number of epochs for these models are different and they are 200, 150 and 200 respectively, highlighting varied training requirements for each geotechnical property. All proposed models were successfully trained and validated for the known data sets. (R^2 Value for training and validation were R^2=0.951 and R^2=0.921 for OMC model, R^2=0.989 and R^2=0.911 for MDD model and R^2=0.993 and R^2=0.915 for UCS_28d (UCS) model respectively.)

Developed models show a reasonable predictive ability towards new data, suggesting that the models can be used as an alternative for conducting experimental studies to predict geotechnical properties of FA stabilized expansive soil. Sensitivity analysis showed that OMC (53%) and MDD (46%) of the natural soil are the most influential parameter for the OMC model and MDD model respectively, whereas FA/Soil ratio (41%) is the most influential parameter for UCS model. It is also recommended that using more data to develop the model gives better accurate model than less used data models.

ACKNOWLEDGMENTS

We take this opportunity to express our gratitude to the Department of Civil Engineering, University of Peradeniya and the panel members of our panel Dr.S.K.Navaratnarajah and Dr. L.C.Kurukulasuriya for their guidance during the research. We extend our gratitude to Ms. Nawanjana Maheepala for her invaluable guidance and support throughout the progress of our research study. We also thank the non-academic staffs of geotechnical laboratory for their support in carrying out the experiments.

REFERENCES

Adhikari, S., Smith, R., & Patel, K. (2019). "Assessment of Expansive Soil Properties with Artificial Neural Networks: A Comprehensive Study." Journal of Geotechnical Research, 21(3), 112-128.

Brown, C., & Taylor, D. (2019). "Predicting Compressive Strength of Expansive Soils Treated with Various Stabi lizers, Including Fly Ash, Using Artificial Neural Networks. Geotechnical Engineering Journal, 22(4), 87-102.

Chew, S. H., Kamruzzaman, A. H. M., & Lee, F. H. (2004). Physicochemical and engineering behavior of cement treated clays. Journal of geotechnical and geoenvironmental engineering, 130(7), 696-706.

Das, S.K., Samui, P., Sabat, A.K. and Sitharam, T.G., (2010). Prediction of swelling pressure of soil using artificial intel ligence techniques. Environmental Earth Sciences, 61(2), pp.393-403.

Eyo, E. U., Ng'ambi, S., & Abbey, S. J. (2020). Incorporation of a nanotechnology-based additive in cementitious prod ucts for clay stabilisation. Journal of Rock Mechanics and Geotechnical Engineering, 12(5), 1056-1069.

Gunasekara, C., Lokuge, W., Keskic, M., Raj, N., Law, D.W. and Setunge, S., (2020). Design of Alkali-Activated Slag-Fly Ash Concrete Mixtures Using Machine Learning. Mate rials Journal, 117(5), pp.263-278.

Jeremiah, J. J., Abbey, S. J., Booth, C. A., & Kashyap, A. (2021). Results of application of artificial neural networks in predicting geo-mechanical properties of stabilised clays—a review. Geotechnics, 1(1), 147-171.

Jones, A., & Brown, R. (2016). "Application of Artificial Neu ral Networks in Modeling Soil Behavior: Focus on Expan sive Soils." Geotechnical Journal, 18(3), 45-58.

Leong, H. Y., Ong, D. E. L., Sanjayan, J. G., Nazari, A., & Kueh, S. M. (2018). Effects of significant variables on com pressive strength of soil-fly ash geopolymer: variable ana lytical approach based on neural networks and genetic pro gramming. Journal of Materials in Civil Engineering, 30(7), 04018129.

Li, J., & Wu, S. (2019). "Prediction of Swelling Potential in Expansive Soils Stabilized with Different Additives using Artificial Neural Networks." Geotechnical Engineering Journal, 22(1), 75-90.

Smith, A., Johnson, B., & Williams, C. (2018). "Impact of Fly Ash on Soil Stabilization: Experimental Analysis." Journal of Geotechnical Engineering, 25(2), 123-137.

Touzet, C., Kieffer, N., & Le Goc, M. (1995). Artificial neural networks forecasting and monitoring scaffold and scaffold ing phenomena in blast furnaces. In 1995 IEEE International Conference on Systems, Man and Cybernetics. Intelligent Systems for the 21st Century (Vol. 4, pp. 3754-3759). IEEE.

Wang, Q., & Zhang, H. (2018). "Predicting the Shear Strength of Stabilized Expansive Soils using Artificial Neural Net works." Geotechnical Engineering Journal, 22(4), 103-118.

Seepage control in earthen dams using Soil-Cement-Bentonite cutoff wall

M.S. Umar and N.H. Priyankara
Department of Civil and Environmental Engineering, University of Ruhuna, Sri Lanka

ABSTRACT: Seepage is a critical challenge in civil engineering, particularly in earthen embarkments. While various methods have been employed to mitigate seepage, Soil-Cement-Bentonite (SCB) cutoff wall emerges as a cost-effective and efficient solution. This study investigates into the complications of SCB cutoff walls, analyzing SCB functions such as permeability, unconfined compressive strength (UCS), and shrinkage crack developments. Findings of this study reveal that SCB cutoff wall performances are extremely affected by the cement and bentonite addition at the same time they highly depend on the soil compositions and its properties. Further, this study emphasizes the balance between cement and bentonite content to enhance cutoff wall functioning while managing the cost. At last, a significant seepage reduction was demonstrated by employing SCB cutoff wall on a case study using SEEP/W software. In conclusion, this research supports the applications of high-performance, cost-effective and durable SCB cutoff walls.

KEY WORDS: SCB cutoff wall, Permeability, UCS, Shrinkage crack

1 INTRODUCTION

Earthen dams are artificial embarkments constructed by compacting earth including soil and rock to store water. According to the Sri Lankan history, most of the earthen dams were constructed for the irrigational purposes by the ancient kings. Since then, these dams have been serving people to fulfill varies purposes. Not only in Sri Lanka, earthen dams have been playing a crucial role globally, serving many purposes including irrigation, flood control, electricity generation and industrial usage.

However, their vulnerability to failure poses a significant risk to the surrounding environment, as evidenced by the tragic Kantale dam disaster in Sri Lanka in 1986, which killed over 100 people and destroyed many houses and lands (Weerasooriya, 2021). Among the various factors contributing to dam failure, seepage control stands out as a supreme concern. Seepage, a common occurrence in dams, can lead to soil erosion and, ultimately, dam failure. Even nowadays, it is possible to observe seepages in the downstream of Parakrama Samudraya, Samanalawewa, Tissawewa and many other reservoirs of Sri Lanka.

Other than seepage failure, the significance of seepage mitigation relays on other factors too. Most of the Sri Lankan earthen dams are only allowed to fill partially, for example Vendrasan dam is filled only up to half of its capacity (Wijayawardhana, 2015), as it can facilitate additional seepage leading to a failure. As a result, rain water which is naturally and sufficiently available in Sri Lanka is not properly utilized, leading to a water scare society.

There are varies methods and techniques which are commonly practiced to mitigate seepage through and beneath the earthen dams. Grout curtains and cutoff walls are two of such widely used methods. Irrigation department of Sri Lanka prefer to use grout curtain methods to control the seepage in existing earthen dams using either clay (bentonite) or cement (Dolage, Gamage and Karunasena, 2012). But it was not as effective as it was thought to be as many evidences for seepage were found even after grouting, for example, Ethimale reservoir in Monaragala district and Vendarasen dam in Trincomalee district (Wijayawardhana, 2015). For Vendersen dam, adopted grouting treatment was satisfactory in 2007 (Dolage, Gamage and Karunasena, 2012) but leakage was experienced later in 2015 (Wijayawardhana, 2015), which raises concern about the long term performance of grouted embarkments. Therefore, slurry cutoff walls can be considered as a better seepage mitigatory option in earthen dams. Fig.1 shows a schematic view of a cutoff wall.

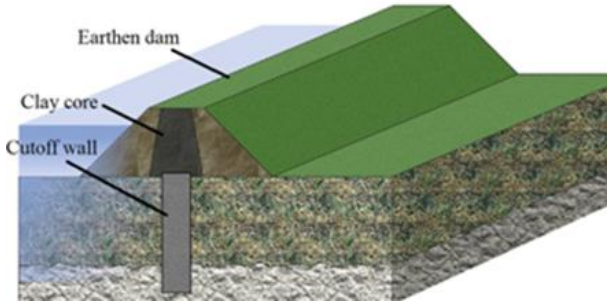

Fig. 1 Schematic view of a cutoff wall (Alós et al., 2020)

There are three prominent slurry cutoff walls with distinct advantages based on their characteristics. Soil-Bentonite (SB) walls excel in reaching low permeability, less than 1×10^{-9} m/s cost-effectively, but their strength is limited to around 15 kPa (Wijayawardhana, 2015) making them unsuitable high-load applications. Cement-Bentonite (CB) walls on the other hand, can easily reach more than 200 kPa but sacrifice permeability, typically around 1×10^{-7} m/s (Ryan and Day, 2002), making them inappropriate to mitigate seepage more effectively. In addition to that, CB cutoff wall is considered to be the costliest slurry wall. However, Soil-Cement-Bentonite (SCB) cutoff walls have a balanced approach, offering high strength, around 100-700 kPa, and permeability less than 1×10^{-8} m/s (Cao *et al.*, 2021; Ryan and Day, 2002; Tian *et al.*, 2020;). SCB walls also prove to be cost-effective, adding minimal cement and bentonite, encouraging excavated soil reuse too, which is environmental friendly.

Thus, there is a growing recognition for the effectivness of SCB slurry cutoff wall to mitigate seepage. However, according to the Sri Lankan context, slurry cutoff wall constructions are not commonly practiced due to the lack of technical knowledge, experience, and researches. Hence, this research study would be helpful to deepen our understanding of SCB cutoff wall. This research aims to obtain an optimum SCB mix proportion to an earthen dam, so that the cutoff wall has a low permeability and sufficient strength, along with the considerations of long-term effects. Finally, this findings would be further supported by estimating the total seepage controlled by the proposed optimum SCB backfill.

2 METHODOLOGY

A comprehensive methodology was adopted in order to achieve the aim of this research study and it is explained below.

2.1 *Soil tests*

Soil sample for this research study was collected from Polpithigama, where a SCB cutoff wall is under construction for Mahakithula dam. Basic soil tests were conducted to obtain the engineering properties of that soil as excavated soil is reused in the SCB wall construction. Moreover, as the major part of SCB backfill is this excavated soil, these properties need special consideration.

2.2 *SCB sample preparation*

To obtain the optimum SCB mix proportion, SCB samples were prepared by varying cement and bentonite contents with the soil. As a first step of sample preparation, 10 % concentrated bentonite slurry (bentonite: water is 1:9) was prepared and hydrated for 24 hours, allowing some time for the bentonite hydration. Then, cement grout was prepared with a Water: Cement ratio of 0.5. Finally, relevant soil sample, cement grout, and bentonite slurry were thoroughly mixed using a mechanical mixer for 10 minutes to produce the SCB mixture. Fig 2 shows the raw materials and prepared SCB backfill.

Fig. 2 Used soil, cement grout, bentonite slurry and prepared SCB backfill in the order

2.3 *SCB sample tests*

According to the SCB cutoff wall, permeability and strength are the most important parameters to be examined. Hence, permeability was measured using falling head apparatus and strength was calculated based on UCS test following the standards ASTM D5856 and D4832 respectively. Accordingly, SCB samples were casted and stored in proper way. In addition to that, some cylindrical samples were prepared, slightly similar to UCS sample, to study the shrinkage crack development. These shrinkage samples were stored under wet-dry cyclic condition to replicate the change in groundwater level, which was useful to analyze the long-term performance of the SCB cutoff wall. Daily monitoring was done to study and analyze shrinkage crack developments. Fig. 3 illustrates some of the prepared permeability, UCS and shrinkage crack analysis samples.

Fig. 3 Prepared permeability (left), UCS (middle) and shrinkage crack analysis samples (right)

2.4 *Obtaining an optimum proportion*

According to the Mahakithula dam cutoff wall specification, 7-day permeability should be less than 1 x 10^{-8} m/s and 7-day UCS should be in between 100-200 kPa. To obtain such an optimum mix proportion, experiments were conducted in three stages.

Firstly, SCB samples were prepared keeping cement content constant as 3% and varying the bentonite content. By analyzing these test results, an optimum bentonite content was obtained. Secondly, SCB samples were prepared by keeping that optimum bentonite value constant (which was 6 %) and

changing cement contents. According to this, an optimum SCB mix ratio was obtained. However, for further understanding a cross check was required with a lower bentonite content (4%) as the third stage of experiments, which was to ensure the durability and cost effectiveness of the SCB cutoff wall. All these SCB mix ratios were tested for permeability, after 7 and 28 days, and for UCS, after 7, 14, 28 and 56 days. Moreover, photos were taken daily on the developed shrinkage cracks for the analysis.

2.5 *Seepage estimation*

To estimate the amount of seepage controlled using proposed optimum SCB cutoff wall, SEEP/W (GeoStudio) software was used. Here, only the steady state flow was analyzed without considering the transient state. Cross section and soil profile of the Mahakithula embarkment was obtained from the respective site, and geometry of the model was drawn according to that. According to the soil profile, sandy soil is available up to 10m depth from the ground surface, the soil that would be used for the cutoff wall construction. Below that, a deep low permeable clayey soil layer is present. And, the earthen dam embarkment is planned to be erected for 25 m from the existing ground level with the proper compaction. Accordingly, seepage through and beneath the embarkment was estimated with and without the SCB cutoff wall.

3 RESULTS AND DISCUSSION

3.1 *Soil test results*

As already mentioned in Chapter 2.1, basic engineering properties of the Mahakithula dam was examined and its results are provided in Table 1.

Table 1. Basic soil properties

Soil Properties	Value
Specific Gravity	2.33
Fine Content	32 %
Liquid Limit	29 %
Plastic Limit	16 %
Plasticity Index	13 %
Soil type	SC
Maximum Dry Density	18.25 kN/m^3
Optimum Moisture Content	13 %
Organic Content	3.63 %
Compressive Strength	68 kN/m^2
Permeability	1 x 10^{-7} ms^{-1}
Saturated moisture content	44 %
Bulk Unit Weight	14.88 kN/m^3

Accordingly, to Table 1, the soil consists of 68% of coarse particle, which was sand. Further, permeability and compressive strength of this soil was not satisfactory for an embarkment even at the maximum compaction.

3.2 *SCB test results*

In the first stage of experiment, SCB samples were prepared keeping cement content constant as 3% and bentonite content varied between 2 to 7%. For which, 7 and 28-day permeability results of these samples are given in Table 2.

Table 2. Permeability of SCB for varies bentonite content

Mix ratio (S: C: B)	Permeability (m/s)	
	7-day	28-day
95: 3: 2	-	-
94: 3: 3	2.9E-07	-
93: 3: 4	4.4E-08	-
92: 3: 5	2.2E-08	1.0E-08
91: 3: 6	8.8E-09	7.2E-09
90: 3: 7	9.4E-09	-

According to Table 2, it is clear that permeability of SCB decreases with increasing bentonite content as well as it further decreases with time same as the study of Ruffing and Evans (2014). This is because, bentonite which is expansive in nature due to the presence of a mineral called montmorillonite, expands and fills the voids of the soil controlling the permeability through the wall.

Fig. 4 illustrates the UCS of SCB samples after 7, 14, 28 and 56 days. Accordingly, strength of the SCB decreases with increasing bentonite content whereas, it increases with time up to 28 days similar to what Owaidat, Andromalos and Sisley (1998) mentioned in his case study. Reason for lower strength with higher bentonite content was the added water content. Bentonite slurry consist of 90% of water, which highly influence the strength of the SCB in a negative way.

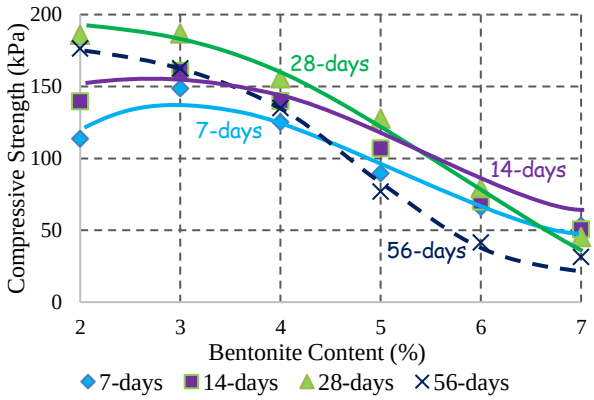

Fig. 4 UCS of SCB for varies bentonite content (3% cem)

However, from the daily monitor, it was found that shrinkage crack development plays a major role in the reduction of SCB strength, especially after 28 days. Strength of the SCB samples were considerably affected due to the shrinkage, even having an impact on its failure pattern. This behavior can be easily understood by looking at Fig. 5, where shrinkage is clearly visible in the 56-day failure sample.

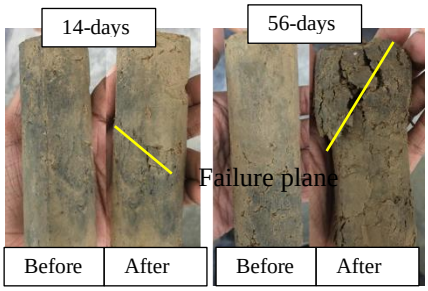

Fig. 5 Effect of Shrinkage in 56-day UCS test

Further, Regarding the shrinkage crack development with various bentonite content, cracks were higher for high bentonite containing samples. This is because of the presence of montmorillonite mineral. When the sample dries, these minerals lose their surrounded water particle casing shrinkage cracks. The effect is higher for SCB with high bentonite content. By looking at Fig. 6 it is clear that shrinkage crack development of 6% bentonite is higher than that of the 6% bentonite.

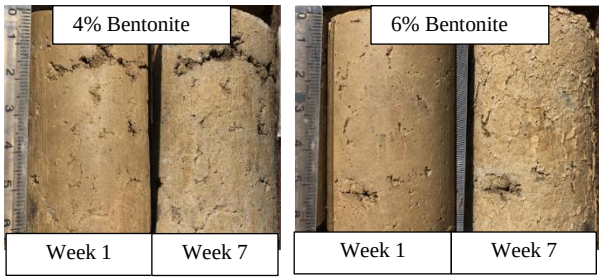

Fig. 6 Shrinkage crack development with bentonite

By analyzing the results of the first stage of experiments, 6% bentonite was considered as the optimum bentonite content. Even though it could not gain the required strength, it achieved the permeability requirement. And, strength can be easily increased by increasing the cement content in the next stage.

In the second stage of the experiments, bentonite of the SCB mixture was maintained as 6% while varying the cement content 2-7%. Table 3 shows the 7 and 28-day permeability test results.

Table 3. Permeability of SCB for varies cement content

Mix ratio (S: C: B)	Permeability (m/s)	
	7-day	28-day
92: 2: 6	1.9E-08	-
91: 3: 6	8.8E-09	7.2E-09
90: 4: 6	8.7E-09	-
89: 5: 6	8.6E-09	5.2E-09
88: 6: 6	7.9E-09	-
87: 7: 6	5.5E-09	-

Table 3 conveniently demonstrates that permeability of SCB decreases even more by increasing the cement content, with further reduction with time. Initially it was assumed that permeability would increase with addition of cement based on some literature. Even though it is contradictory to some findings, other researches including Owaidat, Andromalos and Sisley (1998) and Zhou et al (2023) support a similar pattern. This may be because of the molecular interaction between the cementitious material and the relevant soil particle, which may change from soil to soil depending on the soil composition. This is an example of how complicated SCB sample preparation is. In this case, it supports the soil mitigating seepage with its bonds.

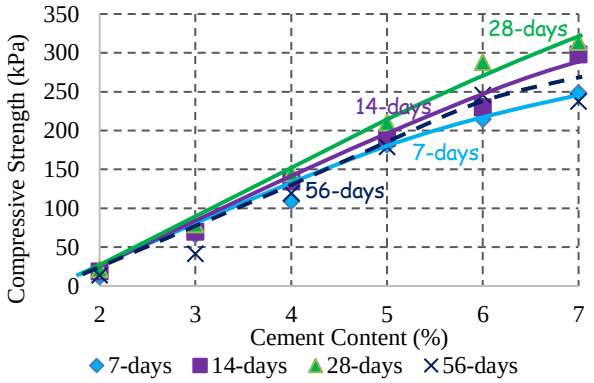

Fig. 7 UCS of SCB for varies cement content (6% ben.)

Fig. 7 describes the UCS of SCB after 7, 14, 28 and 56 days while varying the cement content. Accordingly, strength of the SCB increased while increasing the cement content and it further increased with time up to 28 days. This is because cementitious materials make a strong bond between the soil particles. Similar behavior was found in the case studies of Owaidat, Andromalos and Sisley (1998) and Zhou et al (2023). Same as before, strength of the SCB samples started to reduce after 28 days because of the shrinkage crack development. However, shrinkage crack development did not have much impact with varying cement content. Shrinkage cracks on all the cement contents were almost same, not what was observed in previous stage.

By comparing and analyzing all these results, from stage one and two, it is possible to say that SCB ratio of 90:4:6 is the optimum mix proportion, where both the permeability and strength requirements can be achieved. However, there were three factors that needed further explanation before concluding;

- High raw material requirement because of 6% bentonite and 4% cement.
- Increase in cement content decreased the permeability contradictory to initial assumption. So, why shouldn't we try for lower bentonite!
- High shrinkage crack development on high bentonite SCB samples. With 6% bentonite, long term performance is not guaranteed.

As a result, a cross check was required to find whether a lower mix proportion is possible, satisfying permeability and strength requirement as well as complying with durability and cost effectiveness. So, third stage of experiment was initiated by maintain bentonite content constant as 4% and varying the cement content between 2-5%. Table 4 provides its 7 and 28-day permeability results.

Table 4. Permeability of SCB under the cross check

Mix ratio	Permeability (m/s)	
(S: C: B)	7-day	28-day
94: 2: 4	5.5E-08	-
93: 3: 4	4.4E-08	-
92: 4: 4	5.1E-09	3.7E-09
91: 5: 4	4.4E-09	2.5E-09

According to Table 4, permeability was decreasing with increasing cement content as well as with time. This is so similar to the previous test behavior provided in Table 3, validating the reliability of these tests. And, 7, 14 and 28-day UCS results of the cross check is given in Fig 8, which is also show a similar patter like Fig. 8. UCS strength increased with increasing cement content and with time it further increased.

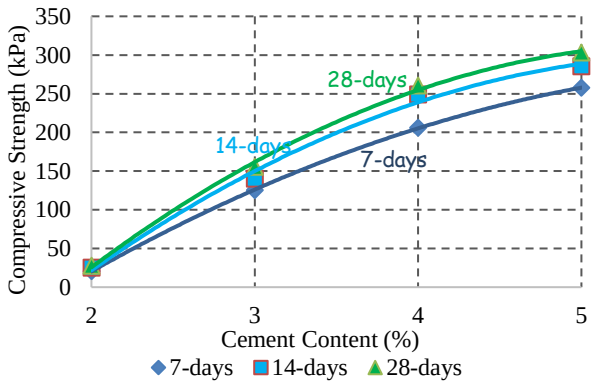

Fig. 8 UCS of SCB under the cross check

From the cross check, it was proved that the specification could be achieved even with a lower SCB mix ratio, 93:3:4. Even though permeability is slightly higher, it is still in the same order of the requirement. Hence, the optimum SCB mix ratio for mahakithula dam is 93:3:4, which can be used to construct high durability and low costly SCB cutoff wall.

3.3 *Estimated seepage through SCB cutoff wall*

As mentioned in Chapter 2.5, Seep/W software was used to estimate the seepage through the Mahakithula earthen dam with and without the proposed optimum SCB cutoff wall. Fig. 9 show the geometry of the dam and Table 5 provides the used soil parameters. Some of these soil properties were calculated from soil tests and some were obtained from past literature.

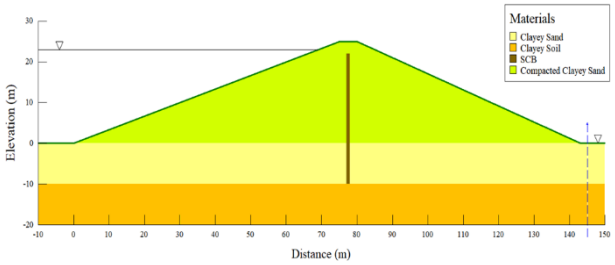

Fig. 9 Geometry and soil profile of Mahakithula dam

Table 5. Soil properties used for the modeling

Soil layer	K (m/s)	Sat VWC	RWC
Compacted SC	1.0E-07	0.132	0.03
Clayey sand	4.0E-05	0.35	0.03
Clayey soil	1.0E-09	0.5	0.09
SCB	4.4E-08	0.12	0.06

When the earthen dam was analyzed only with the compacted embarkment, without SCB cutoff wall, seepage was estimated to be 3.043e-05 m^3/s. Analyzed model is shown in Fig. 10.

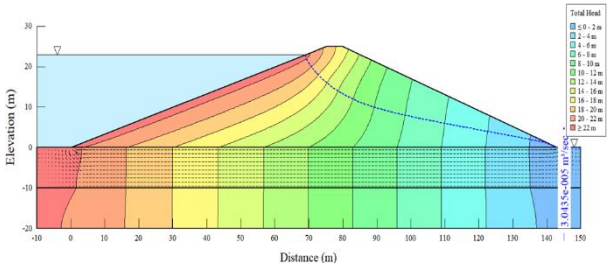

Fig. 10 Seepage through the compacted embarkment

When the model was re-analyzed with the proposed optimum SCB cutoff wall as shown in Fig. 11, seepage was reduced to 1.742e-06 m^3/s, which is 94% seepage mitigation. Hence, it validates that SCB cutoff wall can be used to mitigate seepage considerably.

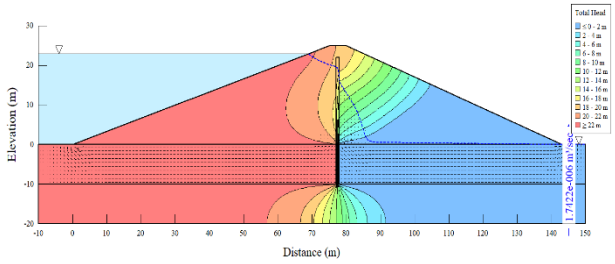

Fig. 11 Seepage through the proposed optimum SCB cutoff wall

4 CONCLUSION

Seepage is one of the most critical and frequently encountered challenge in civil engineering applications, particularly in earthen dams as it may lead to seepage failure. To overcome this challenge, SCB cutoff would be one of the best options which is more effective, economical and durable. However, certain properties of SCB cutoff wall need specific considerations.

From this research study these factors were found:

- Permeability through the SCB cutoff wall decreases with both bentonite and cement addition.
- Strength of the SCB wall increased with cement addition whereas, decreased with bentonite addition.
- Shrinkage crack development can be enhanced by high bentonite content, threatening its long-term performance.
- SCB cutoff wall performance can highly vary depending on the reused soil properties and its compositions.
- Considerable number of experiments and analysis need to be done before selecting an optimum SCB mix ratio for any civil engineering applications.
- SCB cutoff wall with mix ratio of 93:3:4 can be used in Mahakithula dam to have a 94% reduced seepage.

5 RECOMMENDATION

During this research studies, various confusions, problems and challengers were raised. Some of them need to be explored further to have a clear understanding and effective usage of SCB cutoff wall. They are;

- The impacts on the SCB wall performance by varying the mixing time of SCB backfill.
- The effects of soil properties and its composition on SCB wall performance.
  For example: fine content, organic content
- Enhancement of molecular interaction between cementitious material and soil particles.
- Slope stability of the dam, with the widening of SCB cutoff wall.
- Role of clay core in an earthen dam with the introduction of SCB cutoff wall.

ACKNOWLEDGMENTS

We would like to thank Dr. Ruwan Appuhami, Head of the department, all the academic and non-academic staffs of Department of Civil and Environmental Engineering of the Faculty of Engineering, University of Ruhuna for giving all the facilities and guidance to successfully conduct this undergraduate research study.

REFERENCES

Alós Shepherd, D., Kotan, E. and Dehn, F. (2020) 'Plastic concrete for cut-off walls: A review', *Construction and Building Materials*, 255

Cao, B., Xu, J., Wang, F., Zhang, Y. and O'Connor, D. (2021). Vertical Barriers for Land Contamination Containment: A Review. *International Journal of Environmental Research and Public Health*, 18(23), p.12643.

Dolage, D.A.R., Gamage, S.P.P. and Karunasena, T.V.K.I.S. (2012) 'Treatment of Seepage through Vendarasankulum Twin Reservoir in Eastern Sri Lanka - Cost Comparison of Alternative Techniques', *Engineer: Journal of the Institution of Engineers, Sri Lanka*, 45(3), p. 11.

Owaidat, L. M., Andromalos, K. B., and Sisley, J.L., 'Construction of a Soil-Cement-Bentonite Slurry Wall for a Levee Strengthening program', *Proceeding of pan-Am CGS Geotechnical Conferences., 2009*, pp 512-520.

Ruffing, D.G. and Evans, J.C. (2014) ' Case Study: Construction and In Situ Hydraulic Conductivity Evaluation of a Deep Soil-Cement-Bentonite Cutoff Wall ', in. *American Society of Civil Engineers (ASCE)*, pp. 1836–1848.

Ryan, C.R. and Day, S.R. (2002) 'Soil-Cement-Bentonite Slurry Walls', *Deep Foundations 2002*. pp. 713-727.

Tian, Y., He, F., Atsushi, T., Katsumi, T. and Araki, G. (2020). Influence of cement addition on barrier performance of soil-bentonite cut-off wall. *Japanese Geotechnical Society Special Publication*, 8(4), pp.96–101.

Weerasooriya, S. (2021) '*Kantale Dam Disaster 35 years later*.' <https://island.lk/kantale-dam-disaster-35-years-later/> (Mar. 29, 2023].

Wijayawardhana, H.M.J.T. (2015) 'A Study on most suitable slurry cutoff wall material to mitigate seepage in Vendrasan dam, Trincomalee', MS thesis, University of Morattuwa, Morattuwa, SL

Zhou, T., Hu, J., Liu, T., Zhao, F., Yin, Y. and Guo, M. (2023). Engineering Characteristics and Microscopic Mechanism of Soil–Cement–Bentonite (SCB) Cut-Off Wall Backfills with a Fixed Fluidity. *Materials*, 16(14), pp.4971–4971.

Strength Mobilization in Soft Clayey Soils Mixed With Quarry Dust And Cement in Early Curing

R.D.M.P Rajapksha, W.M.N.R Weerakoon
Department of Civil Engineering, University of Sri Jayewardenepura, Sri Lanka

ABSTRACT: This research was conducted to investigate the strength mobilization characteristics of soft clayey soil mixed with quarry dust and cement in early curing. This study provides valuable insights to reduce costs, utilize available resources, overcome soil limitations and promote sustainable construction practices. This study aims to estimate the strength of soil mixture at 3 days, 7 days, 14 days, and 28 days of curing under different proportions of quarry dust and cement. The selected proportions were based on the weight of the composition which contained 5% to 30% quarry dust and 2% to 8% cement. Laboratory mechanical tests including unconfined compressive strength tests and direct shear tests were used in this. According to the results of the tests, it shows that the strength increases with the increase in the cement and quarry dust proportions for different curing periods.

KEY WORDS: Soft clayey soil, Cement, Quarry Dust, Direct shear test, Unconfined compressive strength test

1 INTRODUCTION

Soft clay soils are recent alluvial deposits formed within the past 10,000 years, characterized by their featureless and flat ground surface (Brand and Brenner, 1981). These soils are typically found near or below the water table and consist of large fractions of fine particles such as silt and clay, with high moisture content. (Kamon and Bergado, 1991).

The physical and mechanical properties of soft clays usually vary significantly due to the variations in sedimentary processes associated with different environmental conditions. (Saadeldin and Siddiqua, 2013) The properties of soils have been examined in previous studies using constant confining pressure triaxial testing, variable confining pressure triaxial apparatus, resonant column testing, and shear testing. In general, soft clay soil has the characteristics of low carrying capacity, shallow water table, high water content, high compression, sensitivity, and large touch degeneration. (Zhu et al., 2021). The study conducted by Hussein, Zeena, and Salsabeel in 2015 highlighted several characteristics of soft clayey soils. According to their findings, soft clayey soil has Low undrained shear strength (Cu < 40 kPa), High compressibility (Cc between 0.19 to 0.44), High natural moisture content (typically ranging from 40-60%) and Plasticity index ranging from 45-65%.

Soft clay soils with poor properties can pose significant challenges for irrigation structures, embankments, and road construction. The decreased stiffness and strength of soft clay can lead to excessive settlement and failure of bearing capacity, which can have detrimental effects on the foundations of buildings. (Mubeen, 2007). Soil stabilization methods involve the use of stabilizing agents in soft clayey soils to improve their geotechnical properties such as compressibility, strength, permeability and durability. Cement, lime, gypsum, fly ash, coal ash, marble dust, quarry dust, and different additives are used to increase the strength parameters of soft clayey soil. (Makusa, 2013). In this research, cement and quarry dust are used as additives to improve the strength of soft clay soils.

Quarry dust is characterized by a high fine content, which refers to the proportion of fine particles present in the material. It is a cohesionless, non-plastic material. The unit weight and other material properties of quarry by-products can vary according to the source but are relatively constant at a particular site. The high fine content contributes to improving workability and cohesiveness in certain applications, such as in the production of self-compacting concrete. Quarry dust particles are generally angular in shape due. The angular nature of the particles can provide improved interlocking and stability when used as fill material or in certain construction applications. (Sridharan et al., 2006) Quarry dust has favorable engineering properties such as higher density, good compaction, high shear strength, and reduced permeability compared to natural sands. When added to soft clayey soils, it leads to improvements including reduced plasticity, increased maximum dry density, decreased optimum moisture content, and increased unsoaked and soaked CBR values. (David Suits et al., 2005)

Cement is a fine powder material. It may be considered a primary stabilizing agent or hydraulic binder because it can be used alone to bring about the stabilizing action required (Makusa, 2013). Considering previous researches, the most commonly used type of cement is Portland cement. The addition of cement to the soft clayey soil triggers a chemical reaction, forming cementitious hydrates that bind soil particles together, improving strength, cohesion, and stability for construction purposes.

This research work aims to investigate the strength mobilization of the soft clayey soil by mixing it with quarry dust and cement in early curing. The objectives of this research are to investigate the optimum mixed proportion of quarry dust and cement for high-strength mobilization, to study the strength improvement of soft clayey soil mixed with different mix proportions of cement and quarry dust, to investigate the strength mobilization of the different mix proportions with curing time. and to compare the strength obtained by direct shear test and unconfined compressive test. The study of strength mobilization in soft clay soils mixed with cement and quarry dust provides valuable insights for achieving stability, reducing costs, utilizing available resources, addressing land limitations, and promoting sustainable construction practices.

2 METHODOLOGY

2.1 *Material used*

(i) Soft clayey soil

The disturbed soil samples intended used in this test were collected from Gampaha, the Blugahagoda area. These soils typically consisted of fine particles including clay, silt, and sand.

(ii) Quarry dust

The quarry dust sample which used for the tests was collected from a rubble crusher unit. The quarry dust used here is less than 3.35 mm in diameter.

(iii) Cement

In this study, Ordinary Portland cement was selected as the cement type for the research. The specific grade of cement utilized for this study was 42.5.

2.2 *Sample preparation*

The dry clay samples were collected and crushed into smaller particles, followed by the addition of water to create a homogeneous mixture. The normalized water content was maintained at 1.5 to ensure consistency in all mixing ratios. The normalized initial water content is calculated using the following formula.

$$w_i = \frac{(w-LL)}{LL} \times 100 \quad (1)$$

Where $\mathbf{w_i}$ is the normalized initial water content, **w** is the actual water content of the soil sample, *LL* is the liquid limit of the soil.

In this study, different proportions of quarry dust and cement were mixed with soft clayey soils. The quarry dust proportions included 5%, 10%, 20% and 30% of the soil weight, while the cement proportions consisted of 2%, 4%, and 8% of the soil weight. Before mixing the quarry dust it was dried in an oven for 24 hours to remove moisture. To prevent water evaporation and promote proper curing, it was covered the moulds with polyethene sheets. The purpose of wrapping the moulds is to maintain a consistent moisture content within the specimens during the curing process.

2.3 *Experiments*

2.3.1 *Atterberg limit tests*

Atterberg limit tests were performed on soft clayey soils according to the ASTM D4318 standard test procedures to determine their plasticity and to establish their liquid limit (*LL*), plastic limit (*PL*), and plasticity index (*PI*).

$$PI = LL - PL \quad (2)$$

Fig 1. *LL* test and *PL* test

2.3.2 *Particle size distribution test*

The quarry dust samples used for this purpose were cleaned and properly passed through a 3.35 mm sieve to remove coarser inclusions. Also, it is oven-dried for 24 hours to remove moisture before testing. Then the particle size distribution test was done for quarry dust in accordance with ASTM D1140 Test Method.

2.3.3 *Unconfined Compressive Strength (UCS) Test*

The purpose of this test is to identify the unconfined compressive strength of the soft clayey soil

sample as there is no lateral support. A cylindrical mould of 50mm diameter and 100mm height was used to prepare samples. A UCS test is performed on samples with sufficient strength to stand alone. Due to the low shear strength of soft clay soil treated with cement immediately after mixing, it was not possible to perform unconfined compression tests on the samples. As a result, the decision was made to conduct the first UCS test on the samples on the 3rd day after the sample preparation. The curing periods chosen for this particular test are 3, 7, 14, and 28 days. The UCS test was conducted in accordance with the ASTM D2166 test procedure.

Fig 2. UCS test

2.3.4 Direct shear test

The direct shear tests were performed to determine the effect of the cement and quarry dust inclusion on the shear strength of soft clay soil. The direct shear test is performed under fixed conditions and according to standard ASTM D3080-90. It gives the relation between shear stress and horizontal displacement of clay which is mixed with quarry dust and cement. Dimensions of the shear box for the Direct shear test are 100mm × 100mm × 25mm. The test was carried out for a curing period of 3 days, 7 days, 14 days and 28 days. The test was done as strain-controlled tests by applying a constant rate of 3mm/min displacement. The horizontal displacement was limited to 15 mm.

3 RESULTS AND DISCUSSION

3.1 *Atterberg limit tests results*

Table 1: Results of the Atterberg tests

Liquid Limit	29.375%
Plastic limit	16.88%
Plasticity Index	12.5%

3.2 *Particle size distribution test results*

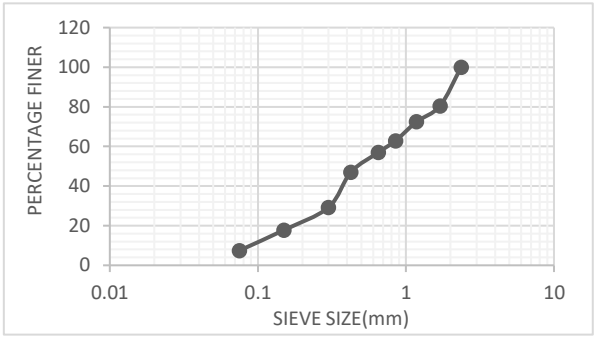

Fig 3. Particle size distribution of quarry dust

3.3 *Unconfined Compressive Strength (UCS) Test results*

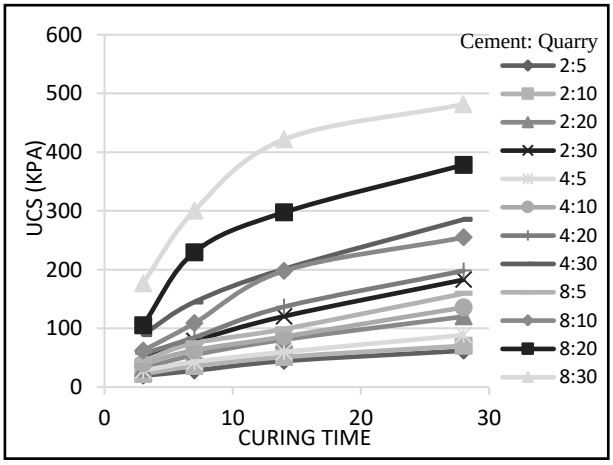

Fig. 4. UCS Value variation with the curing time

The graphs show a consistent relationship between the proportion of quarry dust and the resulting unconfined compressive strength (UCS) values, with a linear fluctuation observed from 5% to 30% quarry dust content. At early curing stages, there is no significant difference in UCS values among different proportions, indicating consistent early strength development. However, after 28 days, the 30% quarry dust proportion exhibits a higher variance in UCS values, suggesting greater variability. Additionally, an 8% cement mixture consistently shows higher UCS values compared to 2% and 4% cement mixtures, indicating improved strength with higher cement content. Overall, increasing curing time leads to higher UCS values, and the sample with 8% cement and 30% quarry dust demonstrates the highest UCS value, indicating its effectiveness in enhancing compressive strength.

3.4 *Direct shear test results*

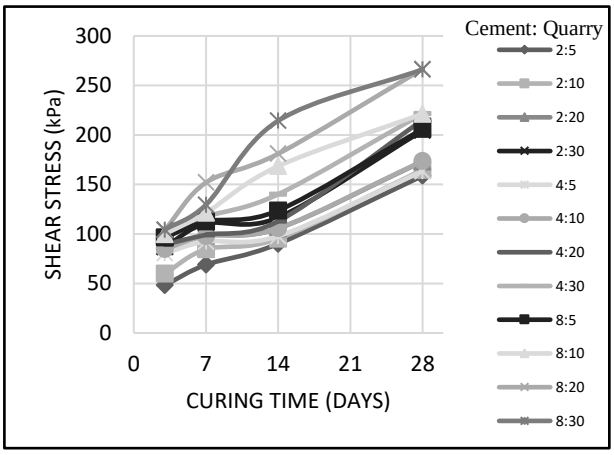

Fig. 5. Shear strength Value variation with the curing time

The graphs indicate that the addition of cement and quarry dust enhances the shear stress of the soft clayey soil. Increasing curing time also leads to improved shear strength. Among the tested cement contents (2%, 4%, and 8%), the sample with 8% cement consistently shows significantly higher shear stress values, indicating the positive effect of higher cement content on shear strength. After 28 days of curing, the soil sample with 30% quarry dust and 8% cement achieves the maximum shear stress value of 266.6 kPa.

3.5 *UCS and Direct shear tests Results compression*

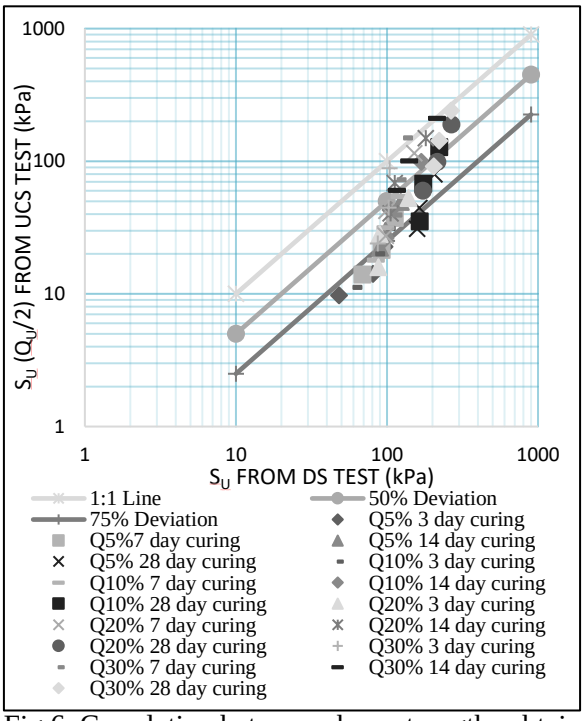

Fig 6. Correlation between shear strengths obtained by two tests

According to this figure shear strength values measured from the direct shear tests were higher than those from the UCS Test for most data points. To assess the deviation between the two types of tests, a 1:1 ratio line was considered. However, it was observed that the *Su* values obtained from the two tests did not align perfectly with this line. As a result, two deviation lines were introduced to better represent the differences between the two test methods. *Su* values obtained at 3 days and 7 days curing are close to 50% deviation and 14 days and 28 days curing are close to 75% deviation line.

4 CONCLUSION

In conclusion, the study focused on investigating the strength mobilization characteristics of soft clayey soil mixed with quarry dust.

- These findings indicate that both the cement content and the proportion of quarry dust significantly influenced the shear strength of the soil samples.
- The combination of 8% of cement and 30% of quarry dust led to substantial improvements in shear strength.
- Curing time was found to play a significant role in the strength development of soil samples. There was a noticeable increase in shear strength with increasing curing time.
- Comparing the test results obtained from these two tests, for most data points the shear strength values obtained from the direct shear tests were higher than the shear strength values measured from the UCS test.
- There is a higher deviation for low shear strength and the deviation reduces with the increase of shear strength between the two tests.

5 REFERENCES

Brand, E.W. and Brenner, R.P. (1981). Soft Clay Engineering. Amsterdam: Elsevier Scientific Publishing Company, pp.27–30.

David Suits, L, et al. “Utilization of Quarry Dust to Improve the Geotechnical Properties of Soils in Highway Construction.” *Geotechnical Testing Journal*, vol. 28, no. 4, 2005, p. 11768, www.researchgate.net/publication/245403560 [Accessed 13 April 2023].

Hussein, K., Zeena, S. and Salsabeel, A. (2015). Geotechnical Properties of Soft Clay Soil Stabilized by Reed Ashes. American

University-Beirut, pp.117–122. < https://www.researchgate.net/publication/311729858> [Accessed 17 September 2022.]

Kamon, M. and Bergado, D.T. (1991). Ground Improvement Techniques. 1st ed. Bangkok, Thailand: 9th Asian Regional Conf.Soil Mech.Found.Eng'g., pp.526–546. [Accessed 29 August 2022].

Makusa, G.P.M. (2013). Soil Stabilization Methods And Materials. pp.1–5. Doctoral thesis, Luleå University of Technology Luleå, Sweden.

Mubeen, M.M. (2007). Stabilization of Soft Clay for Irrigation Structures for Efficient Use of Water. Engineer: Journal of the Institution of Engineers, Sri Lanka, 40(1), p.53. https://doi:10.4038/engineer.v40i1.7128. [Accessed 21 September 2022].

Saadeldin, R. and Siddiqua, S. (2013). Geotechnical characterization of a clay–cement mix. Bulletin of Engineering Geology and the Environment, [online] 72(3-4), pp.601–608. https://doi:10.1007/s10064-013-0531-2. [Accessed 21 September 2022].

Sridharan, A., Soosan, T.G., Jose, B.T. and Abraham, B.M. (2006). Shear strength studies on soil-quarry dust mixtures. *Geotechnical and Geological Engineering*, 24(5), pp.1163–1179. doi: https://doi.org/10.1007/s10706-005-1216-9. [Accessed 05 November 2022].

Zhu, Z., Zhang, C., Wang, J., Zhang, P. and Zhu, D. (2021). Cyclic Loading Test for the Small-Strain Shear Modulus of Saturated Soft Clay and Its Failure Mechanism. Geofluids, 2021, pp.1–13. https://doi:10.1155/2021/2083682. [Accessed 01 November 2022.]

Stabilization of Subgrade Using Geosynthetics

U.D.M. Kumara and N.H. Priyankara
Department of Civil and Environmental Engineering, University of Ruhuna, Sri Lanka

ABSTRACT: In Sri Lanka, according to the CIDA guidelines, 4-day soaked CBR value of the subgrade should be greater than 5% for road construction. Weak subgrades adversely affect road durability, safety, and cost. Current treatment methods, including removal and replacement, soil stabilization, and increasing base thickness, emerge challenges with cost, time, and environment. Research objectives focus on the effect of geosynthetics to improve weak subgrade characteristics, considering the geosynthetic strength and placement within flexible pavement. To predict the 4-day soaked CBR value of subgrade material with the change of moisture content, a mathematical model was developed. The research findings highlight the effect of geosynthetic layer strength at the subgrade-subbase interface and location inside the subbase in significantly improving the ultimate load-bearing capacity of weak subgrades. Geosynthetics can be applied as cost-effective and environmentally friendly solution to mitigate the challenges related to weak subgrades leading to a sustainable road construction.

KEY WORDS: Weak Subgrade, Subbase, CBR, Geosynthetics, Moisture Content

1 INTRODUCTION

Engineers face challenges in road construction projects related to cost reduction, environmental pollution, and long-term road durability. In these cases, both the total cost of the project and the road durability are significantly affected by the strength of the subgrade. Road cross section consists of layers as surface course, base, subbase, and subgrade. The subgrade, which can be either natural ground or an embankment, is considered as the foundation of the pavement. The subgrade is responsible for bearing the traffic loads because the base transfers these loads to the subbase. Consequently, the subgrade needs to have enough bearing capacity to withstand the stresses generated by increased traffic loads. Weak subgrades cause for problems such as settlement, cracks, and ineffective drainage, which significantly reduce pavement durability.

According to CIDA guidelines, for road construction, 4-day soaked California Bearing Ratio (CBR) value of subgrade at maximum dry density (determined by the modified Proctor compaction test) must exceed 5% (ICTAD, 2009). Consequently, the subgrade is defined as weak if the 4-day soaked CBR value is less than 5%. Other than increasing project costs, traditional methods of treating weak subgrades such as removing and replacing, stabilizing the soil, and increasing the base thickness also add to environmental pollution during road construction. In developed countries, geosynthetics have been gained attention as a paramount solution to these problems. Geosynthetics provide an economical and environmentally responsible way to improve the engineering characteristics of subgrades and improving pavement durability, while reducing project costs, construction period, environmental effects,

Geosynthetics are applicable in a wide range of applications. Geosynthetics can be categorized as products including geotextiles, geogrids, geomembranes, geosynthetic clay liners, geofoam, geocells, and geocomposites. Filtration, separation, drainage, barrier construction, reinforcement, and protection are some primary uses of geosynthetics. Geogrids and geotextiles are the main types of geosynthetics used in road construction, mostly for reinforcing purposes.

This research project aims to enhance the engineering characteristics of subgrade materials with the application of geosynthetics. Three objectives have been defined to achieve this aim. The first objective is to determine a relationship between subgrade moisture content and 4-day soaked CBR values. The second objective is to investigate how the improvement of subgrade characteristics is affected by the strength of geosynthetics. The third objective is to determine how the location of geosynthetic layers inside the subbase impacts the subgrade engineering characteristics.

Although plenty of research has been conducted regarding the use of geosynthetics for stabilization of subgrade, less exists in Sri Lanka. Research in this area is vital because stabilization techniques are especially important for subgrades with CBR values less than 5%. Series of plate load tests were conducted to investigate the increased bearing capacity that results from applying a geosynthetic layer at the

interface between the subgrade and subbase. A key part of this study is the analyze of the vertical stress distribution in the subgrade following geosynthetic application, a topic that has not been deeply covered in the literature to date. Unlike previous research that has only examined horizontal stress changes, this study also evaluates the vertical stress distribution along the vertical axis. Furthermore, this study provides a substantial contribution by developing a prediction model for CBR values associated with moisture content variations. Its goal is to develop ultimate results that clarify a precise relationship between moisture content and CBR values. Also, the study explores the impact of various strengths of geosynthetics on CBR values in weak subgrades. A detailed analysis of the vertical stress distribution in the subgrade reinforces this.

2 LITERATURE REVIEW

Use of geosynthetics in road construction possesses several benefits, such as preventing base course material from lateral movements, increasing the flexural stiffness of the base course, and reducing the maximum vertical stress on the subgrade (Perkins ,1999). A predictive model for 4-day soaked CBR value was developed in the study by Wimalasena et al., (2022) by considering moisture content and compaction level variations. A study on "monotonic loading test to investigate the benefits of composite geogrids for subgrade improvement" was undertaken by Kankanamge, Jay- and Prasad, (2022). For the plate load test, they used a steel test box having dimensions 1.0 m in length, 1.0 m in width, and 1.0 m in height. Two test models that were reinforced with composite geogrid and unreinforced were also considered. A 500mm thick, weak subgrade was constructed at the bottom of model box. The granular layer was constructed on top of the subgrade layer to a height of 200 mm for both the reinforced and unreinforced tests. Composite geogrid was applied at the interface.

3 METHODOLOGY

This research was adhered to the following methodology to achieve the objectives.

3.1 *Material selection*

Figure 1 illustrates the subgrade material used in the experiments, which had a 4-day soaked CBR value of less than 5%. Consequently, this subgrade was classified as a weak subgrade.

Fig.1 Subgrade material

Basic engineering characteristics of the subgrade material were determined, and table 1 summarizes these characteristics.

Table 1. Summary of engineering properties of subgrade material

Subgrade Engineering Property	Value	Unit
Fine content	60.79	%
Gravel content	3.62	%
Sand content	35.59	%
Liquid limit	58	%
Plastic limit	43	%
Plasticity Index (PI)	15	%
Soil classification	MH	
Specific gravity	2.481	
Saturated moisture content	60	%
Maximum dry unit weight	15.1	kN/m^3
Optimum moisture content	22	%
4-day soaked CBR @ OMC	2.39	%

3.2 *Determination of a relationship between 4-day soaked CBR value of the subgrade material and moisture content*

The first objective of this research is to develop a relationship between the subgrade moisture content and its 4-day soaked CBR value. The determination of 4-day soaked CBR values at various moisture contents for the same subgrade material is made easier by this relationship. This is crucial as it saves the time and labor cost for conducting number of 4-day soaked CBR trials. This was accomplished by conducting five 4-day soaked CBR tests at different moisture contents while keeping the CBR specimen's dry density range constant. The moisture content, dry unit weight, and experimental CBR values of the CBR specimens are shown in table 2. A regression model was developed based on the experimental CBR data, and it was validated by another

three 4-day soaked CBR trials at various moisture contents.

Table 2. Experimental results of CBR trials

Moisture content (%)	4-day soaked CBR value (%)	Dry unit weight (kN/m3)
4.66	8.07	14.59
8.97	6.06	14.42
14.31	4.22	14.37
21.67	2.39	14.16
29.31	1.65	14.08

3.3 *Plate load tests of stabilized subgrade using geosynthetics*

The following method was followed to achieve the second objective, which is to determine the impact of geosynthetic strength on improving subgrade characteristics, and the third objective, which is to determine the effect of geosynthetic location on improving subgrade characteristics.

Static plate load testing was conducted to evaluate the effect of geosynthetics to enhance the subgrade's load bearing capacity. A steel box with inside dimensions of 580 mm in height, 480 mm in width, and 625 mm in length was used to make the model sections, which is illustrated in figure 2. Four model sections were used to investigate how geosynthetic strength affects weak subgrade stabilization, while two model sections were used to evaluate the effect of geosynthetic location on weak subgrade stabilization.

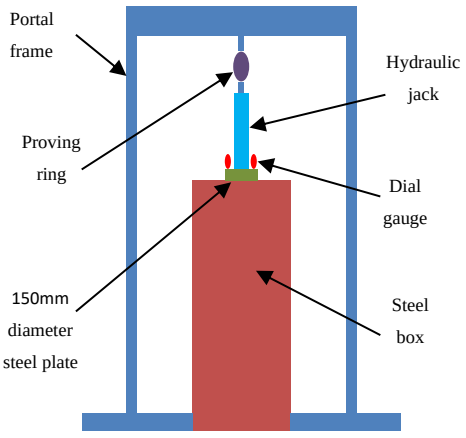

Fig.2 Loading setup for Plate load test

The subgrade's maximum dry unit weight of 15.1 kN/m³ and optimum moisture content of 22% were continuously maintained throughout all model sections, while the maximum dry unit weight of 20.6 kN/m³ and the optimum moisture content of 5.2% were maintained for the subbase. Moreover, the subbase and subgrade thicknesses for each model section were respectively kept as 150 mm and 300 mm. Using a hydraulic jack, the load was transferred to the soil through a 150 mm diameter circular steel plate centered on the top surface of the soil. The force applied by the hydraulic jack was measured with a proving ring, and the settlement of the steel plate was measured using two dial gauges.

An illustration of a pavement model section with earth pressure sensor installation is shown in figure 3. Three earth pressure sensors were placed 50 mm, 100 mm, and 200 mm below the subgrade interface, respectively, below the center of a circular steel plate.

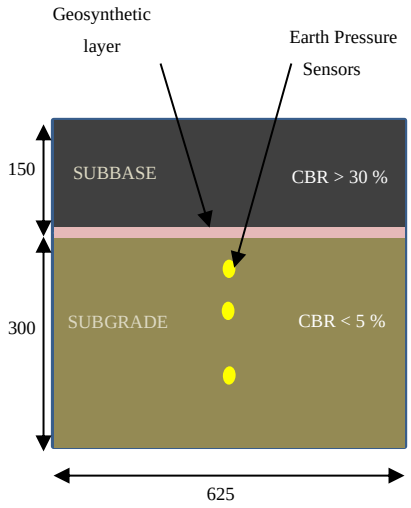

Fig.3 Pavement model section

To achieve second and third objectives, a series of plate load tests were conducted. Firstly, a geosynthetic layer was placed at the interface between the subgrade and subbase to evaluate the effect of geosynthetic strength on improving subgrade characteristics. Four experiments were carried out with different geosynthetic types and strengths. Details on which type of geosynthetic was used in each test are given in Table 3.

Table 3. Type and strength of geosynthetic layer at the interface for each test

Test no.	Type of geosynthetic
1	No geosynthetics
2	100/50 geotextile
3	200/50 geotextile
4	Composite geogrid

A geosynthetic layer was placed at the interface between the subgrade and subbase, while another layer was placed inside the subbase to satisfy the third objective, which is to evaluate the effect of the geosynthetic location on enhancing subgrade characteristics. The locations of geosynthetic layers for every test are listed in table 4.

Table 4. Location of geosynthetic layers for each test

Test no	Location of geosynthetic layers
5	Interface + middle of the subbase
6	Interface + upper one third of subbase

It was determined that the subgrade material at 5% moisture content has a 4-day soaked CBR value of 8.07% using the prediction model developed to satisfy the first objective, which predicts 4-day soaked CBR values at different moisture content. The final model section was constructed by maintaining the subgrade at 5% moisture content and a dry unit weight of 14.1 kN/m³ without placing a geosynthetic layer at the subgrade-subbase interface.

The resulting load vs. settlement curve from this specific model section was then compared to the load vs. settlement curves of the other six model sections. This comparison aimed to confirm whether, with the application of a geosynthetic layer, the ultimate bearing capacity of the weak subgrade exceeds the ultimate bearing capacity of the same subgrade material with a 4-day soaked CBR value greater than 5%.

4 RESULTS AND DISCUSSION

The results of the tests carried out to achieve the objectives are shown in this section. The results include a series of 4-day soaked CBR tests to determine the relationship between moisture content and 4-day soaked CBR values. For analyzing the outcomes, earth pressure sensor records and applied pressure versus settlement curves from a series of plate load tests carried out with various geosynthetic layer applications are also included.

4.1 *Prediction model for 4-day soaked CBR value of subgrade material with the change of moisture content*

The 4-day soaked CBR value versus moisture content is shown graphically in Figure 4. A strong correlation between the moisture content variations and the 4-day soaked CBR value may be predicted by developing a regression model, as indicated by the graph. The coefficient of estimation (R^2) value of 0.9982 for the regression model with the formula $y = 10.824e^{-0.066x}$ confirm that the relationship is strong. As a result, the developed regression model exhibits a good accuracy and can be applied to predict 4-day soaked CBR values in dependence on moisture content variations.

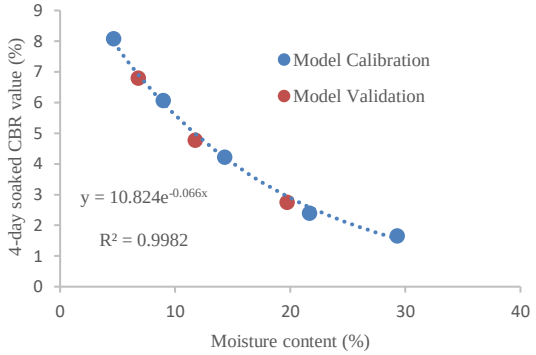

Fig.4 Graph of 4 day soaked CBR value Vs moisture content

4.2 *Effect of geosynthetic strength on stabilization of weak subgrade*

The pressure versus settlement curves of model sections are shown in figure 5, which shows the effect of a geosynthetic layer of different strengths at the subgrade/subbase interface.

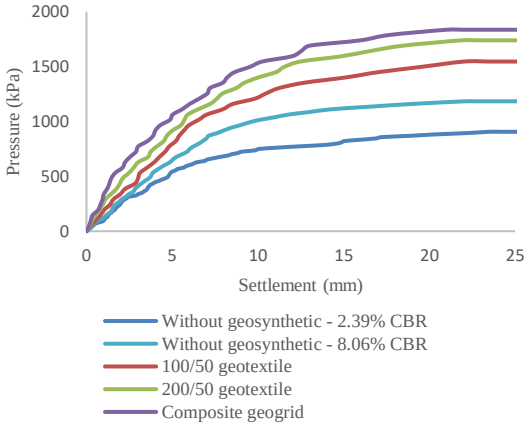

Fig.5 Pressure Vs settlement curves of model sections with the application of a geotextile layer

With a subgrade having a 4-day soaking CBR value of 8.06%, the maximum bearing capacity of subgrade without a geosynthetic layer is determined to be 1184 kPa. Notably, the final bearing capacities of weak subgrades that have been stabilized with a single geosynthetic layer exceed the measured value of 1184 kPa. This finding emphasizes that a geosynthetic layer placed between a weak subgrade and subbase can significantly increase the ultimate bearing capacity of weak subgrade when compared to a subgrade with a 4-day soaking CBR value of more than 5%.

Figure 6 illustrates the bearing capacity ratio of model sections in comparison to the model section possessing a subgrade with a 2.39% 4-day soaked CBR value without a geosynthetic layer.

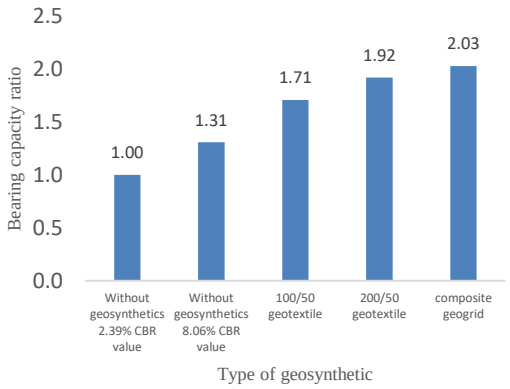

Fig.6 Variation of bearing capacity ratio with type of geosynthetic layer at the interface

The application of a geosynthetic layer results in an increment of weak subgrade bearing capacity by over 70%. Nevertheless, there is no statistically significant improvement in bearing capacity with the further increment of strength of the geosynthetic material.

4.3 *Effect of geosynthetic location on stabilization of weak subgrade*

The pressure versus settlement curves for the model sections with 200/50 geotextile layers at various locations are presented in figure 7.

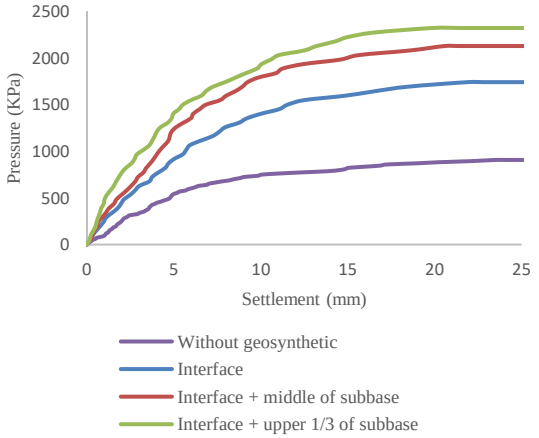

Fig.7 Graphs of pressure Vs settlement with the location of 200/50 geotextile layers

The ultimate load bearing capacity of the weak subgrade increased in proportion to the number of geotextile layers added. Furthermore, putting the second geotextile layer closer to the top surface resulted in a noticeable improvement in the ultimate bearing capacity of weak subgrade. These results demonstrate that the total bearing capacity of the weak subgrade is affected by the number and location of geotextile layers.

Figure 8 depicts the bearing capacity ratio of model sections in contrast to the model section with a subgrade having a 2.39% 4-day soaked CBR value, and a 200/50 geotextile layer at the interface between the subgrade and subbase.

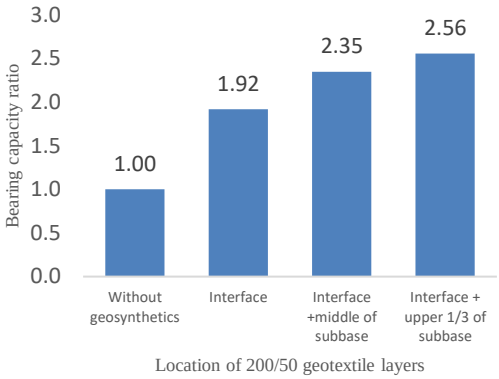

Fig.8 Variation of bearing capacity ratio with the location of 200/50 geotextile layers

The application of two geotextile layers increases the bearing capacity of the weak subgrade by more than 135%. Moreover, bearing capacity can be raised by roughly 20% by placing the second geosynthetic layer at the upper 1/3 of the subbase instead of the second geosynthetic layer at the middle of the subbase.

4.4 *Effect of geosynthetics on vertical stress reduction of subgrade*

The maximum vertical stress variation within the subgrade is shown in figure 9 at three different depths from the interface as 50 mm, 100 mm, and 200 mm. Earth pressure sensors were positioned for recording these measurements.

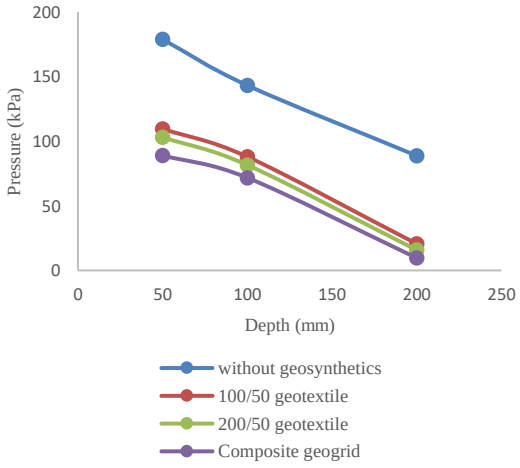

Fig.9 Graph of vertical stress Vs depth of the subgrade from the interface

The graphs presented indicate how the placement of a geosynthetic layer results in a significant reduction in the vertical stress applied to the subgrade with a reduction that exceeds a 50% drop. This pressure drop reduces the subgrade settlement, which decreases the possibility of cracks and potholes developing in a road during its serviceability state.

Figure 10 presents the percentage reduction in vertical stress along the depth of the subgrade, compared with the vertical stress at equivalent depths in the subgrade without a geosynthetic layer.

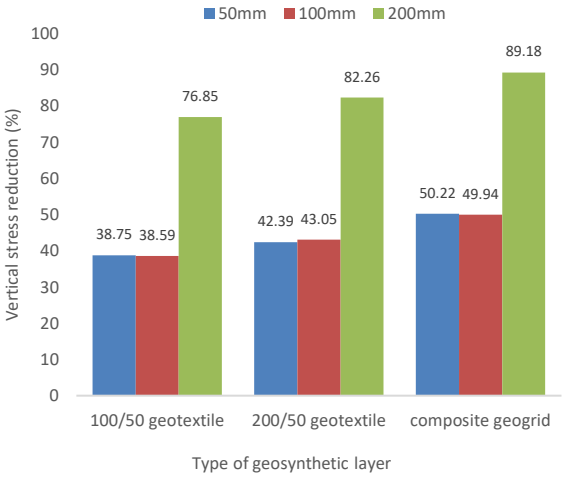

Fig.10 Variation of vertical stress reduction with type of geosynthetic layer

Compared to other types of geosynthetics, composite geogrid shows a significant decrease in vertical stress. Overall, at 200 mm depth in the subgrade, each geosynthetic layer contributes to reduce vertical stress by more than 70%.

Figure 11 shows the percentage reduction in vertical stress along the depth of the subgrade with the location of two 200/50 geotextile layers, compared with the vertical stress at equivalent depths in the subgrade without a geosynthetic layer.

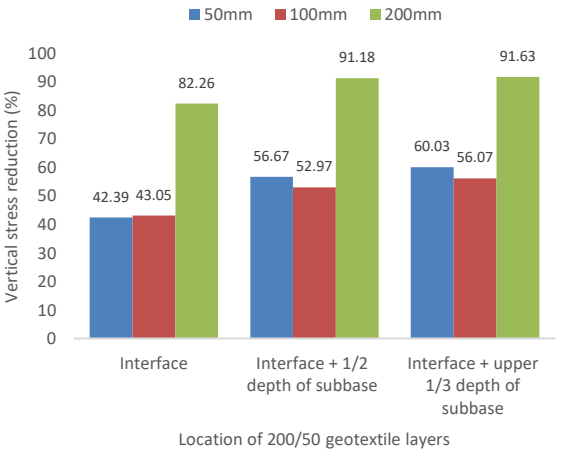

Fig.11 Variation of vertical stress reduction with location of 200/50 geotextile layers

According to the figure 11, the application of two geotextile layers results in a reduction of vertical stress exceeding 90% at a depth of 200mm within the subgrade. Nevertheless, there is no significant reduction in stress observed with the location of second geotextile layer inside the subbase.

5 CONCLUSIONS

Following conclusions can be drawn based on experimental results of the research study.

- A mathematical model can be developed to predict the 4-day soaked CBR value as a function of moisture content. Use of such a model reduces both time and labor requirements, which need for conducting number of CBR trials in road construction.
- The ultimate bearing capacity of a weak subgrade can be significantly enhanced compared to that of a subgrade with a 4-day soaked CBR value exceeding 5% through the application of a geosynthetic layer. Hence, geosynthetics can be used as a sustainable material, which satisfy the CIDA guidelines on road construction in Sri Lanka.
- Further improvement of the ultimate bearing capacity of a weak subgrade can be achieved by introducing two geosynthetic layers at the interface between the subgrade and subbase, as well as inside the subbase.
- The application of a geosynthetic layer within a flexible pavement leads to a substantial reduction in vertical stress inside the subgrade. This reduction is crucial for minimizing pavement settlement, which mitigates road cracks.

6 REFERENCES

ICTAD, I. f. (2009). Standard Specification for Construction and Maintenance of Roads and Bridges (Vol. Publication No: SCA/5).

Kankanamge, M., Jay-, G. and Prasad, C. (2022) 'Monotonic Loading Test to Investigate the Benefits of Composite Geogrids for Subgrade Improvement', pp. 0–14.

Nazzal M., 2007. "Laboratory Characterization and Numerical Modeling of Geogrid Reinforced Bases in Flexible Pavements". PhD dissertation, Louisiana State University, Baton Rouge, LA.

Perkins, S. W. 1999. "Geosynthetic Reinforcement of Flexible Pavements Laboratory Based Pavement Test Sections", Final Report FHWA/MT-99- 001/8138, State of Montana department of transportation research, and development and technology transfer program, Bozeman, Montana, USA, 108 pp.

Wimalasena, et al (2022) 'Predicting California Bearing Ratio (CBR) Value of a Selected Subgrade Material', pp. 0–12.

Partial Soil Replacement Strategies for Enhancing Soft Soil Conditions Beneath Shallow Foundations

G.K.H. Wijesooriya, Prof. L.I.N. De Silva
Department of Civil Engineering, University of Moratuwa, Sri Lanka

ABSTRACT: Soft soil replacement is a widely used technique to enhance the subsurface conditions beneath shallow foundations. It involves replacing weak and unstable soil types like peat, medium or soft clay, and organic soils with more reliable and competent materials such as crushed concrete, granular soil, or rock boulders. By implementing soil replacement, the bearing capacity of the foundation is increased, while the expected settlement is reduced. This leads to improved overall stability and performance of the foundation system. This paper presents the results of the study on partial soft soil replacement under shallow foundations. The effects on the width and depth of the replacement, soft soil properties, and properties of the replacement materials have been studied. A two-dimensional plain strain model is developed using the finite element program, PLAXIS 2D. To ensure its accuracy and reliability, the model is initially validated by comparing its results with a case available in the literature. The results obtained from the analysis indicate that as the width and depth of the replacement increase, the settlement decreases. Based on the results, it is recommended to utilize a replacement width of 1.25 times the width of the footing and a replacement depth of 2 times the width of the footing. As replacement materials, granular soil, and rock boulders can be recommended.

KEY WORDS: Partial Replacement; Shallow Foundations; Ground Improvement; Numerical Modelling; PLAXIS 2D

1 INTRODUCTION

Soft soils have poor shear strength and high-water content. Construction projects face major challenges when dealing with soft soils due to their potential to cause structural damage. Soft soil replacement offers several benefits compared to other methods of improvement and deep foundation. It is more cost-effective and helps in reducing construction time. Additionally, it does not necessitate specialized contractors or specific machinery.

Generally, soft soil replacement is carried out underneath shallow foundations up to the hard strata. However, there are many instances where the depth to the hard layer is significant and it is not possible to replace all the weak soil, due to the significant costs involved. For relatively small-scale projects, using other ground improvement techniques or full soft soil replacement might not be cost-effective. So partial replacement would be a feasible solution. It is necessary to identify the effect of partial soil replacement on the foundation's behaviour.

The findings of this study will be useful when full replacement is not feasible. From this study, the width and depth of partial replacement and the most suitable replacement material that could be used to reduce the settlement under foundations are addressed. So, a set of guidelines/recommendations for the partial replacement of soft soils under shallow foundations can be proposed using the findings. This study is a detailed and fundamental investigation that can be broadly applied for any specified research area and industry purposes, and this can be a guide on how the partial replacement is carried out.

2 PREVIOUS RESEARCH ON SOIL REPLACEMENT

Several studies have been conducted on soft soil replacement techniques, focusing on the concept of selective replacement. The idea of utilizing a grainy trench beneath the foundations was initially proposed by (Madhav A N & Vitkar, 1978). Reference (Madhav A N & Vitkar, 1978) also concluded that the installation of a trench led to a significant increase of over 100% in the ultimate bearing capacity.

The impact of replacement soil on reducing settlement in footings placed on deep soft clays is studied in (Abdel Salam, 2007). The investigation focused on factors such as the modular ratio, thickness of the replacement soil layer, mechanical characteristics of the soft clay, the rigidity of the footing, and the presence of a groundwater table. The findings revealed that an increase in the thickness of the replacement layer resulted in a decrease in vertical settlement. The optimal thickness of the replacement layer falls within the range of 0.5 to 1.25 times the width of the footing (B) based on the study's observations (Abdel Salam, 2007).

A study employing both centrifuge modelling and numerical modelling to investigate the impact of replacing the upper soft soil layer or a portion of it with stronger soil concluded in (Gabr, 2012). The experimental results indicated higher settlement values for thin replacement layers, whereas thick replacement layers exhibited lower settlement values. Interestingly, the numerical model yielded higher settlement values compared to the centrifuge model (Gabr, 2012).

The Settlement Evaluation of Improved Soft Clay Using LECA Replacement was discussed in (Zukri et al., 2018). Lightweight expanded clay aggregate (LECA) material has been used as the replacement. Due to its low weight, high strength, and efficient drainage characteristics, this material is now used in several projects in civil engineering. According to the study's findings, increasing the depth of LECA replacement will help reduce settlement value for all LECA unit weights as well as for normal aggregates. Furthermore, the use of the replacement technique under the loaded area is effective in increasing the settlement factor (Zukri et al., 2018).

A study on partial replacement techniques for soft clay in the Tina Plain, Sinai, Egypt, utilizing geofoam under footings was carried out in (Atta et al., 2012). The study revealed that the reduction in the total settlement is not as significant when the width of the geofoam exceeds 1.5 times the footing width. Consequently, the study recommends using a geofoam width equal to 1.5 times the foundation width, as it proves to be highly effective in reducing settlement while also being cost-efficient (Atta et al., 2012).

Settlement estimation in improved soft clay using sand columns and partial replacement using both numerical and experimental methods were discussed in (Abbas, 2016). Results show that implementing replacement under the loaded area effectively reduces settlement. Based on extensive analysis, the most effective replacement thickness has consistently been found to be below 2 m, ranging between 0.7 and 2 m. Furthermore, the ideal replacement materials have been determined to be sand and a combination of sand and crushed stone (Elhamid et al., 2021).

The improvement of the bearing capacity of footings on soft clay using the partial soil replacement technique was analyzed using experimental methods (Fattah et al., 2015). The effectiveness of substituting soft soil with granular soil to enhance the bearing capacity of footings on soil was observed to reach its maximum level when the soil was partially replaced using a trench pattern (strip). The recommended dimensions for this soil replacement approach involved extending the replacement area by B/2 on all sides, with a depth of 1.5 times the footing width (B) (Fattah et al., 2015).

The effect of partial replacement with crushed concrete on the settlement and bearing capacity of soft clay was discussed using experimental methods in (Mohammed Al-Waily, 2019). According to the study findings, incorporating a partial replacement layer at a depth of 0.4 times the width of the strip footings leads to an average reduction in settlements of 72% and an average increase in bearing capacity of 96% (Mohammed Al-Waily, 2019).

3 METHODOLOGY

The objective of this research is to present some guidelines and recommendations for the partial replacement of soft soils beneath shallow foundations, utilizing numerical models with PLAXIS 2D geotechnical software.

The study focuses on evaluating the impact of the depth and width of partial replacement, as well as the influence of material properties of both the soft soils and the replacement material. Furthermore, the investigation involves an examination of the failure modes experienced by foundations subjected to partial soil replacements.

The study focused on investigating the partial replacement of soft soils beneath shallow foundations through numerical analysis. The model is first verified using the results of two cases available in the literature. Then numerical analysis was conducted without any soil replacement, resulting in a significantly high settlement value. Consequently, the introduction of soil replacement becomes essential. To achieve the objectives, first, the effect of the depth and width of the replacement is investigated. Then, the replacement material and the soft soil properties varied and finally, failure modes were examined.

3.1 *Model Validation*

The verification of the model was conducted using two known cases in (Zukri et al., 2018). In this study, the soft soil was represented by kaolin clay, while the fill material employed was LECA (Lightweight Expanded Clay Aggregates). The Mohr-Coulomb Model (drained) was utilized to capture the behaviour of LECA, and the soft clay behaviour was represented using the Soil Hardening Model (SHM).

Case 01 involves a replacement depth of 1.5 m measured from the footing level and a load of 100 kN/m^2 is applied. In Case 02, a replacement depth of 2.5 m from the footing level and a load of 50 kN/m^2 are applied. The finite element model was created using PLAXIS 2D software.

Table 1. Material properties used in model validation (from (Zukri et al., 2018))

Parameter	Material Properties	
	Kaolin Clay	LECA
Constitutive Model	SHM	MC
Type of analysis	Drained	Drained
ɣ (kN/m^3)	16	9
Young's Modulus, E(kN/m^2)	2420	2520
Cohesion, c' (kN/m^2)	7	0.1
Friction angle, Ø	25	35
Dilation angle, ψ	0	5
Poisson's ratio, v	0.30	0.3
Permeability, k(m/s)	2.58E-10	2.53E-2

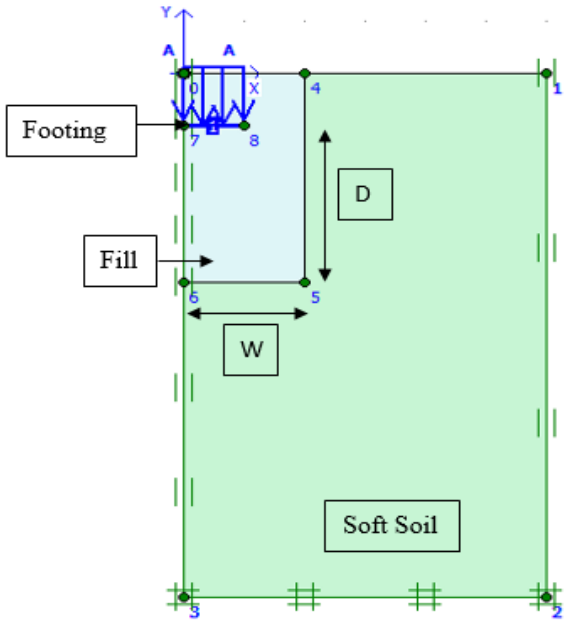

Fig. 1 Finite element model

Figure 01 illustrates the finite element model that was generated using PLAXIS 2D. In this figure, 'D' represents the depth of the partial replacement from the footing level, while 'W' represents the width of the partial replacement.

3.2 *Results of model validation*

Table 2. Results of model validation

Case	Model Validation		
	Actual (Zukri et al., 2018)	Model for Validation	% Deviation of the model from the actual
01	275 mm	289.91 mm	5.42%
02	180 mm	170.22 mm	5.74%

The model results have a good agreement with the actual settlement values. Therefore, this modelling procedure has been used for the analysis of the vertical displacement of shallow foundations.

Then the model results were validated using a numerical method. The settlement calculations consider only the immediate settlement and primary consolidation settlement, as they are particularly relevant in granular soils and soft clayey soils. The immediate settlement is determined using the Schmertmann method, while the primary consolidation settlement is assessed based on stress distribution analysis.

Table 3. Results of model validation (Numerical)

Case (Width, Depth)	Model Validation		
	1.25 m 1 m	1.5 m 2 m	2 m 3 m
Immediate Settlement (mm)	43.80	36.23	28.67
Primary Consolidation Settlement (mm)	34.03	24.83	18.03
Primary Consolidation + Immediate Settlement (mm)	77.83	61.06	46.70
Settlement By PLAXIS Model (mm)	82.75	66.28	52.00

The model results have a satisfactory agreement with the calculated settlement values.

3.3 *Constitutive model*

The selection of an appropriate constitutive model to accurately represent the behaviour of soft soils is of utmost importance when performing numerical analysis. In this study, several well-known models, namely the Mohr-Coulomb Model (MC), Linear Elastic Model (LE), Soft Soil Model (SSM), Soil Hardening Model (SHM), and Soft Soil Creep Model (SSC), were utilized for analysis. After careful consideration, the Mohr-Coulomb Model was chosen as the preferred constitutive model for the study. In Sri Lanka, the Mohr-Coulomb model is predominantly utilized due to the convenience of obtaining material properties using Standard Penetration Test (SPT) "N" values.

3.4 *Parametric study – Model details*

A numerical model was developed using PLAXIS 2D software. In the analysis, a 2D idealization is employed, specifically using a plain strain idealization. A 2-meter strip footing is modelled with model boundaries positioned 5m away from the footing and extending to a depth of 10 m. The total load applied on the footing is assumed to be uniformly distributed across the entire foundation. The uniform load used for this study is 100 kN/m^2. The

groundwater table is assumed to be located at a depth of one meter below the ground level.

In this study, a drained analysis approach was selected to examine the behaviour of the soil. The constitutive model chosen to represent the soil's behaviour was the Mohr-Coulomb model. Material properties used for models are presented in Table 4. For the analysis, a fine mesh was used. The replacement depth is changed to 1B, 2B, and 3B, while the replacement width is adjusted to 1.25B, 1.5B, and 2 B. In this context, B represents the width of the footing, which is 1 m.

Table 4. Material properties used for the model

Parameter	Material Properties	
	Soft Clay	Granular Soil
Constitutive Model	MC	MC
Type of analysis	Drained	Drained
γ_{unsat} (kN/m^3)	14	20
γ_{sat} (kN/m^3)	16	22
Young's Modulus, E(kN/m^2)	5000	20000
Cohesion, c' (kN/m^2)	5	0.1
Friction angle, Ø	18	35
Dilation angle, ψ	0	5
Poisson's ratio, v	0.35	0.3
Permeability, k(m/s)	1.00E-08	0.1

Then the settlement under the footing was investigated by varying the soft soil properties. This was achieved by modifying the soft clay's characteristics. Mainly the cohesion (c), friction angle (ϕ), and Young's Modulus (E) were changed. The analysis focused on evaluating the settlement variation for both soft clay and stiff clay conditions. The replacement depth was maintained at 2 m, while the replacement width was varied. Then, the replacement width was maintained at 2 m, while the replacement depth was varied.

Table 5. Material properties for soft soils

Parameter	Material Properties	
	Soft Clay	Stiff Clay
E (kN/m^2)	5000	10000
Cohesion, c'(kN/m^2)	5	5
Friction angle, Ø	18	25

In industry, low-grade concrete, granular soil, and rock boulders are commonly used as replacement materials. To assess the effect of the replacement material, rock boulders, and granular soil were used as the chosen fill materials, and the replacement depth was kept constant at 2 m, while the replacement width was subjected to variation. Then, the replacement width was maintained at 2 m, while the replacement depth was varied.

Table 6. Material properties for replacement materials

Parameter	Material Properties	
	Granular Soil	Rock Boulders
E (kN/m^2)	20000	60000
Cohesion,c' (kN/m^2)	0.1	0.1
Friction angle, Ø	35	35

4 RESULTS & DISCUSSION

A total of twenty-seven models were developed to simulate the displacement of soft soil. These models were created by varying parameters such as the depth and width of the replacement, replacement material, and the properties of the soft soil.

The initial model, which does not involve any replacement of granular soil, yielded a settlement value of 100 mm.

First, to study the effect of the width of the partial replacement, the replacement width was adjusted to 1.25B, 1.5B, and 2B, where B represents the width of the footing (1 m). The settlement was assessed at various replacement depths of granular soils to examine the impact of the width of partial replacement.

Figure 2 shows the variation of settlement with the replacement width at three different replacement depths. The results show that increasing the width of partial replacement leads to a reduction in settlement across all replacement depths. It can be observed from the results that there is a significant decrease in settlement when the ground width is improved up to 1.25 times the footing width (1.25B). Further improvements beyond 1.25B width do not have a significant impact.

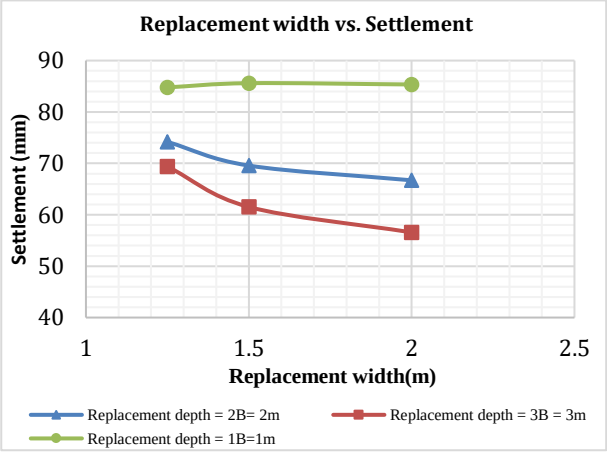

Fig. 2 Variation of settlement with replacement width

The replacement depth was then varied as 1B, 2B, and 3B from the footing level to evaluate the effect of the partial replacement depth, where B indicates the width of the footing (1 m). The replacement depth was then varied as 1B, 2B, and 3B from

the footing level to evaluate the effect of the partial replacement depth, where B indicates the width of the footing (1 m). Figure 3 shows the variation of settlement with the replacement depth at three different replacement widths.

The results show increasing the depth of partial replacement reduces settlement in all replacement widths. The results clearly indicate that there is a significant reduction in settlement when the ground depth is improved up to 2 times the footing width (2B). However, no significant reduction in settlement could be observed after a replacement depth of 2B.

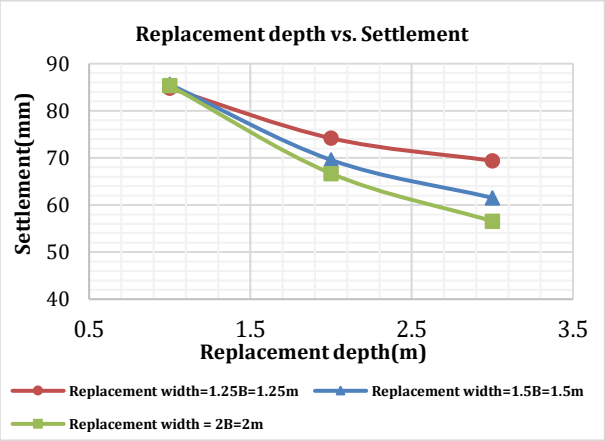

Fig. 3 Variation of settlement with replacement depth

Figures 4 and 5 show the variation of settlement with soft soil properties by varying replacement width and depth respectively. It can be observed that if the c, ϕ, E of soft soil is higher, the settlement will decrease. Stiff clay gives less settlement.

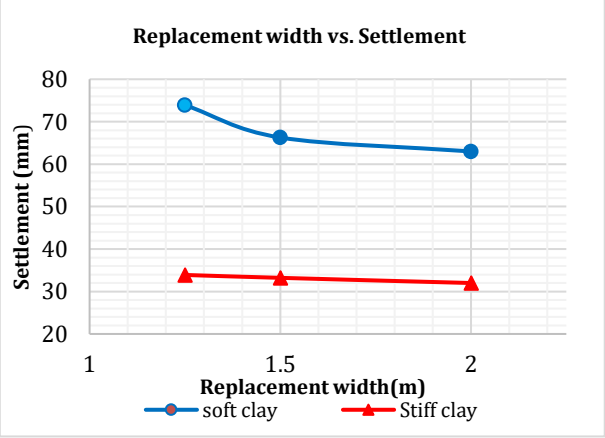

Fig. 4 Variation of settlement with soft soil properties (by varying replacement width)

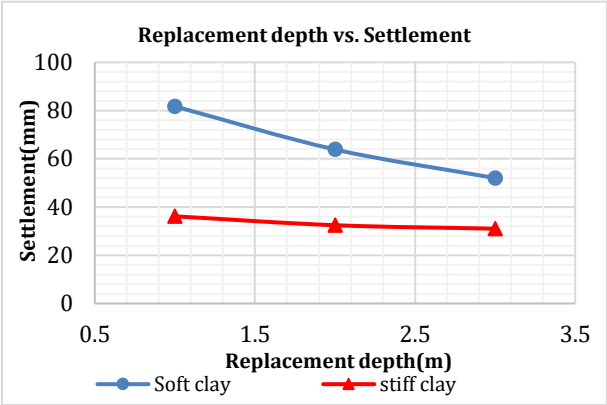

Fig. 5 Variation of settlement with soft soil properties (by varying replacement depth)

Figures 6 and 7 illustrate the variation of settlement with replacement material properties by varying replacement width and depth respectively. When comparing the settlement results, it was observed that the settlement is lower when rock boulders are used instead of granular soil. However, there is no significant difference in settlement observed when employing either granular soil or rock as the filling material.

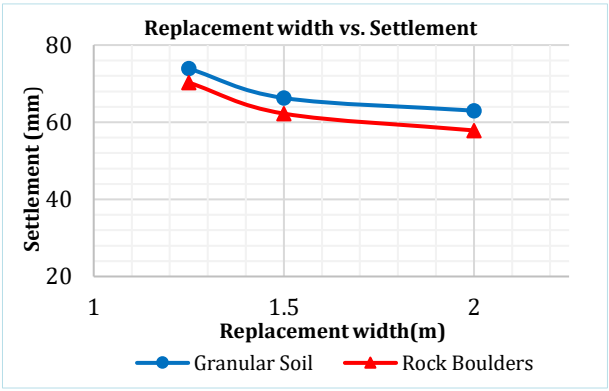

Fig. 6 Variation of settlement with replacement material properties (by varying replacement width)

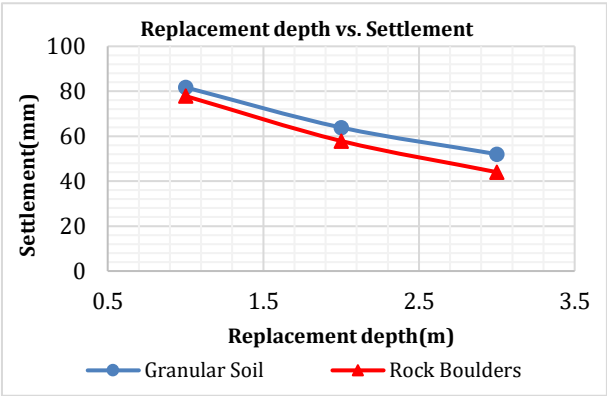

Fig. 7 Variation of settlement with replacement material properties (by varying replacement depth)

The analysis of the failure mode involves comparing the total strain increments with the depth of improvement. The focus was on observing how the wedge-type failure mode varied with changes in the improvement depth. It also provided insight into the point at which further improvement would no longer be economically viable.

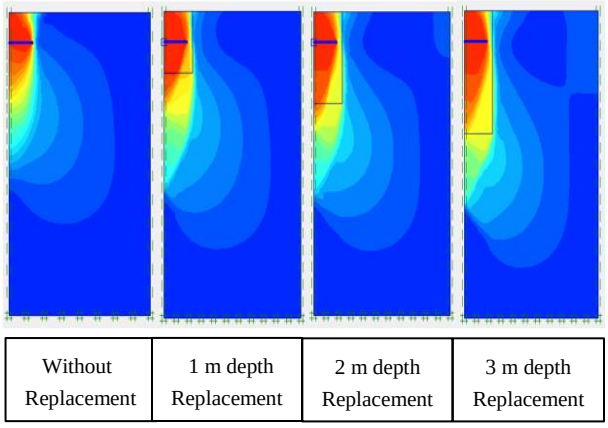

Fig. 8 Variation of total strain increment with replacement depth

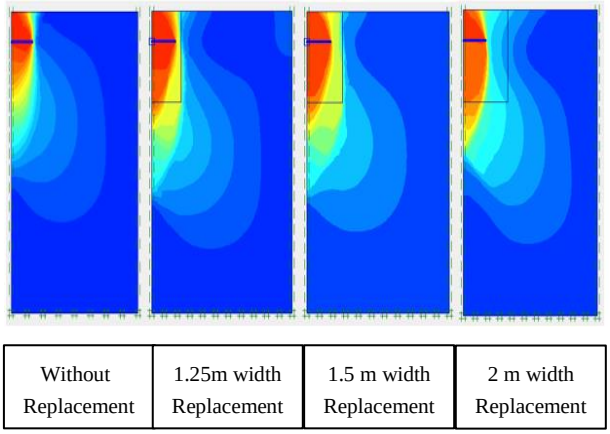

Fig. 9 Variation of total strain increment with replacement width

Figures 8 and 9 illustrate the variation of total strain increment with replacement depth and width respectively. When the improvement depth and width is increased, the total strain increment is also increased.

Within a width of 1.25 meters and a depth of 2 meters, the strain increments are distributed. Therefore, implementing partial improvement within this area is expected to lead to a significant enhancement in the foundation's behaviour.

5 CONCLUSIONS

The settlement behaviour beneath the footing was studied through numerical analysis using 2D models under drained conditions. Several conclusions can be derived from this study.

When no replacement is implemented, the settlement value tends to be significantly higher. However, when partial soft soil replacement is applied, the settlement is reduced. Therefore, the introduction of partial replacement techniques leads to a decrease in settlement.

Increasing the depth of partial replacement leads to a reduction in settlement. However, there is a significant reduction in settlement when the ground depth is improved up to 2 times the footing width (2B). Further improvements beyond 2B do not have a significant impact.

Increasing the width of partial replacement decreases the settlement. There is a significant reduction in the settlement when the replacement width is increased up to 1.25 times the footing width. Increasement beyond 1.25B will not affect more.

The condition of the foundation can be improved by replacing a part of the soft soil with more competent materials such as granular soil or rock boulders. When comparing the use of rock boulders and granular soil as replacement materials, it was found that the settlement of the footing was lower when rock boulders were employed. However, there is no significant difference in settlement between filling with granular soil and rock Therefore, rock boulders and granular soil can be considered suitable replacement material due to their ability to effectively reduce settlement.

If the cohesion (c), friction angle (ϕ), and Young's Modulus (E) of soft soil are higher, there will be a reduction in settlement. Stiff clay results in less settlement than soft clay.

In partial replacement of soft soil, it is recommended to use a width 1.25 times the width of the footing, a depth 2 times the width of the footing, and replacement materials such as granular soil and rock boulders.

ACKNOWLEDGMENT

Continuous support given by the Department of Civil Engineering, University of Moratuwa throughout the research is sincerely appreciated.

REFERENCES

Abbas, B. J. (2016). The Settlement Evaluation of Improved Soft Clay using Sand Columns and Partial Replacement Technique. *International Journal of Engineering Research & Technology*, *5*(7). https://doi.org/10.17577/IJERTV5IS070355

Abdel Salam, S. (2007). *The Effect of Replacement Soil on Reducing Settlement of Footing on Deep Soft Clay Using Numerical Approach*. Cairo University, Giza, Egypt.

Atta, A. A., Salem, T. N., & Badrawi, F. (2012). Partial Replacement of Soft Clay in Tina Plain, Sinai, Egypt by Geofoam Under Footings. *The Egyptian Int. J. of Eng. Sci. and Technology*, *15*(2).

Elhamid, M. A., Abdelaziz, T., & Bassioni, H. (2021). Factors Affecting the Thickness OF Replacement Layer on Medium Clay. In *ASEAN Engineering Journal* (Vol. 11, Issue 4).

Fattah, M. Y., Al-Neami, M. A., & Al-Suhaily, A. S. (2015). Improvement of Bearing Capacity of Footings on Soft Clay by Partial Soil Replacement Technique. *The 2nd International Conference of Buildings, Construction and Environmental Engineering (BCEE2-2015), October*, 203–208.

Gabr, A. K. (2012). The uncertainties of using replacement soil in controlling settlement. *The Journal of American Science*, *8*(12), 662–665.

Madhav A N, M. R., & Vitkar, D. P. P. (1978). Strip footing on weak clay stabilized with a granular trench or pile. In *Can. Geotech. J* (Vol. 15). www.nrcresearchpress.com

Mohammed Al-Waily, M. J. (2019). Effect of Partial Replacement with Crushed Concrete on Settlement and Bearing Capacity of Soft Clay. *IOP Conference Series: Materials Science and Engineering*, *584*(1). https://doi.org/10.1088/1757-899X/584/1/012059

Zukri, A., Nazir, R., & Ng, K. S. (2018). The Settlement Evaluation of Improved Soft Clay Using LECA Replacement Technique. November.

Engineering Properties of Peat Soils - Mixed with Combination of Quarry Dust and Cement

A.R.A. Mohammed and W.M.N.R. Weerakon
Department of Civil Engineering, University of Sri Jayewardenepura, Sri Lanka

ABSTRACT: Peat soil is an extremely soft soil that displays high compressibility, low shear strength, and low bearing capacity and is thus not suitable for construction. The research explores enhancing the engineering properties of peat by stabilizing it with quarry dust and cement. Through experimental methods, peat samples mixed with varying quarry dust (0%, 5%, 10%, 15% by wet weight of peat) and cement (5%, 10%, and 15% by wet weight of peat) were analyzed via Direct Shear Test (DST) and Unconfined Compression Test (UCT) over 3, 7, 14, and 28 days of curing. Results indicated significant strength improvements with higher quarry dust and cement proportions and extended curing times. Maximum strength was achieved with 15% cement and 15% quarry dust. Comparative analysis of DST and UCT results showed consistency within the results. Additionally, consolidation tests display reduced peat compressibility post-stabilization, confirming the efficacy of quarry dust and cement in enhancing peat's geotechnical properties.

KEY WORDS: Peat; Unconfined Compression Strength; Shear Strength; Consolidation

1 INTRODUCTION

Peat is an accumulation of partially decomposed and disintegrated plant remains, preserved under incomplete aeration and high-water content (Huat, Maail and Mohamed, 2005). Peat development is balanced between organic material accumulation and decomposition. The varying type of peat is influenced by plant types contributing to the peat and the varying environmental conditions under which decay occurs. Peat generally forms in areas with persistent high-water tables, such as swamps or marshes, where organic matter remains submerged and relatively preserved (Kazemian et al., 2011)

Peatlands, span approximately 4.5% of the earth's terrestrial surface or about one billion acres globally and span over 2500 hectares in Sri Lanka alone (Zimar, Nasvi, and Jayakody, 2020). Peat is primarily differentiated into fibrous and amorphous types. The Von Post scale further refines this classification, ranging from H1, indicating wholly undecomposed fibrous peat, to H10, denoting fully decomposed amorphous peat. This classification considers humification levels, moisture, fiber content, and plant composition to assess peat's decomposition state (Kazemian et al., 2011)

Peat soil, with its high organic and fiber content coupled with significant moisture levels, is highly problematic for construction due to its low load-bearing capacity, substantial compressibility, high rate of creep and difficulties in access (Kazemian, Huat, and Moayedi, 2012). Peat is prone to severe risks such as instability, slip failure, localized sinking, and considerable long-term settlement even under moderate loading (Zimar, Nasvi, and Jayakody, 2020).

The Stabilization of the peatland can be divided into two categories; mechanical stabilization and chemical stabilization. Mechanical techniques include soil displacement or replacement, staged construction, preloading, stone columns, embankment piling, and synthetic reinforcement. Chemical stabilization utilizes deep in-situ mixing and surface applications of materials like cement, fly ash, bottom ash, bentonite, gypsum, silica fume, and blast furnace slag to strengthen the soil (Vincevica et al., 2021). Many studies have focused on the stabilization of peat soil.

In the study by Zambri et al (Mohd Zambri and Md. Ghazaly, 2018) the efficacy of lime and cement as additives for the stabilization of peat soil was investigated. The research involved a series of direct shear tests conducted on disturbed peat soil samples, which were amended with lime and cement at two different proportions: 10% and 20% by dry weight of the soil. The experimental results indicated an enhancement in shear strength of the treated soil by up to 14%. Comparative analysis revealed that lime as an additive provided marginally superior results, enhancing shear strength by 14.07%, while cement resulted in a 13.5% increase. These outcomes affirm the potential of lime and cement as effective stabilizing agents for peat soils, with lime exhibiting a slight advantage over cement in terms of shear strength improvement.

In the investigation by Venuja et al. (2017), the stabilization potential of fly ash and well-graded sand on peat samples was tested. The study varied

the fly ash proportion from 10% to 30% by weight, complemented by a constant inclusion of 125 kg/m^3 of sand. It was observed that the Unconfined Compressive Strength (UCS) of the samples augmented with the addition of up to 10% fly ash, beyond which a decline in UCS was noted. Furthermore, the UCS values exhibited a positive correlation with the duration of the curing periods, indicating an enhancement in strength over time. Results from Rowe cell tests elucidated an amelioration in the compressibility characteristics of the peat when stabilized with the aforementioned additives. These findings underscore the nuanced effects of fly ash content on the mechanical properties of peat and the beneficial role of extended curing periods on its stabilization.

The study conducted by Pashaki et al. (2017) focused on evaluating the impact of varying proportions of cement and sand on the geotechnical characteristics of peat. Specimens were methodically prepared with 5%, 10%, and 15% of each additive by weight to ascertain the geomechanical influence exerted by these materials. A comprehensive set of tests, including Atterberg limits, compaction, unconfined compressive strength (UCS), and California Bearing Ratio (CBR) assessments, were executed to examine the modifications in the soil's behavior. The outcomes from these examinations revealed a notable enhancement in the geotechnical attributes of the peat, thereby confirming the effectiveness of cement and sand as soil stabilizers in altering the physical and mechanical properties of peat to a significant extent.

Kazemian et al. (2011) explored the stabilization of peat using various proportions of a cement-sodium silicate grout admixed with kaolinite, with the ratios prepared based on the peat's wet weight. Vane shear tests conducted after 3 and 30 days of curing periods manifested that kaolinite integration substantially elevated the shear strength of the peat. In a related study, Celik et al. (2014) investigated the influence of sand content on fibrous peat's compaction, shear strength, and compressibility. By incorporating sand in increments of 10% to 50% by weight, the experiments determined that the sand content critically affected the mechanical properties of peat. Shear strength and consolidation tests on the mixtures, conditioned to their optimum moisture content and maximum dry densities, corroborated the pronounced effect of sand addition on the stabilization process, enhancing the overall geotechnical performance of the fibrous peat. Both studies collectively underscore the role of mineral additives in improving the mechanical stability of peat soils.

However, there is a lack of research on peat soil stabilization using quarry dust either alone or combined with cement or other admixtures. Cement and quarry dust are locally available materials and had shown favorable responses towards peat soil stabilization in the past research. Finding an effective way to stabilize peat soil with locally available admixtures will be very beneficial. Therefore, the major aim of this research study was to determine the geotechnical engineering properties of peat stabilized with a combination of quarry dust and cement.

2 MATERIAL AND METHODOLOGY

2.1 *Materials*

The experimental work for this study incorporated three primary materials: peat, quarry dust, and ordinary Portland cement (OPC). The peat soil was collected as a disturbed sample from the Muthurajawela region, from a depth ranging between 0.1 m and 0.5 m beneath the ground surface. To preserve its natural moisture content, the peat sample was stored in a sealed bag. Initial classification of the peat was conducted using the Von Post system. The peat was categorized as H4 according to the Von Post scale, indicating a certain level of decomposition. Quarry dust, a by-product resulting from the mechanical crushing of rocks, is commonly employed within the construction sector. Sieve analysis was performed to determine its grading.

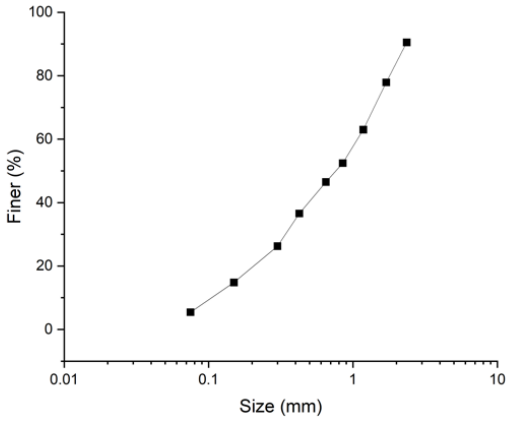

Fig. 1 Particle size distribution of quarry dust

The research utilized Ordinary Portland Cement, a staple binding material in the construction industry, to investigate the stabilization potential when combined with quarry dust for enhancing the geotechnical properties of peat soil.

2.2 *Sample Preparation*

The peat obtained for this research was in a slurry-like consistency, interspersed with organic and inorganic materials such as roots and stones. To ensure uniformity of the samples for laboratory testing, the peat was manually screened to extract large stones, vegetation roots, and other significant

fragments. Subsequently, it was subjected to a wet sieve using a 4.75 mm aperture to achieve homogeneity. Next, the quarry dust was oven-dried at 105 ℃ for 24 hours to remove any moisture and was sieved through a 3.35 mm sieve to discard any coarser particles, ensuring that only the fines were retained for inclusion in the subsequent stabilization experiments with the peat.

The quarry dust and cement were added to the peat soil sample, as a percentage (5%, 10%, and 15%) of the weight of wet peat soil. Samples were prepared for 4 different curing periods including curing days of the 3rd day, 7th day, 14th day, and 28th day.

2.3 *Experimental Procedure*

Moisture content was performed following ASTM D2974-14. Water content was determined by drying the peat soil sample for nearly 24 hours at 105 ± 5 ºC. The specific Gravity of the peat soil was determined in accordance with ASTM D854-02 using a pycnometer. The Fiber content of the peat was determined in accordance with ASTM D1997-91. The organic content test was performed in accordance with ASTM D2974-14 by loss on ignition test. The oven-dried peat sample was placed in a muffle furnace and the temperature was gradually raised to 440 ℃ until the samples were completely ignited.

The Unconfined Compressive Strength test was conducted to find out the unconfined compressive strength of samples on different curing periods (3, 7, 14 and 28 days). For the UCS test, the size of the sample is 50 mm × 100 mm and the test is conducted in accordance with ASTM D2166.

The Direct Shear Test was performed to determine the undrained shear strength of the samples. The size of the sample is 100 mm × 100 mm × 25 mm height. The test was performed according to the standard of ASTM D3080-04. The test was done as strain-controlled tests by applying a constant rate of 1mm/min displacement. The horizontal displacement was limited to 10 mm. To maintain a constant volume during the tests, the vertical loading ram was securely clamped just before shearing. This clamping action prevented any movement of the ram and thus maintained a constant sample height. By doing so, the dilation of the specimen was restrained by the variation in vertical stress during shearing, under constant-volume conditions, which was considered equivalent to undrained conditions.

The consolidation test was performed using an Oedometer. The test was done on raw peat soil and stabilized peat with 15% of both cement and quarry dyst. Loads of 5 kg, 10 kg and 15 kg were applied for a day for each weight to study the consolidation properties of the soil sample.

3 RESULTS AND DISCUSSION

3.1 *Index Properties*

Table 1 shows the index properties of raw peat obtained from laboratory tests.

Table 1. Index Properties of Peat

Property	Value
Moisture Content	107.04 %
Specific Gravity	1.93
Fiber Content	61.13 %
Organic Content	41.54 %

3.2 *Unconfined Compressive Strength*

Figure 1 shows the result of unconfined compressive strength of the samples with curing days. Higher strength is obtained from samples that have been cured for 28 days compared with the 3, 7, and 14-days cured samples. A higher unconfined compressive strength value of 301 kPa was obtained with the sample having quarry dust at 15% and cement at 15%.

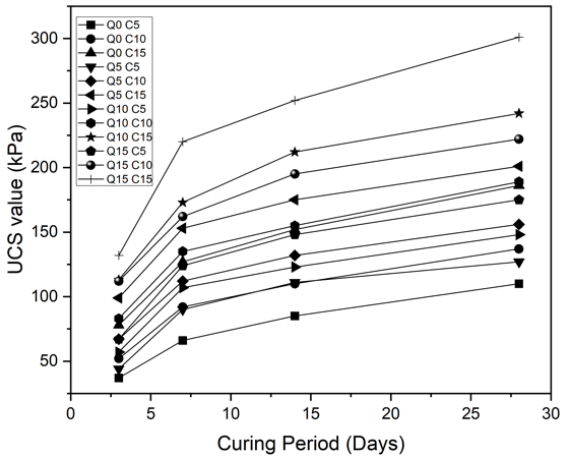

Fig. 1 UCS variation with curing period

The strength development is a result of several factors contributed by both quarry dust and cement. Cement initiates a chemical reaction with water. This reaction is called the hydration of cement. The cement produces free calcium cations (Ca). When it comes in contact with water and replaces dissimilar adsorbed cations on the colloidal surface (pozzolanic reactions). Practically all fine-grained soils display rapid cation exchange and flocculation-agglomeration reactions when treated with cement in the presence of water with increasing curing time and this is also evident in peat (Kazemian, S. et al., 2011).

On the other hand, quarry dust fills the voids in the peat and consumes the excess pore water in the

peat. The addition of quarry dust to the peat soil also strengthens the bond between the soil particle. As a result, the soil particle becomes closer to each other, causing the soil texture to change. This will increase the density and improve the compaction characteristics of the peat soil.

3.3 *Undrained Shear Strength*

In order to examine the impact of cement and quarry dust on the shear strength of peat soil, direct shear tests were conducted on all samples. After placing the sample inside the shear box and setting up the apparatus, a minimal vertical pressure was applied to the top of the sample. This was done to ensure proper contact between the specimen's top surface and the loading plate.

To maintain a constant volume during the tests, the vertical loading ram was securely clamped just before shearing. This clamping action prevented any movement of the ram and thus maintained a constant sample height. By doing so, the dilation of the specimen was restrained by the variation in vertical stress during shearing, under constant-volume conditions, which was considered equivalent to undrained conditions.

The direct shear tests were done on different curing periods (3rd day, 7th day, 14th day and 28th day) to examine the effect of the curing period on the samples. Figure 2 shows the results of the direct shear test obtained on different curing periods. A similar trend to the UCS test was also observed in the direct shear test results.

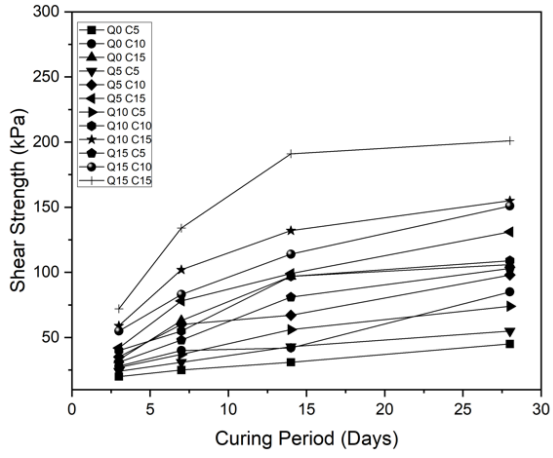

Fig. 2 Shear strength variation with curing period

Higher strength was observed from samples that have been cured for 28 days compared with the 3, 7, and 14-day cured samples. The strengths of the samples were increasing with the increasing amount of both cement and quarry dust. Notably, the stabilized sample consisting of 15% cement and 15% quarry dust exhibited a significant shear strength of 201 kPa on the 28th day.

Figure 1 and Figure 2 clearly demonstrate a noticeable upward trend in strength as the curing period progresses. This can be attributed to the ongoing hydration reaction between the cement and quarry dust, leading to the formation of cementing products. The hydration process contributes to the increase in strength over time.

It should be noted that, in case of stabilization which involves cement, the pozzolanic reaction can continue for months or even years after mixing, resulting in the increase in strength of cement stabilized peat with the increase in curing time (Huat et al, 2005).

3.4 *Comparison of undrained shear strength*

A comparison was made between the undrained shear strength obtained from DST and UCT for curing periods ranging from 3 to 28 days. The shear strength from UCT was taken as half of the unconfined compressive strength. Figure 3 illustrates the comparison of these strength values. It is observed that, for lower strength values, the shear strength measured from UCS is slightly higher, while the opposite is true for higher values of undrained shear strength. This slight variation can be attributed to multiple factors.

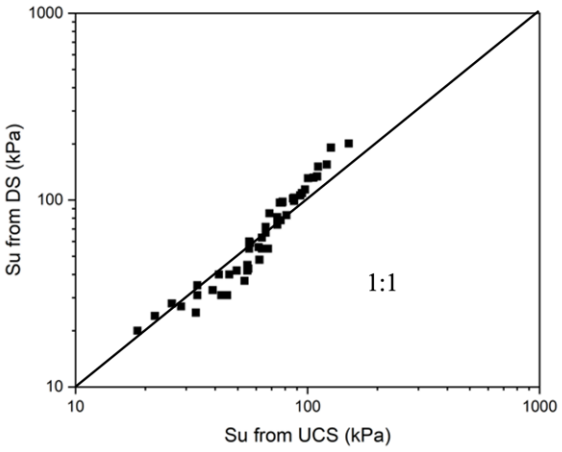

Fig. 3 Correlation between undrained shear strength obtained by DST and UCT

One factor to consider is that the samples prepared for the UCT remained relatively softer even at later curing days. This lack of hardness is a significant contributor to the reduced unconfined compressive strength observed during the later stages of curing. Additionally, the anisotropic properties of the specimens and the variation in loading rates between the UCT and DST may also contribute to the observed differences.

Nevertheless, it is worth mentioning that the results obtained from both methods are comparable and fall within the 1:1 ratio line. This suggests that

despite the slight variations, the two testing methods provide reasonably consistent results in terms of measuring the strength of the samples.

3.5 *Compressibility behavior of peat soil*

Oedometer consolidation test was conducted on raw peat and stabilized peat with 15% of quarry dust and 15% cement (sample composition giving the highest UCS). Figure 4 and Figure 5 show the variation of the settlement with the time of raw and stabilized peat respectively.

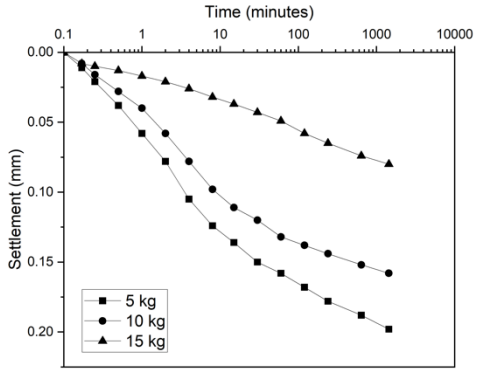

Fig. 4 Variation of settlement with the time of raw peat

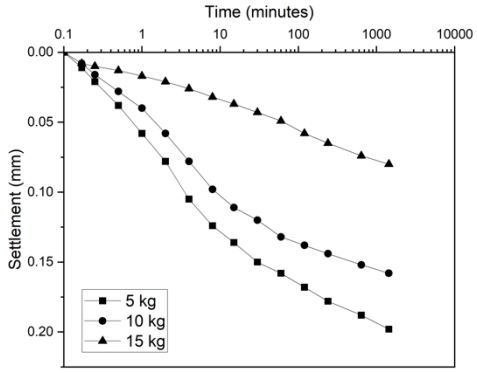

Fig. 5 Variation of settlement with the time of stabilized peat

Table 2 shows the values obtained for the initial void ratio, coefficient of volume compressibility and compressibility index.

Table 2. Values of m_v, C_c of raw and stabilized peat

Parameter	Raw	Stabilized
Initial void ratio	1.95	0.8
m_v (m^2/kN)	0.001225	0.0003482
C_c	0.21	0.0479

The values obtained for these parameters clearly show the improvement in the compressibility parameters after stabilizing the peat with quarry dust and cement. The initial void ratio was significantly reduced in the stabilized peat compared to raw peat. This is because the quarry dust fills the voids in the peat and consumes the excess pore water in the peat. The addition of quarry dust might also strengthen the bond between the soil particle and the soil particle becomes closer to each other, causing the soil texture to change. On the other hand, due to the cement hydration cementitious product was formed which is comparatively very stable and has good strength properties. Table 3 shows the coefficient of consolidation of both raw peat and stabilized peat.

Table 3. Values of the Coefficient of Consolidation

Sample Type	Load (kg)	Cv $(m^2/year)$
Raw Peat	5	2.802
	10	2.425
	15	1.246
Stabilized Peat	5	5.321
	10	4.972
	15	11.187

Table 3 shows that, for the raw peat, there is a tendency to decrease in Cv with the increasing applied pressure indicating a slower rate of consolidation at higher consolidation pressure. Considering the stabilized peat soil, the Cv value is considerably higher compared to the raw peat due to the stabilization. An unusual pattern was observed in the Cv value of the stabilized peat soil. It could be the effect of the hydration of cement which will continue for days. Even though the consolidation pressure was increased, the stability and strength of the soil increased with time (curing time). As time passes, the stabilized peat soil will get hardened and the voids will be filled with hydrated products of cement.

4 CONCLUSION

An experimental study was conducted to study the engineering properties of peat stabilized with quarry dust and cement. The following conclusions could be drawn from the outcome of this study:

- The sample prepared with 15% quarry dust and 15% cement yielded the maximum strength values in both the unconfined compressive test (UCT) and direct shear test (DS). Therefore, it is considered the optimum sample.
- In the UCT, the maximum Unconfined Compressive Strength (UCS) value recorded for the optimum sample was 301 kPa. Similarly, in the direct shear test, the optimum sample achieved a maximum undrained shear strength of 201 kPa.
- A comparison between the results of the direct shear test and the UCT was conducted to assess their reliability and agreement. The

comparison revealed a fair agreement between the test results, indicating consistency between the two testing methods.

- Consolidation tests were performed on both raw peat and the sample with 15% quarry dust and 15% cement, which exhibited higher UCS and shear strength values.
- Comparing the stabilized peat soil to raw peat, the consolidation properties showed clear improvement. The stabilized peat exhibited a significant reduction in the initial void ratio compared to raw peat.
- In raw peat, there was a tendency for C_v to decrease with increasing applied pressure, indicating slower consolidation at higher consolidation pressures. In contrast, the C_v value was considerably higher in the stabilized peat soil due to the stabilization process.

REFERENCES

Celik, F. and Canakci, H. (2014) "An investigation of the effect of sand content on geotechnical properties of fibrous peat," Arabian Journal for Science and Engineering, 39(10), pp. 6943–6948.

Huat, B., Maail, S. and Mohamed, T., 2005. Effect of Chemical Admixtures on the Engineering Properties of Tropical Peat Soils. American Journal of Applied Sciences, 2(7), pp.1113-1120

Kazemian, S., Huat, B. and Moayedi, H., 2012. Undrained Shear Characteristics of Tropical Peat Reinforced with Cement Stabilized Soil Column. Geotechnical and Geological Engineering, 30(4), pp.753-759.

Kazemian, S. et al. (2011) "Influence of cement – sodium silicate grout admixed with calcium chloride and kaolinite on sapric peat," Journal of Civil Engineering and Management, 17(3), pp. 309–318.

Mohd Zambri, N. and Md. Ghazaly, Z., 2018. Peat Soil Stabilization using Lime and Cement. E3S Web of Conferences, 34, p.01034.

Pashaki, e., 2017. Geomechanical properties of peat stabilized with cement and sand. International Journal of ADVANCED AND APPLIED SCIENCES, 4(9), pp.19-25.

Venuja, S., Mathiluxsan, S. and Nasvi, M., 2017. Geotechnical Engineering Properties of Peat, Stabilized with a Combination of Fly Ash and Well-Graded Sand. Engineer: Journal of the Institution of Engineers, Sri Lanka, 50(2), p.21.

Vincevica-Gaile, Z., Teppand, T., Kriipsalu, M., Krievans, M., Jani, Y., Klavins, M., Hendroko Setyobudi, R., Grinfelde, I., Rudovica, V., Tamm, T., Shanskiy, M., Saaremae, E., Zekker, I. and Burlakovs, J., 2021. Towards Sustainable Soil Stabilization in Peatlands: Secondary Raw Materials as an Alternative. Sustainability, 13(12), p.6726.

Zimar, A., Nasvi, M. and Jayakody, S., 2020. Geotechnical Characterization of Peats in Muthurajawela Region in the Western Coast of Sri Lanka. Geotechnical and Geological Engineering, 38(6), pp.6679-6693.

Novel Fly Ash based One-part Geopolymer for Stabilization of Expansive Road Subgrade

K.R.H. Jayawardane, K.S.S. Rangana, M.C.M. Nasvi and L.C. Kurukulasuriya
Department of Civil Engineering, University of Peradeniya, Sri Lanka

ABSTRACT: Expansive soils pose significant challenges in road construction due to their volumetric changes and limited bearing capacity. The predominant approach for soil stabilization is chemical stabilization, but alkali-activated geopolymers are gaining attention as sustainable alternatives. Geopolymers come in one-part (OP-G) and two-part (TP-G) forms, with OP-Gs offering convenience and lower costs for transportation over TP-Gs. This study evaluates strength and swelling characteristics of a fly ash (FA)-based OP-G stabilized road subgrade, comparing results with TP-G and ordinary Portland cement stabilization. Through testing 16 unconfined compressive strength (UCS) specimens with varying binder/dry soil and solid NaOH/FA ratios, the optimal OP-G mix was determined at ratios of 0.2 and 0.1, respectively, based on both cost and UCS. A utility analysis was conducted to rank the stabilized soil samples based on performance indicators like UCS, swell pressure, CBR, cost, and emissions. The findings endorse the efficacy of OP-G in stabilizing expansive road subgrades.

KEY WORDS: Expansive soil, Soil stabilization, Fly ash, One-part geopolymer, Strength

1 INTRODUCTION

Expansive soil is problematic due to its low shear strength, high swelling, and shrinkage. Soil stabilization improves its structural capacity through physical and chemical methods. Physical methods alter soil properties, while chemical methods modify soil properties by adding active materials. Chemical stabilization is popular due to cost benefits and control over setting and curing times. Ordinary Portland Cement (OPC), a popular soil stabilization binder, is becoming unsustainable due to global greenhouse gas emissions (Davidovits, 1991; Bakharev et al., 2001a; Bakharev et al., 2001b).

Alkali-activated binders (AAB) have attracted recent attention as a promising solution to calcium-based stabilizer problems (Davidovits, 2015; Maheepala et al., 2022; Disu et al., 2021). Davidovits (2015) highlights that the use of AABs instead of traditional stabilizers can reduce greenhouse gas emissions (GHG) by 70 to 90%. Geopolymers are divided into two types: one-part and two-part, based on the alkali activator used, with two-part geopolymers (TP-G) using liquid activators and one-part geopolymers (OP-G) using solid activators.

The commercial application of two-part geopolymers is limited due to the difficulty of handling these viscous, corrosive solutions on construction sites.

Therefore, researchers have explored the use of alkali-activated fly ash-based OP-G for stabilizing expansive soils. Tesanasin et al. (2022) studied the use of alkali-activated fly ash-based OP-G for stabilizing marginal lateritic soil. They found that the optimal dosage of solid NaOH (NH) in flake form was 20% or less. The analysis of cost and CO_2 emission of OP-G and TP-G stabilized materials revealed that TP-G had higher CO_2 emissions and lower costs for samples stabilized with OP-G. Zheng et al. (2021) suggested using OP-G as a binder for stabilizing soft clay instead of OPC. The geopolymer binder was created by mixing water with a solid source material, ground granulated blast furnace slag, fly ash (FA), and a solid NH activator. The study found that UCS values increased with FA content up to 10% and reduced with further addition. The Geopolymer-stabilized clay achieved a higher UCS than clay stabilized with OPC. Rios et al. (2016) employed a geopolymer composed of low-calcium FA as a precursor and a combination of sodium silicate and NH as an alkaline activator to stabilize silty roadbeds in the southern region of Bogotá, Colombia. The results demonstrated that the strength of the geopolymer-stabilized silty clay met the pavement engineering's bearing capacity requirements within 7 days.

Despite the advantages of using one-part geopolymers, such as simplified transportation, reduced costs, and improved safety, the number of studies conducted on this specific application is limited, hindering a comprehensive understanding of their efficacy and potential. Therefore, there exists a significant knowledge gap regarding the utilization of one-part geopolymers in soil stabilization.

2 MATERIALS AND METHODS

2.1 *Materials*

The soil sample was obtained from Hettipola area in Mahiyanganaya (Coordinates of 7.543038, 80.914474). A series of characterization tests were carried out for expansive soil and the results are presented in Table 1. The expansive soil was classified as CLAY of high plasticity in accordance with the Unified Soil Classification System.

Table 1. Properties of the expansive soil

Characteristic	Value
Liquid Limit (%)	55
Plastic Limit (%)	29
Plasticity Index (%)	26
Clay (%)	47
Silt (%)	25
Sand (%)	27
Maximum dry density (kN/m^3)	14.91
Optimum moisture content (%) (under standard proctor compaction)	23.8
Specific gravity	2.67
Swell pressure (kPa)	163.7
Unconfined compressive strength (MPa)	0.32

Fly ash (FA) was collected from the Lakwijaya coal power plant in Norochcholai. The solid alkaline activator employed for OP-G synthesis was sodium hydroxide (NaOH), while the liquid alkaline activator utilized in TP-G formulation was a combination of sodium silicate solution (Na_2SiO_3) and NaOH. These materials were purchased from the local market in Colombo. The Ordinary Portland Cement (OPC) used in the study was sourced from local markets.

2.2 *Mix optimization of OP-G samples*

The optimized mix parameters for OP-G were extracted from the relevant literature. To determine the optimal mix for OP-G stabilization in terms of strength and cost, a series of 16 UCS specimens were casted with variations in binder (FA + NaOH)/ dry soil (B/S) ratio and solid NaOH/ FA (NH/FA) ratio. It should be noted that for the preparation of OP-G in this study, B/S ratio and NH/FA were varied within the range of 0.2-0.35 and0.1-0.25 respectively according to relevant literature (Wu et al. 2021 and Zheng et al. 2021). The sample mixture types and corresponding designations are presented in Table 2. The optimum OP-G stabilized soil sample was found based on UCS test results and cost per unit volume of stabilized soil.

Table 2. Summary of sample mixture types and corresponding mix ratios

Sample ID	B/S ratio	NH/FA ratio
S1	0.2	0.10
S2	0.2	0.15
S3	0.2	0.20
S4	0.2	0.25
S5	0.25	0.10
S6	0.25	0.15
S7	0.25	0.20
S8	0.25	0.25
S9	0.3	0.10
S10	0.3	0.15
S11	0.3	0.20
S12	0.3	0.25
S13	0.35	0.10
S14	0.35	0.15
S15	0.35	0.20
S16	0.35	0.25

2.2.1 *Sample preparation and testing*

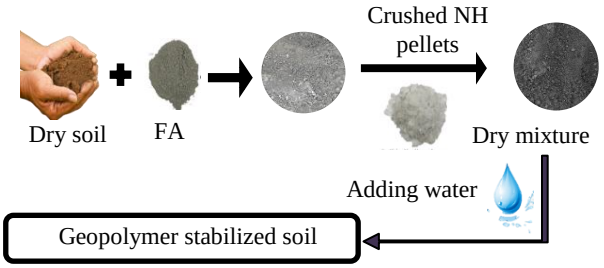

Fig. 1: Mixing method 2

To prepare the raw soil for testing, the soil was first oven-dried at a temperature of 105–110 °C for 24 hours. In accordance with the mixing method shown in Fig. 1, the soil was mixed with FA for an approximate duration of 5 minutes to ensure proper mixing. Following this, crushed solid NH pellets were mixed with the soil mixture, with the mixing process continuing for an additional 8 minutes. The next step involved the addition of the required quantity of water, taking into account both the soil and geopolymer binder. The soil, FA and solid NH mixture underwent a thorough mixing with the water to achieve a homogenous consistency (see Fig. 2).

Fig. 2 Properly mixed geopolymer binder and soil

Once the soil mixture was properly mixed with water, it was compacted in a 1-liter compaction mold under standard compaction conditions. Three specimens were then extracted for UCS testing from one compacted sample.

Three alternative water contents were evaluated experimentally in an effort to determine the necessary total water content for each sample. Ultimately, the total water content calculated by multiplying the total weight of solids by the optimum moisture content (OMC) was selected as the most suitable option, informed by the results obtained from the trial tests.

The UCS of prepared OP-G stabilized samples was tested after 7 days of curing under a rate of platen displacement was maintained at 0.1 mm/min. The reported UCS values are averages of 3 test specimens.

2.2.2 *Optimization of OP-G mix based on UCS and cost*

The optimum OP-G stabilized soil sample was found based on UCS test results and cost per unit volume of stabilized soil. A comprehensive cost analysis, focusing solely on manufacturing expenses, was conducted for all samples. The overall utility for each sample was calculated considering UCS and cost/UCS assigning same weights for both responses.

2.3 *Sample preparation and testing of OP-G, TP-G, and OPC stabilized soils*

In this study, the OP-G stabilized soil sample was compared with an optimal TP-G stabilized soil mixture and an 8% OPC stabilized soil sample. The optimum OP-G stabilized soil sample (obtained in section 3.2) was prepared following the sample preparation outlined in Section 2.2.1. For the synthesis of the TP-G stabilized soil sample, a liquid alkaline activator composed of Na_2SiO_3(NS) and NH was utilized, with a NH molarity of 5 M. The NS to NH ratio was set at 70:30, as per Kishor et al. (2021) and Yaghoubi et al. (2018). The same optimal ratios employed for OP-G in terms of B/S and activator to FA were adopted for TP-G formulation. The procedure employed for preparing the OP-G stabilized soil was replicated for the TP-G stabilized soil, substituting solid alkaline activator with liquid alkaline activator. For the OPC stabilized soil sample, 8% OPC was initially mixed with the soil, followed by the addition of the optimum water content.

The stabilized soil samples (OP-G, TP-G, and OPC) were subjected to various tests after 28 days of curing. These tests, including the swell pressure test (BS 1377: Part 5: 1990), Atterberg Limit test (BS 1377: Part 2:1990), UCS test (BS 1377: Part 7:1990), and CBR test (BS 1377: Part 4:1990), aimed to evaluate the mechanical and physical properties of the samples. The CBR samples underwent a curing period of 24 days followed by a soaking duration of 4 days before testing.

2.4 *Cost and emission analysis*

A comprehensive analysis was conducted to assess the cost and carbon footprint of all three samples, focusing solely on the manufacturing of raw materials. The cost analysis involved determining the mass of FA, OPC, and activator per unit volume of each stabilized soil sample (kg/m³). Local market prices were utilized to determine the unit cost for each material, resulting in a unit cost of 0.15 USD/kg for OPC, 0.96 USD/kg for NH, 0.8 USD/kg for NS, and 0.04 USD/kg for FA. Subsequently, the cost per unit volume of stabilized soil (cost/m³) was computed.

Emissions for the unit volume of each stabilized sample were calculated based on inventory data and functional equations sourced from Fernando et al. (2021).

2.5 *Utility analysis using MAUT*

In this study, a simplified version of Multi-Attribute Utility Theory (MAUT) was utilized to rank the stabilizers. Initially, several criteria, including swell pressure, UCS, CBR, cost per UCS (cost/UCS) and emission per UCS (emission/UCS), were identified. Subsequently, weights were assigned to each criterion to reflect their relative importance. Specifically, weights of 0.2, 0.15, 0.15, 0.3 and 0.2 were allocated to swell pressure, UCS, CBR, cost/UCS and emission/UCS, respectively, with cost and strength exerting the most significant influence on the selection of the optimal mix. To facilitate a fair comparison among criteria with differing units, a normalization step was incorporated. Utility functions were then developed for each criterion. Linear utility functions were employed for criteria where higher values were preferred, such as UCS, while concave utility functions were utilized for criteria where lower values were desired, such as cost/UCS and swell pressure. Subsequently, an overall utility score was computed for each stabilizer percentage, guided by the utility functions and weights. The selection of the most suitable stabilizer percentage was determined based on the highest overall utility score, with higher overall utility values indicative of a superior mix. The analysis adhered to the methodology outlined by Taufik et al. (2021).

3 RESULTS AND DISCUSSION

3.1 *Unconfined compressive strength*

Fig. 3 and 4 shows the UCS of OP-G stabilized soil at different NH/ FA ratios and B/S ratios.

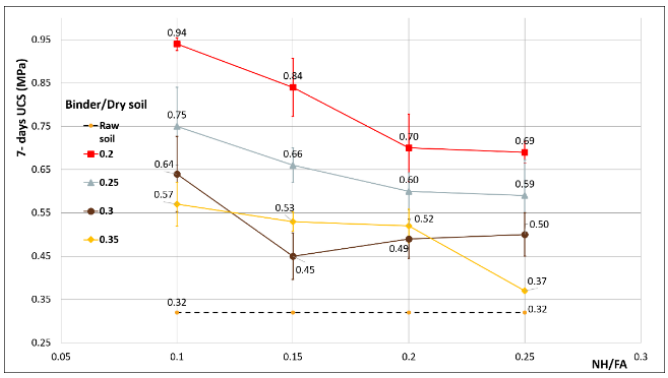

Fig. 3 The variation of 7-D UCS with NH/FA ratios

According to Fig.3, optimum B/S ratio was found as 0.2.

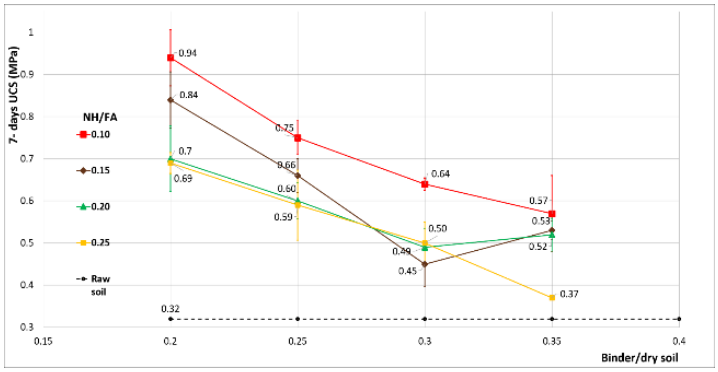

Fig. 4 The variation of 7-D UCS with B/S ratios

According to Fig. 4, optimum NH/FA ratio was found as 0.1.

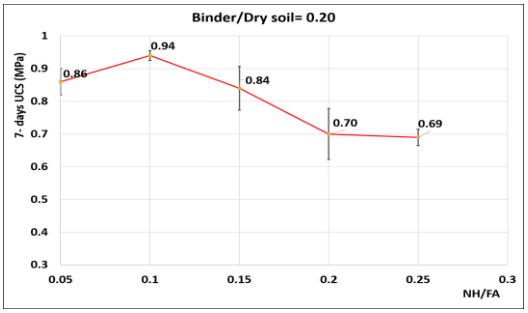

Fig. 5 The variation of 7-D UCS with NH/FA ratio for optimum B/S ratio (0.2)

The highest UCS was found in the mix with B/S ratio of 0.2 and solid NH/FA ratio of 0.1 in which the UCS value reached 0.94 MPa at 7 days curing time. According to Fig. 5, the UCS values of stabilized soil increased to an optimum and again decreased with the increasing of NH/FA ratio. This indicated that higher or lower NH content would not improve the mechanical property of expansive clay. The increase in UCS was due to the formation of C-A-S-H gels from polymerization reactions. The decrease in UCS with NH/FA higher than 0.1 was because of the heat generation of NH which led to expansion and cracking (Tesanasin et al. 2022).

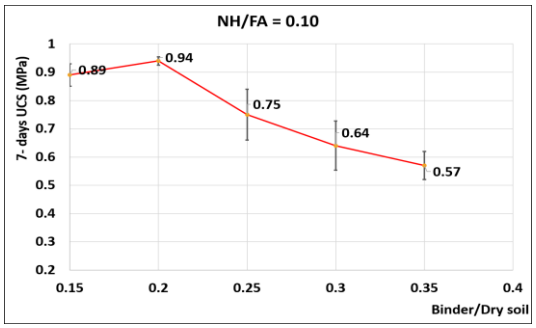

Fig. 6 The variation of 7-D UCS with NH/FA ratio for optimum NH/FA ratio (0.1)

According to Fig. 6, the UCS values of stabilized soil increased to an optimum and again decreased with the increasing of B/S ratio. This indicated that when the FA was beyond the certain amount, it also would perform negative impact on early UCS values of stabilized soil high strength due to formation of N-A-S-H gels which only reduces the porosity (Zheng et al. 2021).

3.2 *Optimized mix based on UCS and cost*

According to the overall utility calculated for each sample considering UCS and cost/UCS, all mixes were ranked. The optimum mixing proportion of OP-G stabilized soil was found to be B/S ratio of 0.2 and solid NH/FA ratio of 0.1 (S1) based on both UCS and cost/UCS as shown in Table 3. Table 3 displays the top 5 mixtures out of a total of 16 samples, selected based on their utility in terms of UCS and cost/UCS ratio.

Table 3. Results of Utility Ranking

Sample ID	Cost/UCS (USD/MPa/m^3)	UCS (MPa)	Overall utility	Rank
S1	34.04	0.94	9.16	1
S5	51.19	0.75	7.07	2
S3	70.57	0.7	6.04	3
S4	82.59	0.69	5.64	4
S6	74.68	0.66	5.59	5

3.3 *Strength and swell characteristics of OP-G, TP-G and OPC stabilized samples*

The results imply that adding geopolymeric binders leads to a decrease in soil plasticity. In comparison to the untreated soil, the plasticity index (PI) values for OP-G, TP-G, and OPC have decreased by 56%, 48%, and 34%, respectively. Interestingly, when

compared to OPC, the geopolymer-stabilized soil samples show a significant decrease in PI (see Fig.7 (a)).

The swell pressure values of the TP-G, OPC-stabilized, and OP-G soil samples are lower than those of the natural soil sample, as shown in Fig.7 (b). For OP-G, TP-G, and OPC, the observed percentage reductions in swell pressure are 52%, 47%, and 34%, in that order. This indicates that even if OPC is more efficient in developing strength, the OP-G formulation suggested in this study is much more beneficial in minimizing swelling.

Fig.7 (c) illustrates the UCS values of the OP-G, TP-G, and OPC stabilized soil samples, which were determined to be 1.23, 0.98, and 2.77 MPa, respectively. These figures indicate a significant increase in UCS over the untreated soil. After 28 days, the percentage increase in UCS for the TP-G, OPC, and OP-G stabilized samples was 206%, 765%, and 284%, respectively. According to the subgrade application standards outlined by ICTAD (Sri Lanka) guidelines, the UCS range for stabilized soil is set between 0.75 MPa and 1.5 MPa. The UCS results indicate compliance with these specified standards for all stabilized samples.

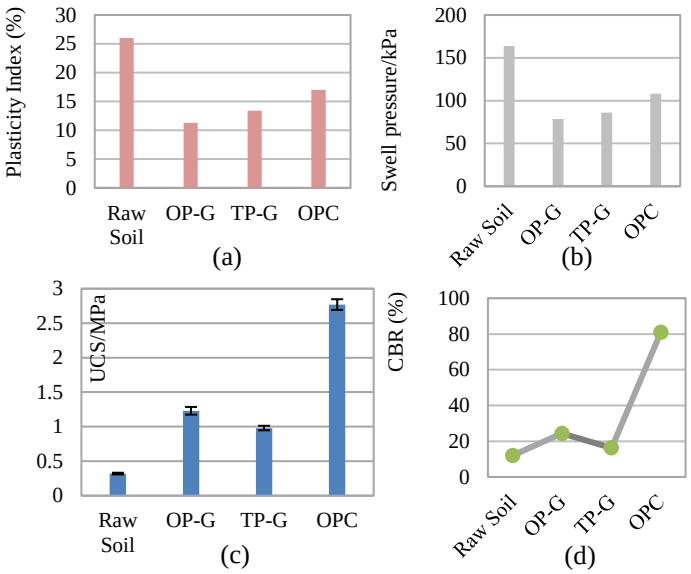

Fig. 7 The variation of strength and swell characteristics of stabilized soil after 28 days

After 4 days of soaking for OP-G, TP-G, and OPC stabilized soil samples, the CBR values were determined to be 24%, 16%, and 81%, respectively, as shown in Fig.7 (d). The CBR standards of ICTAD for stabilized subgrade soil, which state that the CBR should be higher than 15%, are met by all three stabilized samples.

3.4 *Cost and emission comparison*

The cost and emissions associated with OP-G, TP-G, and OPC-stabilized soils are presented in Table 4. Notably, the cost of OP-G and TP-G stabilizers is considerably higher than that of OPC, despite FA being a lower-cost by-product. The costs attributed to NH and NS significantly contribute to the total cost, rendering it economically unfavorable as a binder. Additionally, the emissions from OPC-stabilized samples are notably higher compared to OP-G and TP-G.

3.5 *Optimum stabilizer based on utility analysis*

Table 5 details a utility analysis that makes use of MAUT, with ranks determined by total utility values. Overall, OPC ranked first with an overall utility value of 0.6, indicating its overall superior performance across all criteria. OP-G ranked second with an overall utility value of 0.41, while TP-G ranked third with an overall utility value of 0.35. The results highlight the superior performance of the OPC-stabilized sample compared to the OP-G and TP-G-stabilized samples, as evidenced by the combined performance of UCS, CBR, and cost/UCS values. As the OP-G mixture shows acceptable UCS values along with lower emission levels and reduced swell pressures, it can be recommended as the best alternative to OPC over its poor performance in limiting swelling and its higher environmental impact.

Table 5. Results of MAUT for stabilized samples

Sample	OP-G	TP-G	OPC
U(Swell pressure)	1	0.74	0
U(UCS)	0.14	0	1
U(CBR)	0.12	0	1
U(Cost/UCS)	0.15	0	1
U(Emission/UCS)	0.64	1	0
Overall Utility	0.41	0.35	0.6
Rank	2	3	1

Table 4. Cost analysis of the stabilized soils

Item	Cost (USD/m^3)					Emission (kg CO_2-eq/ m^3)					28-day UCS (MPa)	Cost/UCS (USD/m^3/ MPa)	Emission/UCS (kg CO_2-eq/ m^3/MPa)
	FA	OPC	NH	NS	Total	FA	OPC	NH	NS	Total			
OP-G	9.78	-	23.71	-	33.49	2.72	-	35.19	-	37.91	1.23	27.23	30.82
TP-G	9.83	-	3.32	17.1	30.25	2.73	-	4.93	16.67	24.33	0.98	30.87	24.83
OPC	-	18.24	-	-	18.24	-	114.61	-	-	114.61	2.77	6.58	41.38

4 CONCLUSIONS

- The highest UCS of OPG formulation was found in the mix with binder/ dry soil (B/S) ratio of 0.2 and solid NaOH/ fly ash (NH/FA) ratio of 0.1 in which the UCS value reached 0.94 MPa at 7 days curing time.
- The optimum mixing proportion of OP-G stabilized soil was found to be binder/ dry soil (B/S) ratio of 0.2 and solid NaOH/ fly ash (NH/FA) ratio of 0.1 based on both UCS and cost/UCS.
- Notably, geopolymer-stabilized soil samples demonstrated a significant decrease in PI compared to OPC.
- The UCS values for OP-G, TP-G, and OPC stabilized soil samples after 28 days were 1.23 MPa, 0.98 MPa, and 2.77 MPa, respectively. These results signify a substantial increase in UCS compared to untreated soil, meeting subgrade application standards outlined by ICTAD guidelines.
- 4 days of soaked CBR values for OP-G, TP-G, and OPC stabilized soil samples were determined to be 24%, 16%, and 81%, respectively, all exceeding the CBR standard of 15% set by ICTAD for stabilized subgrade soil.
- The observed percentage reductions in swell pressure for OP-G, TP-G, and OPC were 52%, 47%, and 34%, respectively, suggesting the superior swell reduction capability of OP-G despite OPC exhibiting greater strength development.
- Cost and emissions analysis reveal that the cost of OP-G and TP-G stabilizers is notably higher than OPC, primarily due to expenses associated with sodium hydroxide (NH) and sodium silicate (NS). But emissions from OPC-stabilized samples are significantly higher compared to OP-G and TP-G.
- The utility analysis utilizing MAUT revealed OPC as the top performer with an overall utility value of 0.6, followed by OP-G and TP-G with values of 0.41 and 0.35 respectively. Despite OPC's superior performance across criteria, the acceptable UCS values, lower emissions, and reduced swell pressures of the OP-G mixture make it a viable alternative, surpassing OPC's limitations in swelling control and environmental impact.

ACKNOWLEDGMENTS

We would like to express our heartfelt gratitude to Nawanjana Maheepala and all the laboratory staff whose invaluable guidance and unwavering support have been instrumental in the progress and success of this endeavor.

REFERENCES

Bakharev, T., Sanjayan, J. G., and Cheng, Y.-B. 2001a. Resistance of alkaliactivated slag concrete to alkali-aggregate reaction. Cem. Concr. Res. 31 (2), 331–334.

Bakharev, T., Sanjayan, J. G., and Cheng, Y.-B. 2001b. Resistance of alkaliactivated slag concrete to carbonation. Cem. Concr. Res. 31 (9), 1277–1283.

Davidovits, J. (1991). Geopolymers. J. Therm. Anal. 37, 1633–1656. doi:10.1007/ bf01912193

Davidovits, J., 2015. False Values on CO_2 Emission for Geopolymer Cement/concrete Published in Scientific Papers, pp. 1–9. Technical paper, 24

Disu, A.A., Kolay, P.K., 2021. A critical appraisal of soil stabilization using geopolymers: the past, present and future. Int. J. Geosyn. Ground Eng. 7 (2), 1–16. https://doi.org/10.1007/s40891-021-00267-w.

Fernando, S., Gunasekara, C., Law, D.W., Nasvi, M.C.M., Setunge, S. and Dissanayake, R., 2021. Life cycle assessment and cost analysis of fly ash–rice husk ash blended alkali-activated concrete. Journal of Environmental Management, 295, p.113140

Kishor, R., Singh, V.P. and Srivastava, R.K. (2021) "Mitigation of expansive soil by liquid alkaline activator using rice husk ash, sugarcane bagasse ash for highway subgrade," *International Journal of Pavement Research and Technology*, 15(4), pp. 915–930.

Maheepala, M.M.A.L.N., Nasvi M.C.M., Robert D.J., 2022, "A comprehensive review on geotechnical properties of alkali activated binder treated expansive soil," *Journal of Cleaner Production*, 363, p. 132488

Rios S., Ramos C., Fonseca A.V, Cruz N., Rodrigues C., 2016, Colombian soil stabilized with geopolymers for low cost roads, Procedia Eng., 143 (2016), pp. 1392-1400

Taufik, I., Alam, C.N., Mustofa, Z., Rusdiana, A. and Uriawan, W., 2021, March. Implementation of Multi-Attribute Utility Theory (MAUT) method for selecting diplomats. In IOP Conference Series: Materials Science and Engineering (Vol. 1098, No. 3, p. 032055). IOP Publishing

Tesanasin, T. Suksiripattanapong C., Duc B., Tabyang W. 2022 Engineering properties of marginal lateritic soil stabilized with one-part high calcium fly ash geopolymer as Pavement Materials.

Wu, J., Min Y., Li B., Zheng X. 2021 Stiffness and strength development of the soft clay stabilized by the one-part geopolymer under one-dimensional compressive loading, *Soils and Foundations*, 61(4), pp. 974–988

Yaghoubi, M., Arulrajah A., Disfani M. (2018) "Effects of industrial by-product based geopolymers on the strength development of a soft soil," *Soils and Foundations*, 58(3), pp. 716–728.

Zheng, X. and Wu, J. 2021 'Early strength development of soft clay stabilized by one-part ground granulated blast furnace slag and fly ash-based geopolymer', *Frontiers in Materials*, 8.

Investigation of consolidation parameters of Sri Lankan peat soil

C. H. Nerangama and W.M.N.R.Weerakoon
Department of Civil Engineering, University of Sri Jayewardenepura, Sri Lanka

ABSTRACT: Peat is one of the problematic soil types because of its characteristics such as high compressibility, high water content, low shear strength and complexity of peat soil properties. Because of that, peat soils are generally weak in their natural states, but can be subjected to significant gain with consolidation. Compressibility characteristics are used to predict the settlement of the soil. To determine compressibility characteristics, a one-dimensional oedometer consolidation test was used with different particle sizes of reconstituted peat samples for 5 kg, 10 kg and 15 kg with loading and unloading processes. To identify the type of peat soil, the Von post classification system was used at the peat deposit location. By using disturbed soil samples, Index properties tests were done to determine the water content, specific gravity and organic content of the peat soil samples. Based on results, there was an impact of the particle size distribution on compressibility characteristics.

KEY WORDS: Peat, compressibility characteristics, one-dimensional oedometer consolidation test, reconstituted peat samples, Von-post classification system

1 INTRODUCTION

The growth of the human population determines a huge demand for development. Nowadays, developments are hindered by a dearth of suitable land in many countries. But there is some land that can't be used to develop any construction projects, because of the unsuitable soil type of the land. Therefore, many research papers have been established by considering the properties and behavior of different types of soil. The reason for that is to ensure that any construction works on different soil types of ground is safe after the construction. Among these different soil types, peat soil is one of the important soil types. Fig. 1 presents the peat deposits in the world.

Fig. 1 Peat deposits Veloo et al (2014)

According to Adnan and Wijeyesekera (2008), peat soil is formed naturally through the decomposition of plant and animal matter under anaerobic conditions. Also, that process takes place over long periods. Furthermore, Peat has high compressibility, low shear strength, high moisture content and low bearing capacity; it has been found by Bujang (2004) and cited by Adnan and Wijeyesekera (2007). Not only that, peat has high organic content and fiber content; it has been found by Whitlow (2001) and cited by Johari, Bakar and Aziz (2015). On the other hand, the properties of peat soil vary from one deposit to another, furthermore vary from point to point in the same deposit. So, peat soil has huge complexity when compared to mineral soil.

When consider the definitions and classifications for peat soil, there are wide variations, but no internationally accepted definition or classification for peat soil. Johari, Bakar and Aziz (2015) have highlighted the three types of peat soil; fibric, hemic and sapric. Also, that can be found according to the Von-post classifications system (H1 –H10) and the fiber content of the peat soil. When considering the peat distribution of the world (Xu et al. 2018), the total global peat land area is 4.23 million km², also approximately 2.84% of the world's land area. Further, estimated peat land areas in Asia account for about 38.4% of the total estimate of global peatland cover.

First step of a construction project is to analyze the soil type, soil behavior and composition of the soil in order to use that soil as a foundation. Among different soil types, Peat soil is the one of problematic soil. Main problem of the peat soil is not acceptable to be used as foundations (Savo and sozi 2019). Because peat soil shouldn't be stronger to take the all loads of the structure. So, main purpose is to gather information about the peat soil profile, specially consolidation properties to predict the settlement of the peat soil. Although the peat lands have got the attention globally, Sri Lanka is still lagging behind the other countries regarding that subject. Peat soil is so complex that global studies are not compatible with Sri Lanka. Main reason for that complexity of

peat soil. So, study of complexity and compressibility characteristics of the peat soil are needed. For studying the compressibility characteristics, the one-dimensional oedometer consolidation test is a suitable test for the laboratory, because of the easiness of the procedure. So, this research paper mainly focused on index properties of peat soil and the influence of the particle size to the compressibility characteristics of peat soil.

2 METHODOOGY

2.1 *Introduction*

This study was based on Quantitative research which concentrate on the investigation of compressibility characteristics of Sri Lankan peat soil. In this research, there were two types of tests:
1) Index properties test and
2) One- dimensional oedometer consolidation test. Under index properties test, Organic content, specific gravity and water content were tested according to the ASTMD 2974-14, ASTMD 854-14 and ASTMD 2974-87 respectively. One- dimensional oedometer consolidation test was done by referring the BS 1377: Part 5: 1990 standard.

2.2 *Peat soil sampling*

Peat soil samples were collected from Muthurajawela marsh area in Sri Lanka. To collect disturbed peat soil samples, excavated depth was 0.3 m to 1.0 m below ground surface. Peat soil samples were collected from five locations and three points from each location. Those soil samples were immediately placed in Polythene bags with sealing the peat soil samples. After that, bags were kept in a plastic basket with a lid (Fig. 2). Especially, peat soil sampling was done quickly to avoid collecting more water for the peat soil samples. Because of ground water level of peat was very high. When peat soil samples were brought to laboratory, kept at a constant temperature. Von Post classification test was done at the peat deposit location with fresh peat.

Fig. 2 Placed peat soil samples

2.3 *Preparation of peat soil samples*

Reconstituted disturbed samples were prepared for the one- dimensional oedometer consolidation test and another disturbed soil sample were prepared to determine the index properties of the peat soil. There are three steps, before testing the one-dimensional oedometer test: 1) Sieving 2) Reconstituting and 3) extrusion. At the sieving step, Disturbed peat soil sample was sieved by using 3.35 mm, 2.36 mm and 1.7 mm sieve apertures. After that, some water was aided to sieve apertures and conducted the wet sieving process to remove the larger particles retained. After that, remaining slurry soil samples from the 2.36 mm, 1.70 mm and pan of the sieve apparatus were collected and those were placed in three molds and applied small pressure for that in a same way for all three samples. Fig. 3 is shown the sieving process and a slurry sample. Next, those soil samples were placed in three consolidation rings. Above procedure was used to prepare of soil for the one-dimensional consolidation test. Disturbed soil samples were used to determine index properties of peat soil. Three soil samples were prepared and tested in each index properties test.

Fig. 3 Preparation and place peat soil samples

2.4 *Index properties test*

Three main tests were conducted to determine the index properties of the peat soil in this research. They are organic content, specific gravity and water content. Organic content was determined by using muffle furnace (burned at 750 ºC) nearly 10 hours. Specific gravity was determined by using the pycnometer. Moisture content was determined by using oven with drying nearly 24 hours at 105±5 ºC.

2.5 *One-dimensional oedometer consolidation test*

All three peat soil samples were placed in three consolidation rings with three different particle sizes. 2 kg seating load was maintained for 24 hours. Reason for that is to adjust the unevenness of the surface of the soil specimen. After that,5 kg,10 kg and 15 kg were loaded for all three soil specimens through 10 days. Also, those loads were unloaded through 10 days. Height of the soil specimen in three soil samples were recorded with the time intervals 0.1,0.25,0.5,1,2,4,8,16,30,60,120,240,480,960,1440,2880,5760,11520 and 14400 minutes.

2.6 *Analysis of test results*

On this research, graphical method was used to determine the compressibility characteristics. Taylor' s method was used determine the Coefficient of consolidation (C_v). For that, settlement against square root time graph can be used at loading stage.
Void ratio against log P (applied pressure) at the loading stage graph can be used to find the Compression Index (C_c) and Pre-consolidation Pressure (P_c). It can be found from the loading stage.
And also, Swelling Index (C_s) can be found from the Void ratio against log P (applied pressure) graph at the unloading stage.
Compression ratio (Cr) can be obtained by using the Compression Index (C_c). It can be used to determine by using below equation (1).

$$C_r = \frac{C_c}{1+e_0} \quad (1)$$

Where e_0 is the initial void ratio of the peat soil sample.
Coefficient of volume compressibility(m_v) can be determined from the void ratio against P (applied pressure) at the loading stage. Slope of the graph gives the Compressibility Coefficient (a_v). Coefficient of volume compressibility (m_v) can be found by using below equation (2).

$$m_v = \frac{a_v}{1+e_0} \quad (2)$$

Where e_0 is the initial void ratio of the peat soil sample.

2.7 *Analysis of output*

Output of the analysis were compressibility characteristics from One- dimensional Oedometer consolidation test and index properties test outputs. C_v, P_c, m_v, C_c, C_s and C_r and water content, specific gravity as well as organic content of the peat soil samples were determined.

3 RESULTS AND DISCUSSION

3.1 *Introduction*

Results of Von post classification system, index properties tests and One-Dimensional Oedometer Consolidation Test are included and discussed under the research objectives.

3.2 *Soil classification*

Von post classification system was done at the peat deposit location with the fresh peat. It was done with the present visual composition of the water and soil including the color and plant structure. By squeezing the soil, behavior of the paste was observed to recognize the type of the peat according to the Von post classification.

Fresh peat soil sample is shown in the below Fig. 4.

Fig. 4 Peat soil observations at the peat location

The observations are presented in the below. Table 1 presents the observations of the peat soil considering the present visual composition before squeezing process.

Table 1. Observations for Von post classification- before squeezing process

Features	Observations
Color of the soil	Dark grey
Plant structure	Hardly recognizable

The observations of the peat soil (after squeezing process) are presented in the Table 2.

Table 2. Observations for Von post classification- after squeezing process

Features	Observations
Color of the water	Muddy water
When squeeze the soil (passing between fingers)	Fairly uniform paste
Nature of the remaining part	Very strongly paste

Degree of humification and symbol were presented in the below table 3. Peat humification is a measure of initial plant breakdown and decomposition (Chambers et al. 2010).

Table 3. Results of the peat soil after Von post classification test

Details	Results
Degree of Humification	H9
Symbol	a

It can be introduced as sapric/ amorphous peat.

3.3 *Index properties test results*

Three samples were tested for each test for water content, specific gravity and organic content. Those final average outputs of the test are summarized in the below Table 4.

Table 4. Results of the index properties test in three soil samples

Parameter	Average Results
Water content (%)	107.621
Specific gravity (G_s)	1.706
Organic content (%)	51.117

According to the results of this research and results which were established Adnan and Wijeyesekera (2008), index properties test values are different with the peat deposit location.

3.4 *Compressibility characteristics*

Three types of particle sizes were used for the three-consolidation test apparatus. Remaining soil samples from the 2.36 mm, 1.70 mm and pan of the sieve apparatus were tested as three samples of the consolidation test apparatus. Those are described as Test 1, Test 2 and Test 3 respectively.

Void ratio against log P was used to determine C_c (Compression Index) and P_c (Pre-consolidation Pressure) at loading stage. At the unloading stage, C_S (Swelling Index) was determined. There were three graphs for Test 1, Test 2 and Test 3. Fig. 5 is shown the graph for Test 1.

With the results of the Compression Index (C_c), C_r (Compression ratio) was obtained using the above-mentioned equation (1).

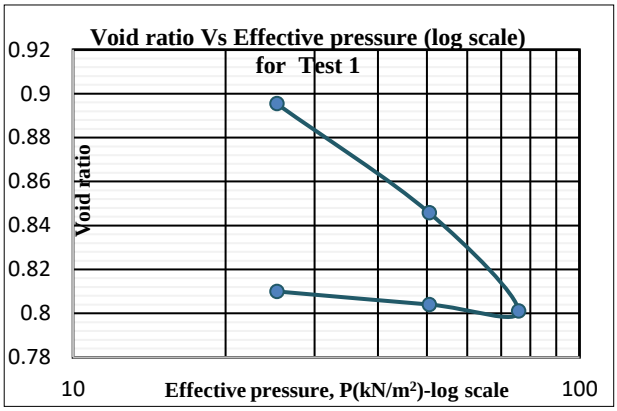

Fig. 5 Void ratio Vs effective pressure (log scale) for R2.36

Void ratio against P graph (Fig. 6) was used to recognize a_v (Compressibility Coefficient). The slope of the graph was given the a_v value. After that, m_v (Coefficient of volume compressibility) was obtained using the equation (2). There were three graphs. All the three graphs are shown together in the Fig.6 below.

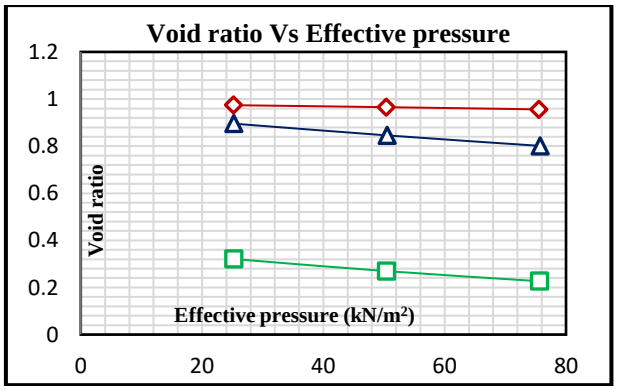

Fig. 6 Void ratio Vs effective pressure (for all tests)

Settlement against Square root time (Fig. 7) was used to determine C_v (Coefficient of consolidation). There were nine graphs. For Test 3, there were three graphs including 5 kg, 10 kg and 15 kg. Likewise, there were six graphs for Test 2 and Test 1. According to the Taylor's method, nine values were determined. Fig. 7 is presented the graph for the Test 3 at 5kg load.

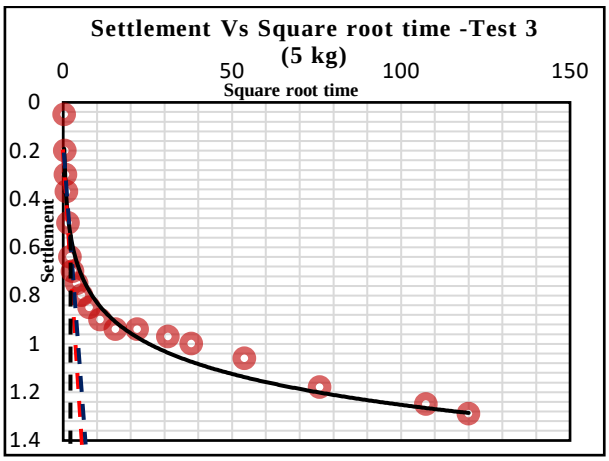

Fig. 7 Settlement Vs square root time for Test 3 (5 kg)

Results for the e_0, P_c, a_v, m_v, C_c, C_s and C_r are summarized in the below Table 5. Results of the Coefficient of consolidation (C_v) is shown in Table 6.

Table 5. Results of compressibility characteristics

Apparatus Name	Test 1	Test 2	Test 3
e_0	0.9927	0.4108	1.1093
C_c	0.1977	0.1974	0.0374
C_S	0.0198	0.0350	0.0035
C_r	1.1904	0.6082	0.0177
$a_v(kN^{-1}m^2)$	0.001868	0.001868	0.000354
$m_v(kN^{-1}m^2)$	0.99459	0.41266	0.00017
P_c(kPa)	58	57	55

Table 6. Results of compressibility characteristics (C_v)

Load (kg)	Apparatus name	C_v (m^2/yr)
5	Test 1	2.537
	Test 2	4.373
	Test 3	9.864
10	Test 1	1.540
	Test 2	2.272
	Test 3	4.347
15	Test 1	2.291
	Test 2	3.771
	Test 3	9.686

Where e_0 is initial void ratio of the sample. C_c is Compression Index. C_S is the Swelling Index, C_r is the Compression ratio, m_v is the Coefficient of volume compressibility, a_v is the Compressibility Coefficient, C_v is the Coefficient of consolidation and P_c

is Pre-consolidation Pressure. P is the applied pressure.

Results for the initial void ratio of the three different soil samples are also different from each other. When consider the soil mass, it can be divided into three; solid, water and air. The ratio of the volume of the voids (water and air) to the volume of solids can be introduced as the void ratio of the soil sample. Initial void ratio is larger when size of the soil particle is smaller. When consider the results of the research, volume of the voids is increased with the smaller size particles sizes. On the other hand, volume of the solids is decreased with the smaller size particles sizes. The coefficient of consolidation (C_v) is measured to know the rate at which compression can occur in the soil when the load is increasing. When particle size of the sample is increased, coefficient of consolidation (C_v) has been decreased. On the other hand, when applied load is increased, generally coefficient of consolidation (C_v) has been decreased. It means with the higher particle sizes, rate of the compression that can occur in the soil has been decreased.

The compression index (C_c) can also be used to determine the settlement of the soil. When particle size of the soil sample is increased, Compression index value has been increased. Settlement of the soil sample is increased, when particle size is also increased. On the other hand, settlement of the soil sample is increased, when there is smaller initial void ratio. Swelling Index (C_s) can be known as the ability of the soil samples to swell with the applied pressure. With the increasing particle size of the sample, Swelling Index is also increased in a soil sample. If Swelling Index is higher value, the ability of a soil to swell is increased.

Compression ratio (C_r) is used for classification of compressibility of a soil. According to the Johari et al. (2015), they have divided the peat soil samples into four classes by using the Compression ratio of the soil sample; very slightly compressible ($C_r = 0 – 0.05$), slightly compressible ($C_r = 0.05 – 0.10$), moderately compressible ($C_r = 0.10 – 0.20$) and very compressible ($C_r = > 0.20$). According to the results as mentioned above, Test 3, soil sample is moderately compressible and other two samples are very compressible samples. Also, with the particle size increasing, Coefficient of volume compressibility is also increased. Particle size is increased; Pre-consolidation Pressure has been increased. It means, if there are large particle sizes of soil samples, that soil sample can bear higher maximum vertical pressure.

4 CONCLUSION

According to observations at the peat deposit location, it gives the type of peat soil as sapric/amorphous in the Muthurajawela marsh area in Sri Lanka. It was found that there was higher water content value and organic content value with the correct range for the specific gravity according to the published data for Muthurajawela peat soil. Based on the findings of this study and previous studies, it can be indicated that there are different values for the index properties test for the different locations.

Furthermore, it was found that there were different values for different particle sizes for the same compressibility characteristics. And also, the particle size distribution of the peat soil samples is also affected by the initial void ratio.

As Civil Engineers need to analyze the soil type, soil behavior, and composition of the soil to use that soil as a foundation for a any design. There are many soil types; peat soil is one of the problematic soil types in the world. For example, peat soil causes a fire and it can burn rapidly (Savo and Sozi 2019). The main problem of the peat soil is not acceptable to be used as foundations (Savo and Sozi 2019). So, Researchers are finding solutions for that; They are avoid building structures on peat soil and change the properties and characteristics of the peat soil. However, the study of the consolidation properties and index properties of peat soil is essential for any situation before the construction. In this research main focus is to identify the correlation between the compressibility characteristics and initial void ratio and particle size. When planning the ground improvement method for the peat land, initially void ratio of the sample can be checked. By using those data can be determined the required technique for the land. Because of the results of the research will be shown the better understanding of Muthurajawela peat for the design and construction processes.

This research is limited because of the complexity of the peat soil. Those results of index properties test and compressibility characteristics are only valid for sapric/amorphous type peat soil in Muthurajawela marsh area. But the methodology can be used for any other peat deposit. However, the impact of the particle size distribution doesn't normally vary with the location of the peat deposit.

The impact of the particle size distribution on the compressibility characteristics is checked only for this type of peat soil. Furthermore, this study can be developed for other types of peats, such as fibric and hemic. After the investigation, those results can be justified with the different types of peat soils.

And also, with the time limitation of the research, the fiber content of the peat soil was not determined. By using the fiber content of the soil, it gives the type of the peat soil. So, Von post classification results can be justified with the fiber content value.

ACKNOWLEDGMENTS

The authors would like to give special thank and acknowledge to Department of Wildlife Conservation for providing the peat soil samples and Department of Chemistry, Faculty of Applied Sciences of University of Sri Jayewardenepura for providing laboratory facilities to conduct the organic content test.

REFERENCES

Adnan, Z. and Wijeyesekera, D.C. (2007), "Geotechnical Challenges with Malaysian Peat", Advances in Computing and Technology Conference, University of East London, Crowne Plaza Hotel, Docklands, London, 2nd Annual Conference 27 January 2007.

Adnan, Z. and Wijeyesekera, D.C. (2008), "Geotechnical Characteristics of Peat", Advances in Computing and Technology Conference, University of East London, Crowne Plaza Hotel, Docklands, London, 2nd Annual Conference 27 January 2008.

DAS, B. M., 2009. Principles of Geotechnical Engineering. Seventh Edition ed. Stamford.

Johari, N.N., Bakar, I. and Aziz, M.H.A. (2015), "Consolidation Parameters of Reconstituted Peat Soil: Oedometer Testing", Applied Mechanics and Materials, Vol.1470, pp. 1466–1470.

Johari, N.N., Bakar, I., Razali, S.N.M. (2015), "Fiber Effects on Compressibility of Peat", Soft Soil Engineering International Conference 2015 (SEIC2015).

Karunawardena, W.A. (2007), "Consolidation Analysis of Sri Lankan Peaty Clay using Elasto-viscoplastic Theory", Vol.177, pp. 01–70.

Savo, K. and Sozi, H. (2019), "Organic and peat engineering properties, and their suitability for construction projects", Vol.28, pp. 01–25.

Tham, F. N., John, K. R. and Roslan, H. (2013), "Definitions and engineering classifications of tropical lowland peats", Bulletin of Engineering Geology and the Environment, Vol. 553, pp.547-552.

Veloo, R., Ranst, E.V. and Selliah, P. (2014), "Peat Characteristics and its impact on oil palm yield", Vol. 40, pp. 34–40.

Investigation of the stability of Embankments on soft soil deposits

C.F. Robinson
B.Sc Undergraduate, Department of Civil Engineering, SLIIT

T.M.D. Thilakarathne
Research Assistant, SLIIT

H.S. Thilakasiri
The Dean, Faculty of Engineering, SLIIT

ABSTRACT: The stability of embankment sections that failed in the Colombo-Katunayake Motorway project is investigated in this study, even though the placement of stone columns was used to enhance the ground. The study uses observational methods, such as Matsuo and Kawamura's construction control diagram and a construction control chart from an embankment trial in Tokai, Malaysia, and focuses on failed sections K6 + 230 – 320, K7 + 890 – 980, and PK1 + 700 – 800. Fill height, lateral displacement, and vertical settling are among the metrics. These techniques are also applied to successful CKE project segments analysis for future validation and application. Because soft soil deposits are likely to experience lateral spreading and settlements, the goal of the research is to identify the best method for detecting and resolving embankment stability concerns. It is possible to improve embankment construction techniques and reduce the risks connected to soft soil conditions by using observational approaches.

KEY WORDS: embankment stability, observational approach, soft soils.

1 INTRODUCTION

Stability is a critical design consideration for embankments built on soft soils. Due to the rapid urbanization, infrastructure expansion, and industrialization, embankments must now be constructed even on soft soil, which was earlier regarded to be undesirable. The necessity for widened development to satisfy the demands of rising population, the lack of suitable land, and the rising value of land has made embankments on soft soil important today. Due to unfavorable geotechnical characteristics, such as low bearing capacity, slope instability, and excessive settlement the construction of embankments on soft soil may encounter a number of challenges(Ye et al., 2017) (Basack et al., 2016)(Indraratna et al., 2013). Several strategies, including the use of stone columns, Deep Mixed (DM) columns, preloading with PVDs, and light fill, have been used successfully to strengthen soft soil.

Large-scale facility development on soft clay raises a number of questions regarding the stability and deformability of the foundation and may need expensive foundation designs to achieve the necessary performance. Allowing staged loading to consolidate foundation soils and hence increase strength and stiffness before applying a complete load is an alternative to deep foundations or expensive structural solutions. Having a performance monitoring program available is a crucial component of staged loading since it allows for continuous improvement in the characterization of on-site circumstances as work progresses(Baecher & Ladd, 1997).

The application of the observational approach method in embankment stability is based on the fact that soil behavior and ground conditions are dynamic and frequently unpredictable. Traditional engineering designs for embankments are predicated on calculations and predetermined hypotheses based on the geotechnical information at hand. These hypotheses, however, would not always account for the whole complexity of the subsurface, which could result in design uncertainties and the possibility of unanticipated difficulties during construction. The observational approach provides a practical and adaptable remedy for these problems(Peck, 1969).

This research is mainly focused on investigating the instability of some embankment sections that was taken place in the Colombo – Katunayake Expressway project (CKE) which is constructed over soft soil . The three embankment sections are analyzed using two available observational approaches

in order to check the most appropriate method for these embankments and hence come up with a method suitable for Sri Lankan context. The importance of this study is that we have the fill height vs vertical and horizontal deflection data of the actual embankment failures in the CKE project and hence accurate conclusions can be drawn from this study.

2 METHODOLOGY

In CKE – Colombo-Katunayake Expressway project three major failure sections were observed due to embankment instability. K6 + 230 – 320, K7 + 890 – 980, PK1 + 700-800 are the three failure sections. There are several methods to identify the stability of the embankment that is built on soft soils. However, in this research construction control charts developed by plotting monitored parameters such as fill height, lateral displacement and vertical settlement have been utilized. There are 2 construction control charts that have been chosen for this research. Which are,

- Diagram for construction control developed by Matsuo and Kawamura
- Construction control chart developed from instrumented trial embankment on soft ground at Tokai of Kedah, Malaysia

2.1 *Diagram for construction control developed by Matsuo and Kawamura*

(Matsuo & Kawamura, 1977)has stated that, the soil characteristics, soft layer thicknesses, and other environmental factors varied, numerous embankments that were built under various circumstances failed close to this curve in the image. This curve is approached as construction moves forward in failure cases, while on the other hand, in non-failure cases, there is a tendency to be distant from this curve, even when it is reached once right after construction.

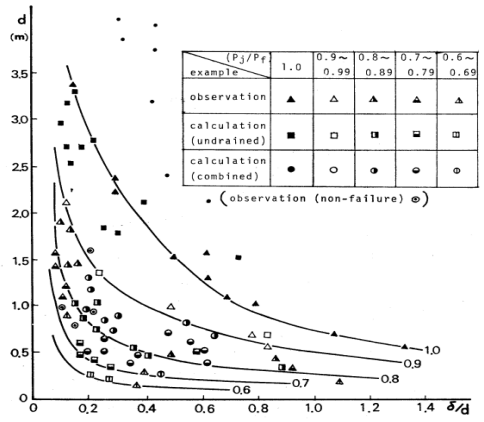

Figure 1 Matsuo and Kawamura chart

This is the diagram for construction control developed by Matsuo and Kawamura. The curves in this diagram were all created using the approach described below. All displacement curves on the (d - δ/d) figure have known loads Pj, loads in the jth loading stage, and loads at failure Pf. Each contour line has a different value representing the stability of the embankments. The contour line having a value of 1.0 is known as failure boundary and beyond that line known as failure zone. Without saying more, the displacement curve's progression towards the smaller contour line indicates that ground stabilization has increased as a result of consolidation.

2.2 *Construction control chart developed from instrumented trial embankment on soft ground at Tokai of Kedah, Malaysia*

A construction control chart titled "Fill Height (fill thickness) versus Lateral Displacement" (FHLD plot) was prepared by the Authors based on the findings of FEM analyses and the actual lateral movement of a set of displacement markers installed at the toe of the trial embankment. The created FHLD map is used in conjunction with a Matsuo stability plot that the authors adjusted to fit the project during the construction stage to monitor the stability of the embankment as it is being built (the filling stage).

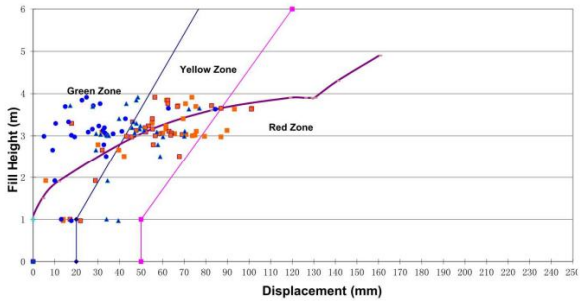

Figure 2 Construction control chart developed from trial embankment of Tokai, Malaysia(Yean-Chin et al., 2016))

To ensure safe embankment construction and hence save expensive and time-consuming corrective work, the FHLD was categorized into Green, Yellow Orange, and Red Zones, respectively. While Table below outlines the steps that must be followed on-site as soon as the monitoring findings change color zones(Yean-Chin et al., 2016)

Zone	Action
Green	Embankment filling can continue.
Yellow	Supervising Engineer to inform design office and embankment filling can continue. For area with PVD, the embankment filling rate reduced to 0.5m/week.
Orange	Supervising Engineer to inform design office immediately. Embankment filling work only can proceed with permission from the design office
Red	Supervising Engineer to stop the embankment filling immediately and inform design office. Design office to review instrumentation data and advise on next course of action.

Figure 3 Necessary actions required during construction

Monitored data measurements were obtained from MCC – China Metallurgical Group of Company. They have specifically monitored the embankment construction due to its beneficiary. It acts as an early warning system, enabling the quick detection of deviations, problems, and threats. For each construction control method different charts having different parameter connection have been used. Matsuo and Kawamura chart has the connection between ratio of horizontal displacement and vertical displacement (δ/d) vertical displacement (d) and Construction control chart developed from trial embankment at Tokai has the connection between horizontal displacement and fill height. Tools used to sketch these graphs are Microsoft excel and Plot digitizer.

Both charts were used to plot, to obtain the statement of the stability of failed as well as successful embankment sections to compare and select the most suitable option that can be used for Sri Lankan context.

3 RESULTS

Colombo-Katunayake Expressway project's successful and unsuccessful embankment sections have been plotted using the two observational approaches, and the findings are shown below. This portion provides a comprehensive overview of the observed construction control charts, variations of the curves for each section respect to its x and y axis parameters. From the plotted charts for each section, the accuracy of each method related to its actual state of the embankment sections can be compared to identify the most suitable method.

3.1 *Failed embankment sections*

- PK1+800

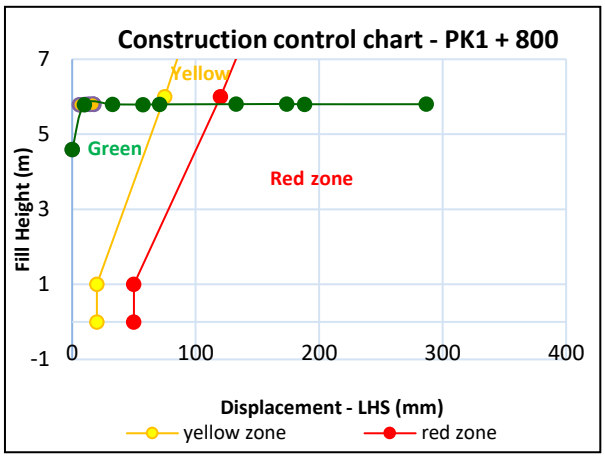

Figure 4 Construction control chart for PK1+800

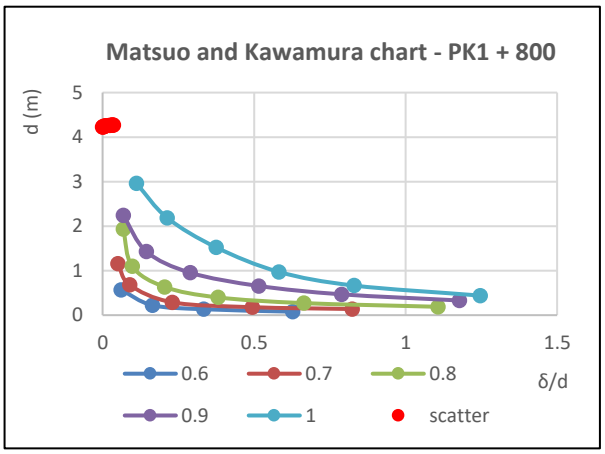

Figure 5 Matsuo and Kawamura chart for PK1+800

- K6+300

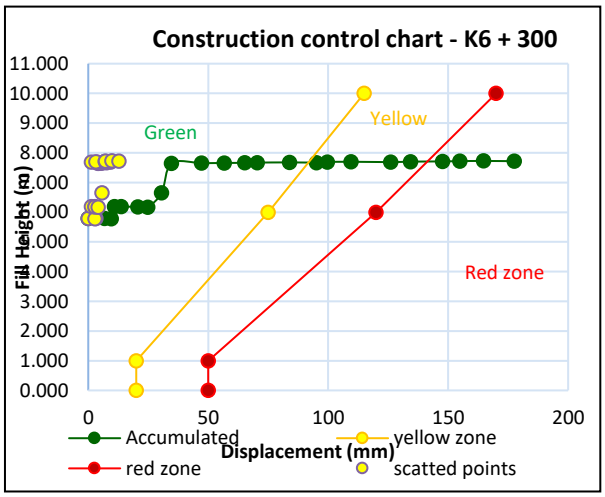

Figure 6 Construction control chart for K6+300

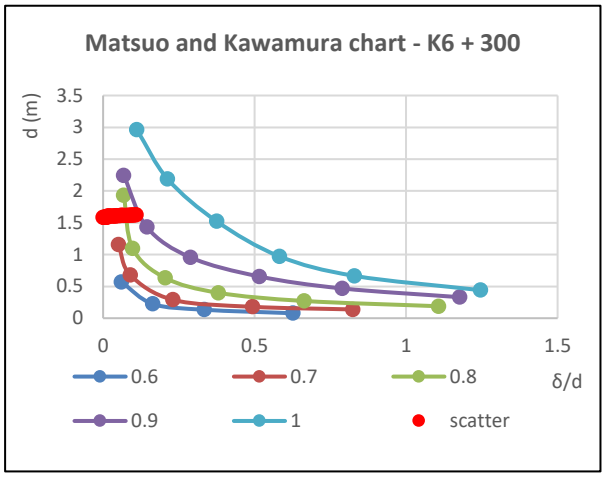

Figure 7 Matsuo and Kawamura chart for K6+300

- K7+935

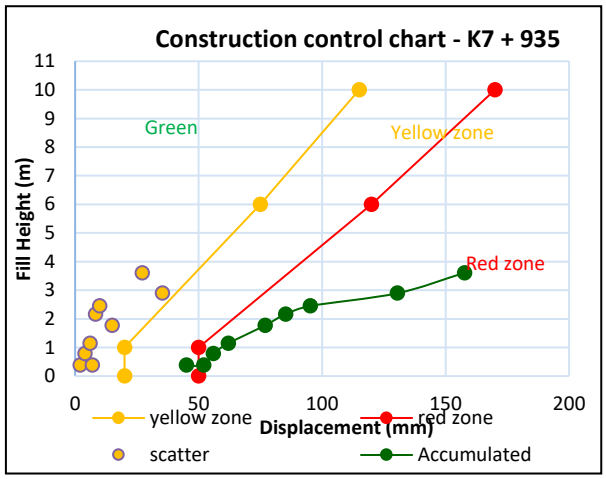

Figure 8 Construction control chart for K7+935

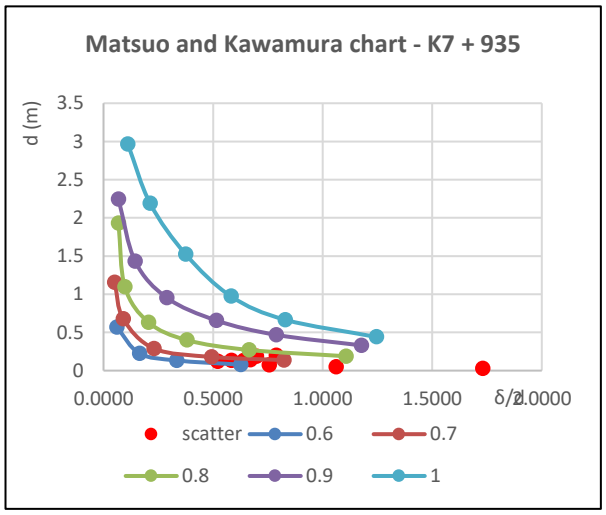

Figure 9 Matsuo and Kawamura chart for K7+935

3.2 *Successful embankment sections*

- K24+180-280

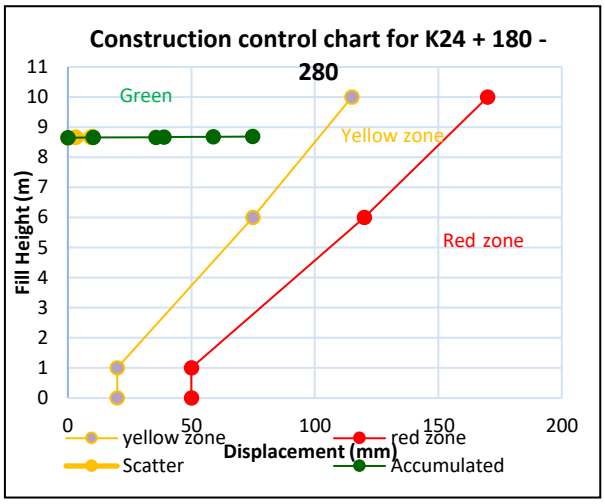

Figure 10 Construction control chart for K24+180-280

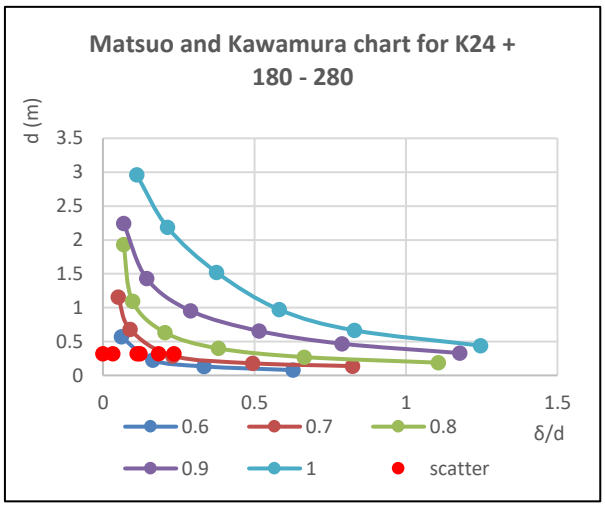

Figure 11 Matsuo and Kawamura chart for K24+180-280

- K0+800

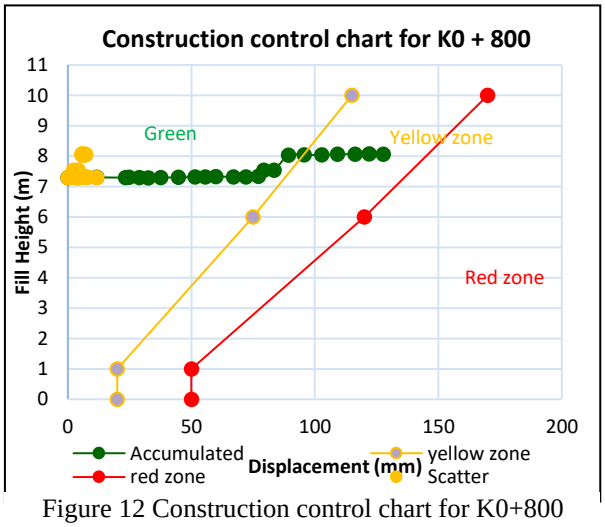

Figure 12 Construction control chart for K0+800

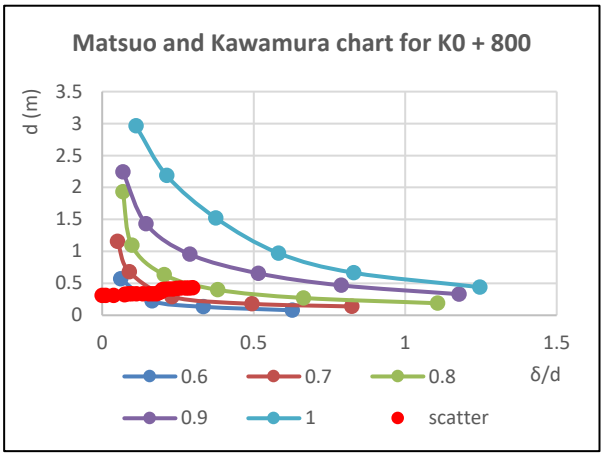

Figure 13 Matsuo and Kawamura chart for K0+800

4 DISCUSSION

Construction control charts are often preferred over traditional stability analysis methods due to their real-time monitoring capabilities and practical applicability in predicting embankment stability on soft soils. Unlike stability analysis, which primarily relies on theoretical models and assumptions, control charts offer a dynamic, on-the-ground assessment of construction processes. Control charts enable continuous monitoring of various parameters during construction, providing immediate feedback on the performance and behaviour of the embankment. Control charts demonstrate their capacity to provide an immediate, useful, and preventive method of guaranteeing embankment stability in soft soil circumstances.

The above results have provided the observational charts plotted for each embankment sections of Colombo-Katunayake Expressway project. Each section's plotted curves and scatter points differ from others due to the embankment sections real time monitored parameters. From the construction control chart developed from trial embankment results, its possible to say that the expected results were obtained for failed sections and successful sections. However, the results obtained from Matsuo and Kawamura chart has not been satisfactory. The construction control chart satisfies with all the failed and successful sections compared to the Matsuo and Kawamura chart. Matsuo and Kawamura chart provides the FoS predictions regarding the state of embankment section while monitoring the construction. However, for CKE embankment sections the validity and accuracy has been obtained from construction control chart developed from trial embankment method.

5 CONCLUSION

This research identified how important to investigate the stability of the embankment that was built on soft soils and how it affects the engineering field due to its necessity of constructing it. Got to know the importance of investigating the stability of the embankment in order to prevent the collapse and failure of the structures while constructing or after construction to protect human lives and avoid environmental, economic and social impacts. Additionally, it has been discussed the stability of embankments and how it plays a crucial role in urban planning decisions, influencing land use and development considerations. By using control charts, construction professionals can identify deviations from expected performance early in the construction process. This early detection enables prompt intervention and corrective measures to address potential stability issues before they escalate. Utilizing these both methods is essential because in practical situations it is meaningless if failure can be realized after it has occurred. However, among these two observational charts construction control chart developed from trial embankment of Tokai, Malaysia has provided the true statement regarding the stability of the embankment sections. Which never means that Matsuo and Kawamura chart has provided false statement regarding the stability. For the soil condition of Colombo Katunayake expressway, the most suitable observation method was selected as Construction control chart. So finally, it's possible to apply this chart as a construction control chart for the sections in CKE project to monitor the behavior of the soil deformation which will state the stability of the embankment sections.

ACKNOWLEDGMENTS

I extend my heartfelt gratitude to all those who contributed to the completion of this manuscript. I am thankful to Ms. Dilmini Tilakarathne, for her insightful feedback and contributions. Additionally, I appreciate the support from MCC – China Metallurgical Group of Company for providing necessary data needed for this research. The collaborative efforts of everyone involved have played a significant role in shaping this manuscript, and I am truly grateful for their dedication and expertise.

REFERENCES

Baecher, G. B., & Ladd, C. C. (1997). Formal Observational Approach to Staged Loading. *Transportation Research Record: Journal of the Transportation Research Board*, *1582*(1), 49–52. https://doi.org/10.3141/1582-08

Basack, S., Indraratna, B., & Rujikiatkamjorn, C. (2016). Analysis of the Behaviour of Stone Column Stabilized

Soft Ground Supporting Transport Infrastructure. *Procedia Engineering*, *143*, 347–354. https://doi.org/10.1016/j.proeng.2016.06.044

Indraratna, B., Basack, S., & Rujikiatkamjorn, C. (2013). Numerical Solution of Stone Column–Improved Soft Soil Considering Arching, Clogging, and Smear Effects. *Journal of Geotechnical and Geoenvironmental Engineering*, *139*(3), 377–394. https://doi.org/10.1061/(ASCE)GT.1943-5606.0000789

Matsuo, M., & Kawamura, K. (1977). Diagram for Construction Control of Embankment on Soft Ground. *Soils and Foundations*, *17*(3), 37–52. https://doi.org/10.3208/sandf1972.17.3_37

Peck, R. B. (1969). Advantages and Limitations of the Observational Method in Applied Soil Mechanics. *Géotechnique*, *19*(2), 171–187. https://doi.org/10.1680/geot.1969.19.2.171

Ye, G., Cai, Y., & Zhang, Z. (2017). Numerical study on load transfer effect of Stiffened Deep Mixed column-supported embankment over soft soil. *KSCE Journal of Civil Engineering*, *21*(3), 703–714. https://doi.org/10.1007/s12205-016-0637-8